NASA TECHNICAL MEMORANDUM

NASA TM X-2367

NASA TM X-236

LONGITUDINAL AERODYNAMIC CHARACTERISTICS AT MACH 1.50 TO 4.63 OF A MISSILE MODEL EMPLOYING VARIOUS CANARDS AND A TRAILING-EDGE FLAP CONTROL

by Charles D. Trescot, Jr.

Langley Research Center
Hampton, Va. 23365

NATIONAL AERONAUTICS AND SPACE ADMINISTRATION • WASHINGTON, D. C. • OCTOBER 197

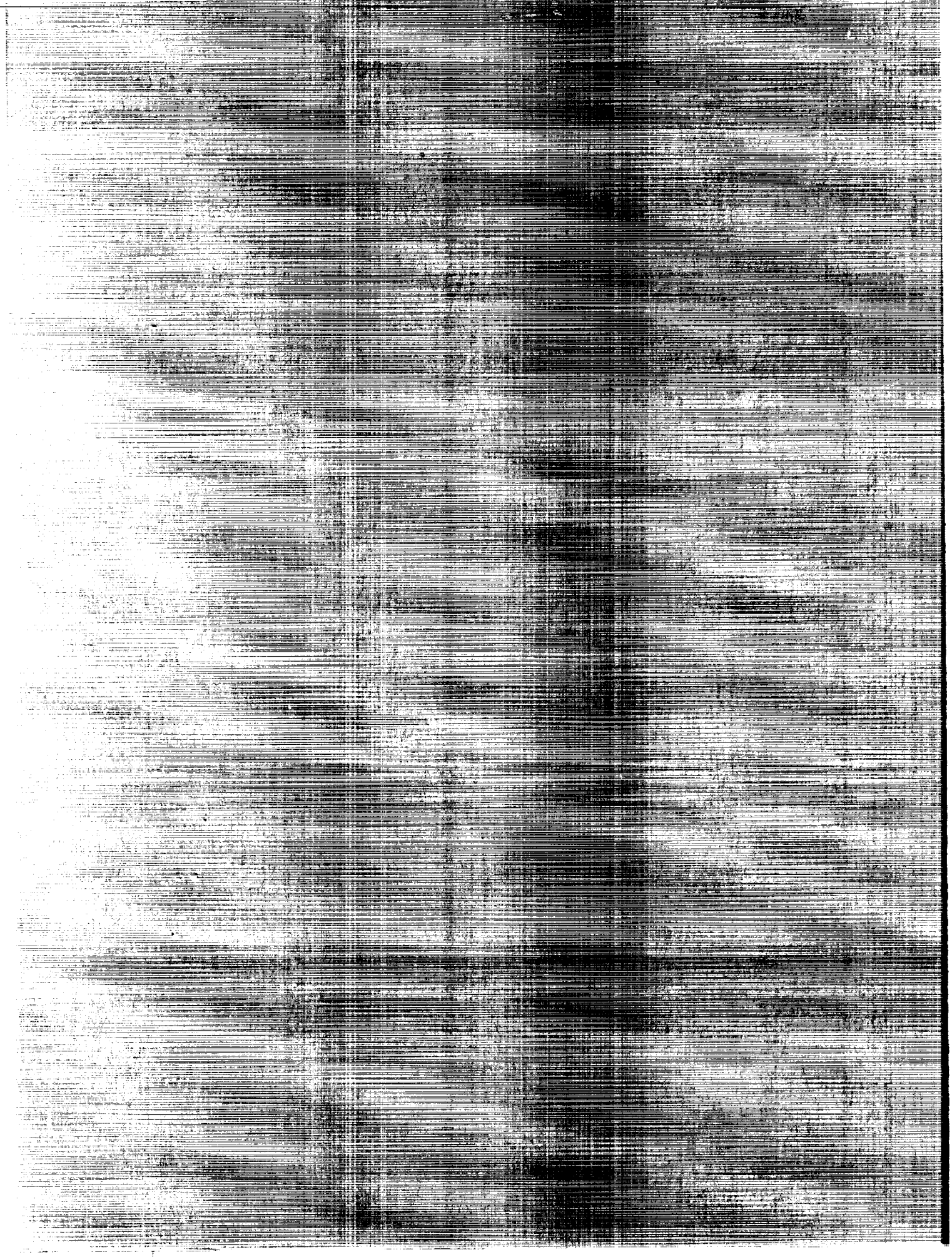

1. Report No.	2. Government Accession No.	3. Recipient's Catalog No.
NASA TM X-2367		

4. Title and Subtitle	5. Report Date
LONGITUDINAL AERODYNAMIC CHARACTERISTICS AT MACH 1.50 TO 4.63 OF A MISSILE MODEL EMPLOYING VARIOUS CANARDS AND A TRAILING-EDGE FLAP CONTROL	October 1971
	6. Performing Organization Code
7. Author(s)	8. Performing Organization Report No.
Charles D. Trescot, Jr.	L-6163
9. Performing Organization Name and Address	10. Work Unit No.
NASA Langley Research Center Hampton, Va. 23365	760-74-01-03
	11. Contract or Grant No.
12. Sponsoring Agency Name and Address	13. Type of Report and Period Covered
National Aeronautics and Space Administration Washington, D.C. 20546	Technical Memorandum
	14. Sponsoring Agency Code

15. Supplementary Notes

16. Abstract

An investigation has been made in the Langley Unitary Plan wind tunnel to determine the static longitudinal stability and control characteristics of a missile configuration with cruciform delta wings and various horizontal canards. The controls consisted of three different trapezoidal canards and a wing trailing-edge flap located on the horizontal wings only. The tests were made at Mach numbers from 1.50 to 4.63, through an angle-of-attack range from about -4° to 30°, at an angle of sideslip of 0°, and at a Reynolds number of 8.20×10^6 per meter (2.5×10^6 per foot).

The results are summarized in the form of various pertinent aerodynamic parameters as a function of Mach number. Although no detailed analysis of the results has been made, the summary of results is useful in demonstrating the importance of certain parameters and should be useful in providing a source of systematic experimental data for correlation with analytical techniques.

17. Key Words (Suggested by Author(s))	18. Distribution Statement
Missile controls Canard Flap	Unclassified – Unlimited

19. Security Classif. (of this report)	20. Security Classif. (of this page)	21. No. of Pages	22. Price*
Unclassified	Unclassified	113	$3.00

*For sale by the National Technical Information Service, Springfield, Virginia 22151

LONGITUDINAL AERODYNAMIC CHARACTERISTICS AT MACH 1.50 TO 4.63 OF A MISSILE MODEL EMPLOYING VARIOUS CANARDS AND A TRAILING-EDGE FLAP CONTROL

By Charles D. Trescot, Jr.
Langley Research Center

SUMMARY

An investigation has been made in the Langley Unitary Plan wind tunnel to determine the static longitudinal stability and control characteristics of a missile configuration with cruciform delta wings and various horizontal canards. The controls consisted of three different trapezoidal canards and a wing trailing-edge flap located on the horizontal wings only. The tests were made at Mach numbers from 1.50 to 4.63, through an angle-of-attack range from about -4° to 30°, at an angle of sideslip of 0°, and at a Reynolds number of 8.20×10^6 per meter (2.5×10^6 per foot).

The results are summarized in the form of various pertinent aerodynamic parameters as a function of Mach number. Although no detailed analysis of the results has been made, the summary of results is useful in demonstrating the importance of certain parameters and should be useful in providing a source of systematic experimental data for correlation with analytical techniques.

INTRODUCTION

The National Aeronautics and Space Administration has investigated various types of controls and lifting surfaces for supersonic and hypersonic missiles to determine their effectiveness in providing maneuverability through a range of Mach numbers. (See refs. 1 to 31.) For these missile configurations, both canard controls and tail controls, either in line or interdigitated with respect to the wings, are employed to provide the maneuvering capability. Generally, the missile lifting surfaces are low-aspect-ratio wings which offer advantages such as small center-of-pressure travel, low drag penalty, and minimum space for stowage.

The present investigation was undertaken to determine the static aerodynamic stability and control characteristics of a missile configuration with cruciform delta wings swept 72.9° and various in-line horizontal canards. The controls consisted of various interchangeable trapezoidal canards and a wing trailing-edge flap on the horizontal wings

only. The configuration was identical with that of reference 14, which was tested at $M = 2.01$ only.

The present tests were conducted in the Langley Unitary Plan wind tunnel and extend the Mach number range from 1.50 to 4.63 through an angle-of-attack range from about -4° to 30°. The Reynolds number was 8.20×10^6 per meter (2.5×10^6 per foot).

SYMBOLS

Values are given both in the International System of Units (SI) and in the U.S. Customary Units. Measurements were made in U.S. Customary Units. The force and moment coefficients are referenced to both the body and stability axes. The coordinate origin was taken on the body axis of symmetry at a point 64.35 percent of the body length from the nose.

A cross-sectional area of body

b_c canard span

C_A axial-force coefficient, $\frac{\text{Axial force}}{qA}$

$C_{A,b}$ base axial-force coefficient, $\frac{\text{Base axial force}}{qA}$

C_D drag coefficient, $\frac{\text{Drag}}{qA}$

C_L lift coefficient, $\frac{\text{Lift}}{qA}$

C_m pitching-moment coefficient, $\frac{\text{Pitching moment}}{qA\ell}$

C_{m_α} longitudinal stability parameter measured near zero angle of attack

$C_{m_{\delta,c}}$ pitch-control effectiveness of canards measured between control deflections of 0° and 20° at zero angle of attack, per degree

$C_{m_{\delta,f}}$ pitch-control effectiveness of wing trailing-edge flap measured between control deflections of 0° and -20° at zero angle of attack, per degree

C_N normal-force coefficient, $\frac{\text{Normal force}}{qA}$

C_{N_α} normal-force-curve slope measured near zero angle of attack, per degree

d body diameter

l length of body

L/D lift-drag ratio

M free-stream Mach number

q free-stream dynamic pressure

r radius

$\frac{x_{a.c.}}{l}$ aerodynamic-center location referenced to body length (positive rearward)

α angle of attack of body center line, degrees

δ_c canard deflection with respect to body center line, positive trailing edge down, degrees

δ_f flap deflection with respect to wing-chord plane, positive trailing edge down, degrees

Model-component designations:

B body

C_1, C_2, C_3 canard surfaces (horizontal only, fig. 1)

W wing

MODEL

A drawing of the model with pertinent dimensions is shown in figure 1 and a photograph of the model is shown as figure 2. The geometric characteristics of the model are given in table I.

The body was composed of a modified ogive forebody and a cylindrical afterbody. The forebody, which had provisions for mounting the canard surfaces, had a rounded nose followed by a conical taper which faired into the ogive section. The ratio of overall length to diameter was 8.67.

Both the wings and the canards were flat plates with wedge-shaped leading and trailing edges. The cruciform wings had a delta planform and a leading-edge sweep of 72.9°. The area of the plain rectangular flaps, which were located on the trailing edge of the horizontal wings only, was 11.53 percent of the exposed wing area. Provisions were made for manual variation of the deflection angle of these flaps from 0° to -30° in 10° increments.

Three different canards, each having a trapezoidal planform and a common hinge line (10.54 percent of the body length), were employed for pitch control only in the plane of the horizontal wings. (See fig. 1.) Provisions were made to vary the canard deflection angles manually from 0° to 20° in 10° increments. Canard C_1 had an exposed area equal to 9.58 percent of the exposed wing area and a total span that was equal to the body diameter $\left(b_c/d = 1.0\right)$. Canard C_2 had an exposed area approximately the same as that of canard C_1 (9.77 percent of the exposed wing area) but had a greater span $\left(b_c/d = 1.47\right)$ and consequently a higher aspect ratio. Canard C_3 maintained the same aspect ratio as canard C_2 but had an exposed area that was approximately 50 percent larger (15.23 percent of the exposed wing area) than that of canard C_2 and a larger span $\left(b_c/d = 1.67\right)$.

APPARATUS AND TESTS

The tests were made in both the low and high Mach number test sections of the Langley Unitary Plan wind tunnel. The test sections are approximately 1.22 meters (4 feet) square and 2.13 meters (7 feet) long. The nozzles leading to the test section are of the asymmetric-sliding-block type; this allows continuous variation in Mach number from about 1.5 to 2.9 in the low Mach number test section and from about 2.3 to 4.7 in the high Mach number test section. For the present tests, the Mach numbers, stagnation pressures, and stagnation temperatures were as follows:

M	Stagnation pressure		Stagnation temperature	
	kN/m^2	lb/ft^2	^oK	^oF
1.50	66.60	1391	339	150
1.90	75.94	1586		
2.30	93.61	1955		
2.96	129.75	2710		
3.95	229.35	4790	353	175
4.63	315.05	6580		

The stagnation dewpoint was maintained sufficiently low (238.7° K (-30° F)) to insure negligible condensation effects in the test section. The model was mounted on a six-component, internal, strain-gage balance which was sting supported in the tunnel. The tests were made through an angle-of-attack range from about -4° to 30° at a side-slip angle of 0° and at a Reynolds number of 8.20×10^6 per meter (2.5×10^6 per foot). The Reynolds number based on body length was 5.42×10^6. The angles of attack have been corrected for sting and balance deflection due to aerodynamic loads and for tunnel airflow misalinement. The axial-force and drag data have been adjusted to a condition of free-stream static pressure at the model base. Typical variations of base axial-force coefficient as a function of angle of attack at the test Mach numbers are shown in figure 3 for several configurations.

Tests were made to determine the control effectiveness of the canards and the wing trailing-edge flaps separately. In addition, tests were made to evaluate the effects of the various components on the aerodynamic characteristics of the model. All tests were made with the boundary-layer transition point fixed by means of roughness strips. The leading edges of the 0.16-cm-wide $\left(\frac{1}{16}\text{-inch}\right)$ transition strips were located about 3.05 cm (1.2 inches) aft of the body nose and 1.02 cm (0.4 inch) streamwise behind the leading edges of the wings and canards. All roughness strips were composed of carborundum grains having a nominal diameter of 0.030 cm (0.012 inch).

PRESENTATION OF RESULTS

The results of the investigation are presented in the following figures:

SUMMARY OF RESULTS

The longitudinal aerodynamic characteristics of the models as affected by the various components are summarized in figure 7 for the test Mach number range. The addition of canard C_1 to the body alone resulted in essentially a constant increase in C_{N_α} throughout the test Mach number range. Maintaining the area of C_1 but increasing the aspect ratio (canard C_2) resulted in a further increase in C_{N_α} except at the higher Mach numbers. Increasing the area of the canard (C_3) while maintaining the aspect ratio of C_2 led to increases in C_{N_α} across the Mach number range. The addition of the wing to the body provided the greatest increase in C_{N_α}, as would be expected. However, when any of the canards were added to the wing-body configuration, a decrement in C_{N_α} resulted throughout the test Mach number range. This decrease in C_{N_α} is a result of the interference flow field imposed on the wing by the canard. A decrease in stability ($+C_{m_\alpha}$) always results from addition of the canards, whereas the addition of the wing always provides a stabilizing increment ($-C_{m_\alpha}$). The aerodynamic-center location as a fraction of body length is shown in figure 7(b).

For the canard-body configurations, there is little change in C_A or C_{N_α} (fig. 7(a)) with increasing Mach number as contrasted to the wing-body-canard configurations where C_A and C_{N_α} decrease with increasing Mach number.

Figures 8, 9, and 10 present the control-deflection data for canards C_1, C_2, and C_3, respectively, and for the trailing-edge flap at $\delta_f = -20^\circ$. The data indicate reasonably linear variations of pitching moment with angle of attack for each configuration. The canards and the trailing-edge flaps are effective pitch-control devices, although the effectiveness $\left(C_{m_{\delta,c}}\right)$ for the canards tested is somewhat greater than for the trailing-edge flap (fig. 13). The control effectiveness of canard C_1 is less than that of canards C_2 and C_3 but remains essentially invariant with Mach number, whereas the control effectiveness for canards C_2 and C_3 and for the trailing-edge flap decreases appreciably with Mach number. (See fig. 13.)

A comparison of the wing trailing-edge flap control with the canard off (fig. 11) and with canards on (figs. 8, 9, 10, and 12) indicates little or no effect of the canards on the flap-control effectiveness.

Deflection of the trailing-edge flap to trim results in a decrement in lift, but deflection of the canard to trim is such that a positive lift increment generally occurs.

Langley Research Center,
National Aeronautics and Space Administration,
Hampton, Va., August 24, 1971.

REFERENCES

1. Spearman, M. Leroy: Aerodynamic Characteristics in Pitch of a Series of Cruciform-Wing Missiles With Canard Controls at a Mach Number of 2.01. NASA TN D-839, 1961. (Supersedes NACA RM L53I14.)

2. Spearman, M. Leroy: Component Tests To Determine the Aerodynamic Characteristics of an All-Movable 70° Delta Canard-Type Control in the Presence of a Body at a Mach Number of 1.61. NACA RM L53I03, 1953.

3. Spearman, M. Leroy: Effect of Large Deflections of a Canard Control and Deflections of a Wing-Tip Control on the Static-Stability and Induced-Roll Characteristics of a Cruciform Canard Missile at a Mach Number of 2.01. NACA RM L53K03, 1953.

4. Spearman, M. Leroy; and Robinson, Ross B.: Aerodynamic Characteristics of a Cruciform-Wing Missile With Canard Control Surfaces and of Some Very Small Span Wing-Body Missiles at a Mach Number of 1.41. NACA RM L54B11, 1954.

5. Spearman, M. Leroy; and Driver, Cornelius: Wind-Tunnel Investigation at a Mach Number of 2.01 of the Aerodynamic Characteristics in Combined Pitch and Sideslip of Some Canard-Type Missiles Having Cruciform Wings and Canard Surfaces With 70° Delta Plan Forms. NACA RM L54F09, 1954.

6. Robinson, Ross B.: Aerodynamic Characteristics of Missile Configurations With Wings of Low Aspect Ratio for Various Combinations of Forebodies, Afterbodies, and Nose Shapes for Combined Angles of Attack and Sideslip at a Mach Number of 2.01. NACA RM L57D19, 1957.

7. Robinson, Ross B.: Wind-Tunnel Investigation at a Mach Number of 2.01 of the Aerodynamic Characteristics in Combined Angles of Attack and Sideslip of Several Hypersonic Missile Configurations With Various Canard Controls. NACA RM L58A21, 1958.

8. Katzen, Elliott D.; and Jorgensen, Leland H.: Aerodynamics of Missiles Employing Wings of Very Low Aspect Ratio. NACA RM A55L13b, 1956.

9. Foster, Gerald V.: Sideslip Characteristics at Various Angles of Attack for Several Hypersonic Missile Configurations With Canard Controls at a Mach Number of 2.01. NASA TM X-134, 1959.

10. Stone, David G.: Maneuver Performance of Interceptor Missiles. NACA RM L58E02, 1958.

11. Spearman, M. Leroy; and Robinson, Ross B.: Longitudinal Stability and Control Characteristics at Mach Numbers of 2.01, 4.65, and 6.8 of Two Hypersonic Missile Configurations, One Having Low-Aspect-Ratio Cruciform Wings With Trailing-Edge Flaps and One Having a Flared Afterbody and All-Movable Controls. NASA TM X-46, 1959.

12. Robinson, Ross B.; and Bernot, Peter T.: Aerodynamic Characteristics at a Mach Number of 6.8 of Two Hypersonic Missile Configurations, One With Low-Aspect-Ratio Cruciform Fins and Trailing-Edge Flaps and One With a Flared Afterbody and All-Movable Controls. NACA RM L58D24, 1958.

13. Church, James D.; and Kirkland, Ida M.: Static Aerodynamic Characteristics of Several Hypersonic Missile-and-Control Configurations at a Mach Number of 4.65. NASA TM X-187, 1960.

14. Robinson, Ross B.; and Spearman, M. Leroy: Aerodynamic Characteristics for Combined Angles of Attack and Sideslip of a Low-Aspect-Ratio Cruciform-Wing Missile Configuration Employing Various Canard and Trailing-Edge Flap Controls at a Mach Number of 2.01. NASA MEMO 10-2-58L, 1958.

15. Robinson, Ross B.; and Foster, Gerald V.: Static Longitudinal Stability and Control Characteristics at a Mach Number of 2.01 of a Hypersonic Missile Configuration Having All-Movable Wing and Tail Surfaces. NASA TM X-516, 1961.

16. Spearman, M. Leroy; and Robinson, Ross B.: Longitudinal Stability and Control Characteristics of a Winged and a Flared Hypersonic Missile Configuration With Various Nose Shapes and Flare Modifications at a Mach Number of 2.01. NASA TM X-693, 1962.

17. Corlett, William A.; and Fuller, Dennis E.: Aerodynamic Characteristics at Mach 1.60, 2.00, and 2.50 of a Cruciform Missile Configuration With In-Line Tail Controls. NASA TM X-1112, 1965.

18. Fuller, Dennis E.; and Corlett, William A.: Supersonic Aerodynamic Characteristics of a Cruciform Missile Configuration With Low-Aspect-Ratio Wings and In-Line Tail Controls. NASA TM X-1025, 1964.

19. Foster, Gerald V.; and Corlett, William A.: Aerodynamic Characteristics at Mach Numbers From 0.40 to 2.86 of a Missile Model Having All-Movable Wings and Interdigitated Tails. NASA TM X-1184, 1965.

20. Hayes, Clyde; and Fournier, Roger H.: Effect of Fin-Flare Combinations on the Aerodynamic Characteristics of a Body at Mach Numbers 1.61 and 2.20. NASA TN D-2623, 1965.

21. Corlett, William A.; and Richardson, Celia S.: Effect of First-Stage Geometry on Aerodynamic Characteristics in Pitch of Two-Stage Rocket Vehicles From Mach 1.57 to 2.86. NASA TN D-2709, 1965.

22. Corlett, William A.: Aerodynamic Characteristics of a Maneuverable Missile With Cruciform Wings and In-Line Canard Surfaces at Mach Numbers From 0.50 to 4.63. NASA TM X-1309, 1966.

23. Spearman, M. Leroy; and Corlett, William A.: Aerodynamic Characteristics at Mach Numbers of 3.95 and 4.63 for a Missile Model Having All-Movable Wings and Interdigitated Tails. NASA TM X-1332, 1967.

24. Spearman, M. Leroy; and Corlett, William A.: Aerodynamic Characteristics at Mach Numbers From 1.50 to 4.63 of a Maneuverable Missile With In-Line Cruciform Wings and Canard Surfaces. NASA TM X-1352, 1967.

25. Spearman, M. Leroy; and Corlett, William A.: Aerodynamic Characteristics of a Winged Cruciform Missile Configuration With Aft Tail Controls at Mach Numbers From 1.60 to 4.63. NASA TM X-1416, 1967.

26. Hayes, Clyde: Supersonic Aerodynamic Characteristics of a Model of an Air-to-Ground Missile. NASA TM X-1491, 1968.

27. Fuller, Dennis E.; and Richardson, Celia S.: Aerodynamic Characteristics at Mach 2.50 of a Cruciform Missile Configuration With In-Line Inlets, Wings, and Tail Surfaces. NASA TM X-1492, 1968.

28. Corlett, William A.: Aerodynamic Characteristics of a Modified Missile Model With Trapezoidal Wings and Aft Tail Controls at Mach Numbers of 2.50 to 4.63. NASA TM X-1751, 1969.

29. Fuller, Dennis E.: Aerodynamic Characteristics of a Cruciform Winged Missile With Trailing-Edge Controls at Mach Numbers From 1.60 to 4.63. NASA TM X-1743, 1969.

30. Corlett, William A.: Aerodynamic Characteristics of a Modified Missile Model With Cruciform Wings and In-Line Tail Controls at Mach 1.60 to 4.63. NASA TM X-1805, 1969.

31. Spearman, M. Leroy; and Trescot, Charles D., Jr.: Effects of Wing Planform on the Static Aerodynamics of a Cruciform Wing-Body Missile for Mach Numbers Up to 4.63. NASA TM X-1839, 1969.

TABLE I.- GEOMETRIC CHARACTERISTICS OF MODEL

Body:		
Length, cm (in.)	66.04	(26.00)
Diameter, cm (in.)	7.62	(3.00)
Cross-sectional area, cm^2 (in^2)	45.61	(7.07)
Length-diameter ratio	8.67	
Moment-center location, percent length	64.35	
Wing:		
Area, exposed, cm^2 (in^2)	335.48	(52.00)
Root chord, exposed, cm (in.)	33.02	(13.00)
Tip chord, cm (in.)	0.00	
Span, total, cm (in.)	27.94	(11.00)
Aspect ratio, exposed	1.23	
Leading-edge sweep, deg	72.90	
Ratio of total span to diameter	3.67	
Trailing-edge flaps:		
Span, each, cm (in.)	7.62	(3.00)
Chord, each, cm (in.)	2.54	(1.00)
Area, both, cm^2 (in^2)	38.71	(6.00)
Exposed wing area, percent	11.53	

Canards:

	C_1		C_2		C_3	
Area, exposed, cm^2 (in^2)	32.13	(4.98)	32.77	(5.08)	51.10	(7.92)
Total span, cm (in.)	7.62	(3.00)	11.18	(4.40)	12.70	(5.00)
Exposed wing area, percent	9.58		9.77		15.23	
Ratio of total span to diameter	1.00		1.47		1.67	
Hinge-line location, percent body length	10.54		10.54		10.54	

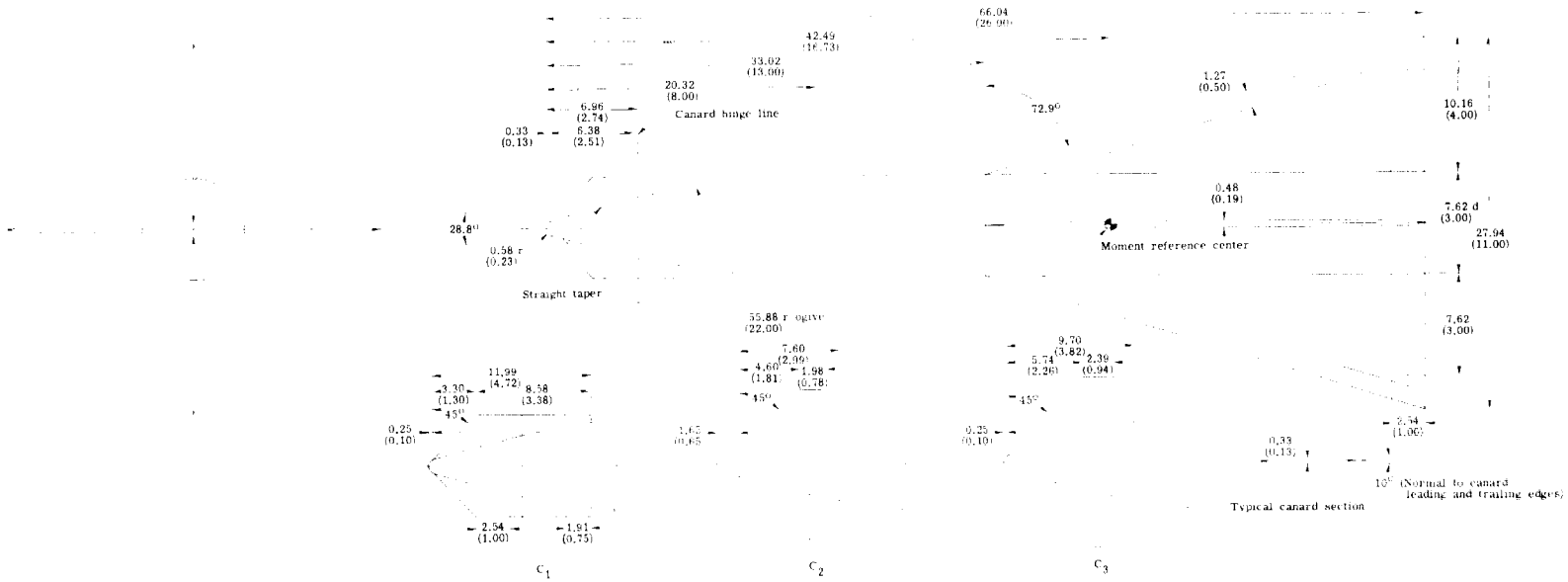

Figure 1.- Drawing of the model. All linear dimensions are in centimeters (inches).

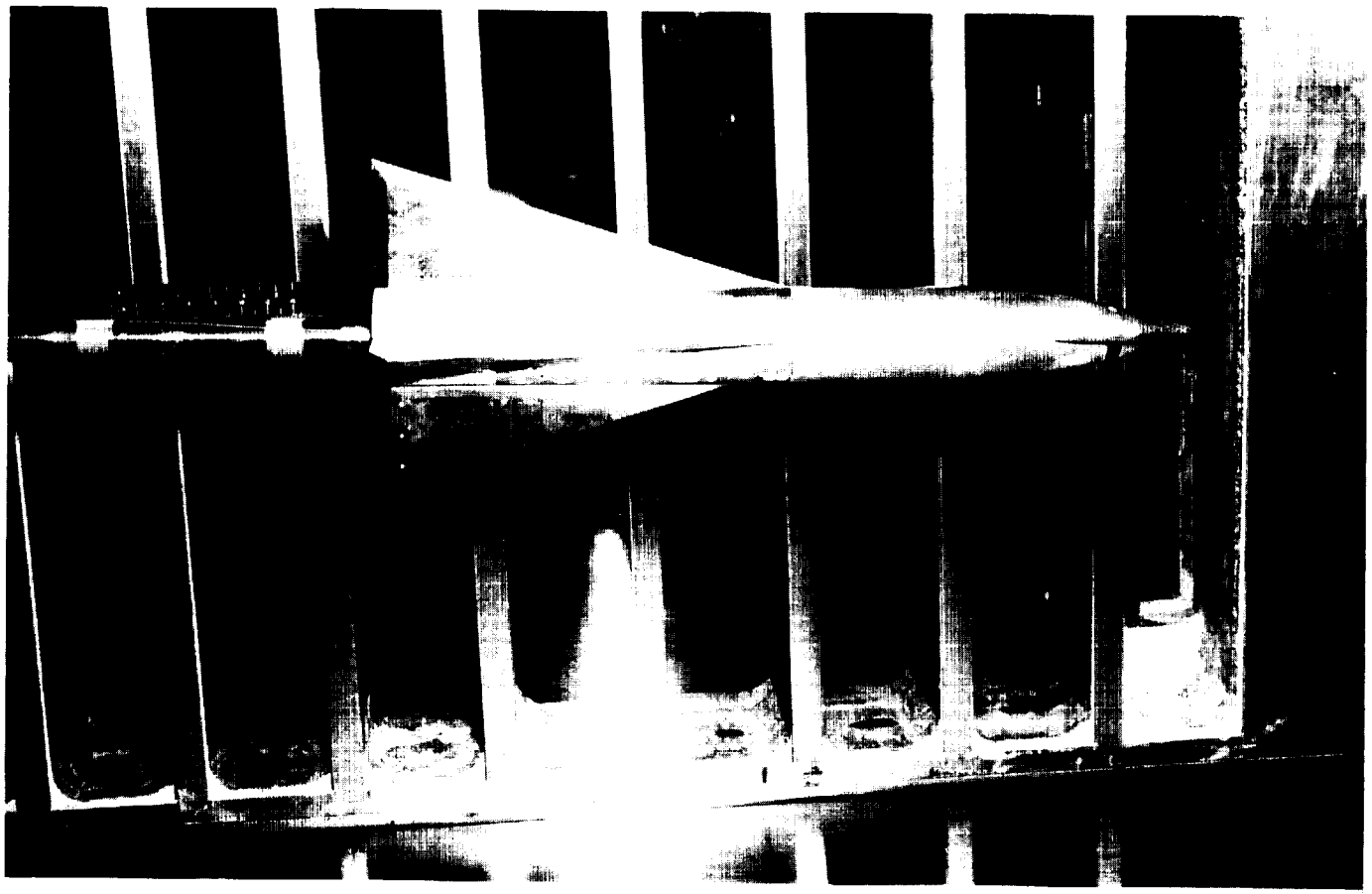

L-66-8195

Figure 2.- Model photograph.

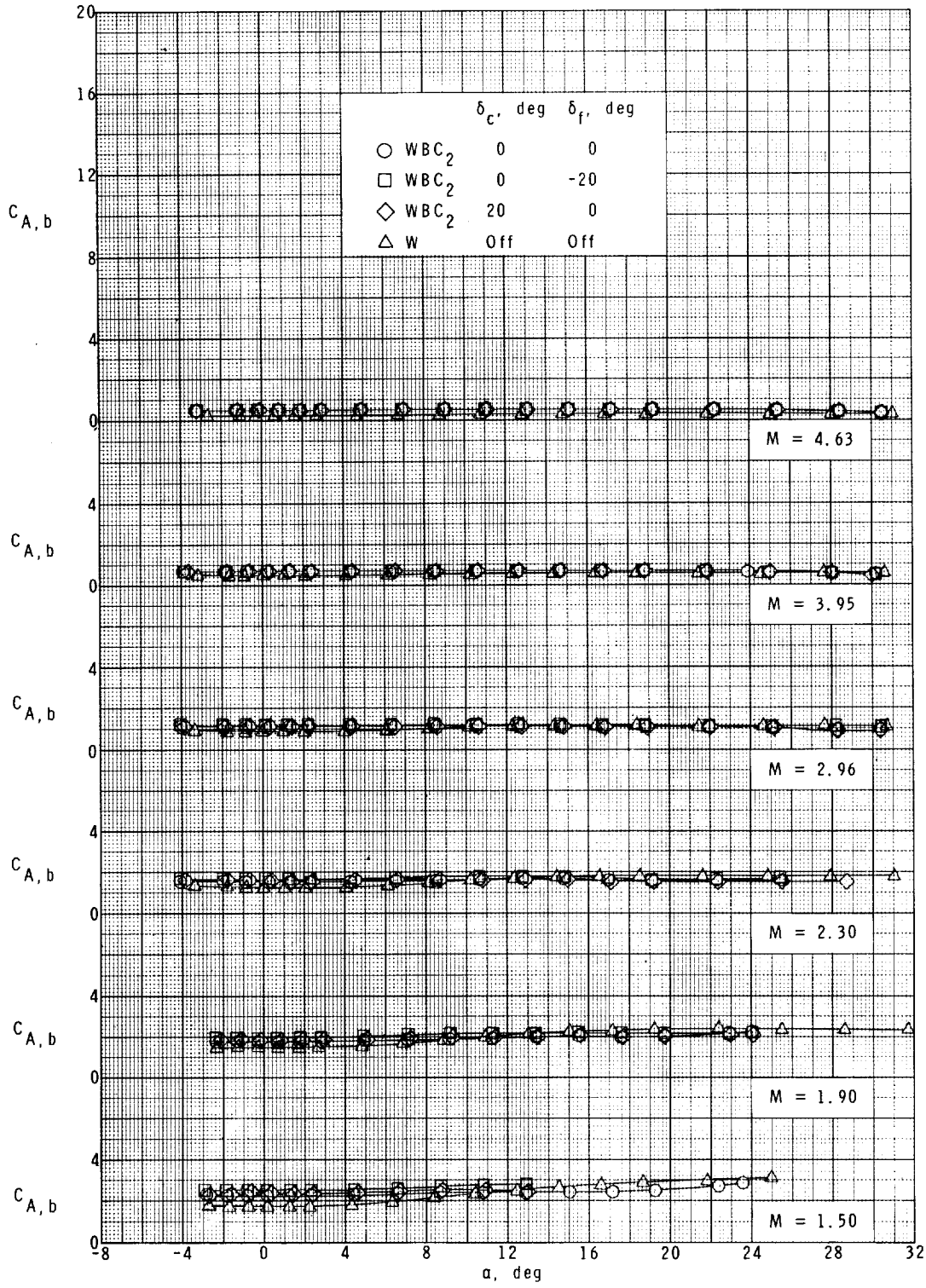

Figure 3.- Typical variations of base axial-force coefficient with angle of attack.

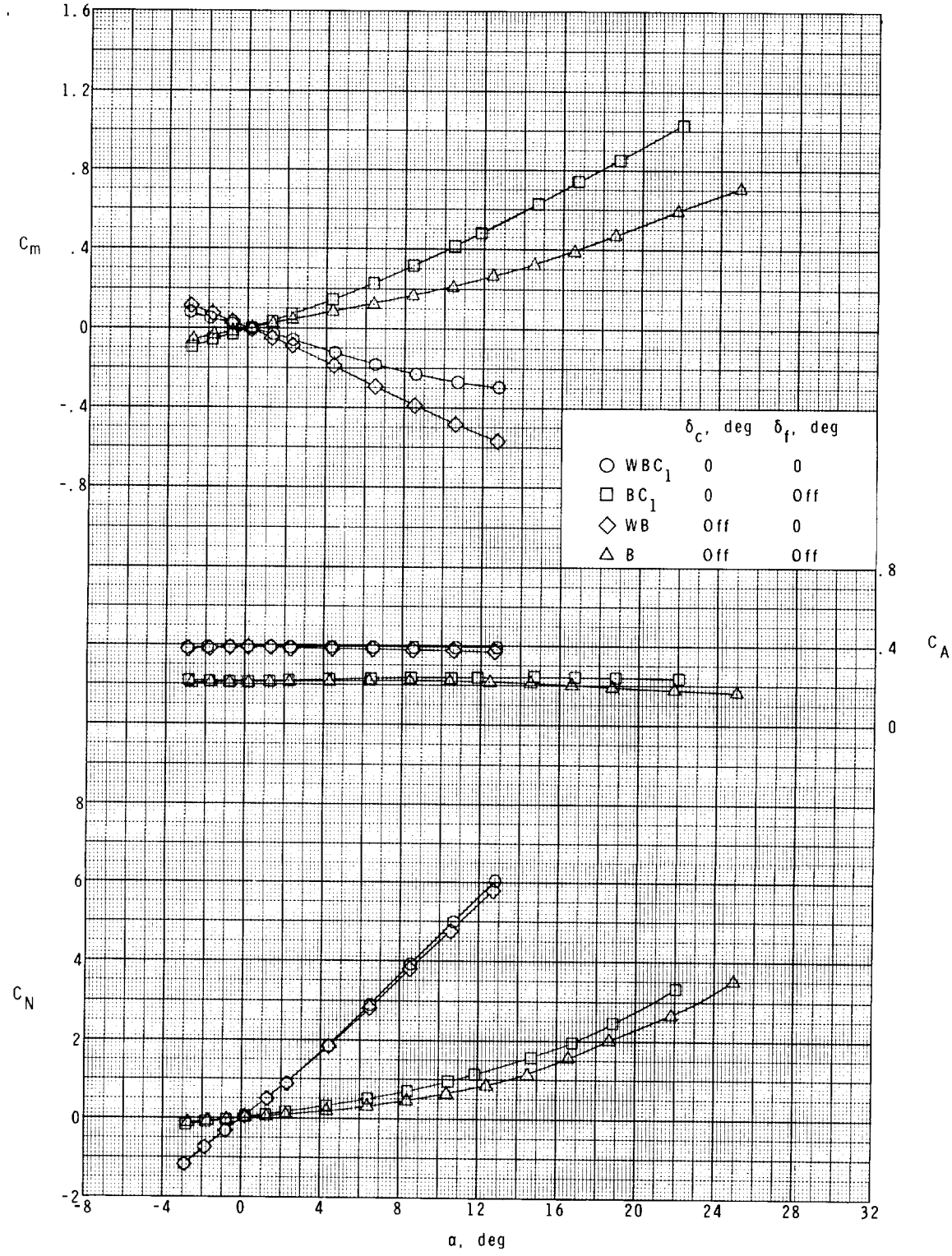

(a) M = 1.50.

Figure 4.- Effects of the wing and canard C_1 on the longitudinal aerodynamic characteristics of the model.

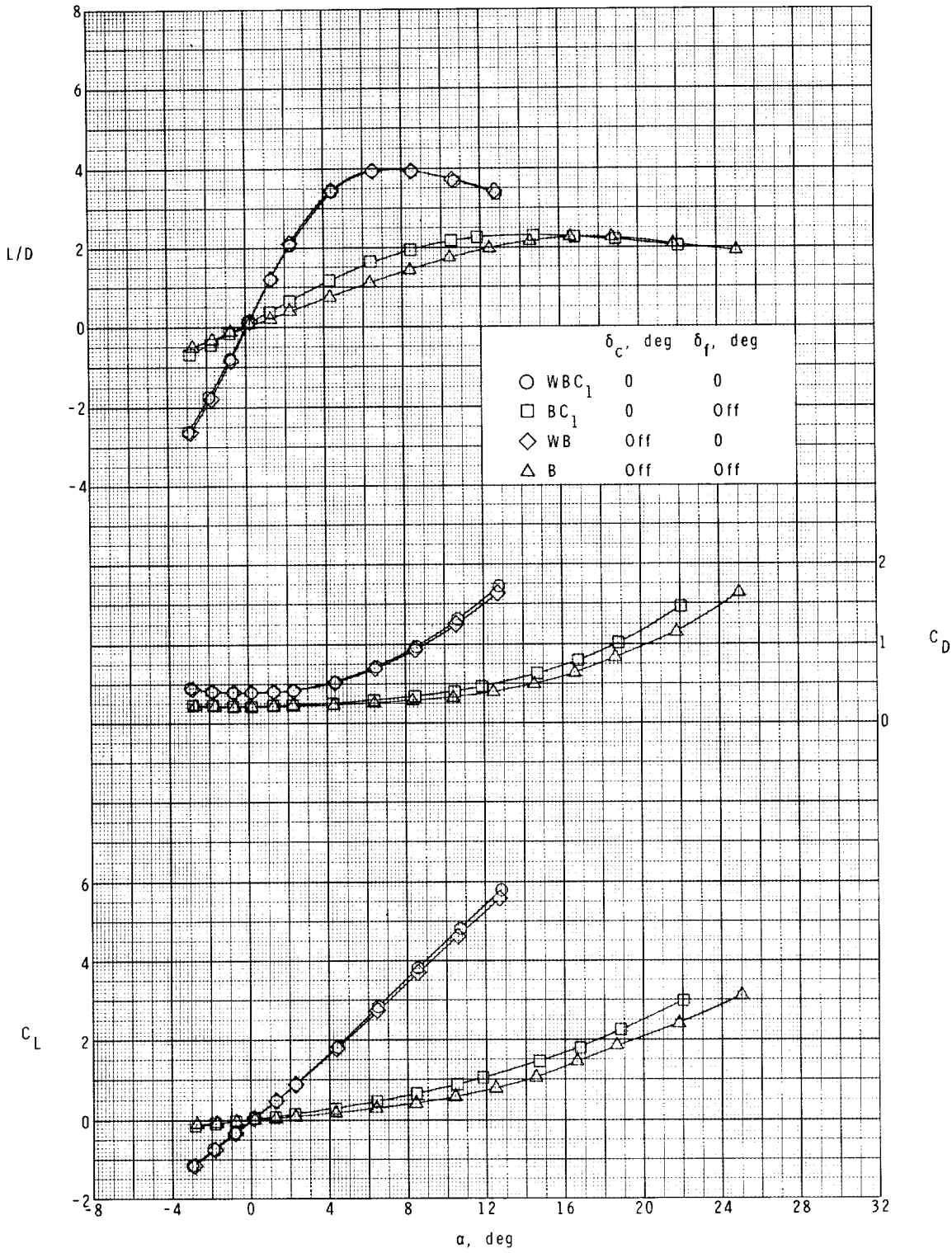

(a) Concluded.

Figure 4.- Continued.

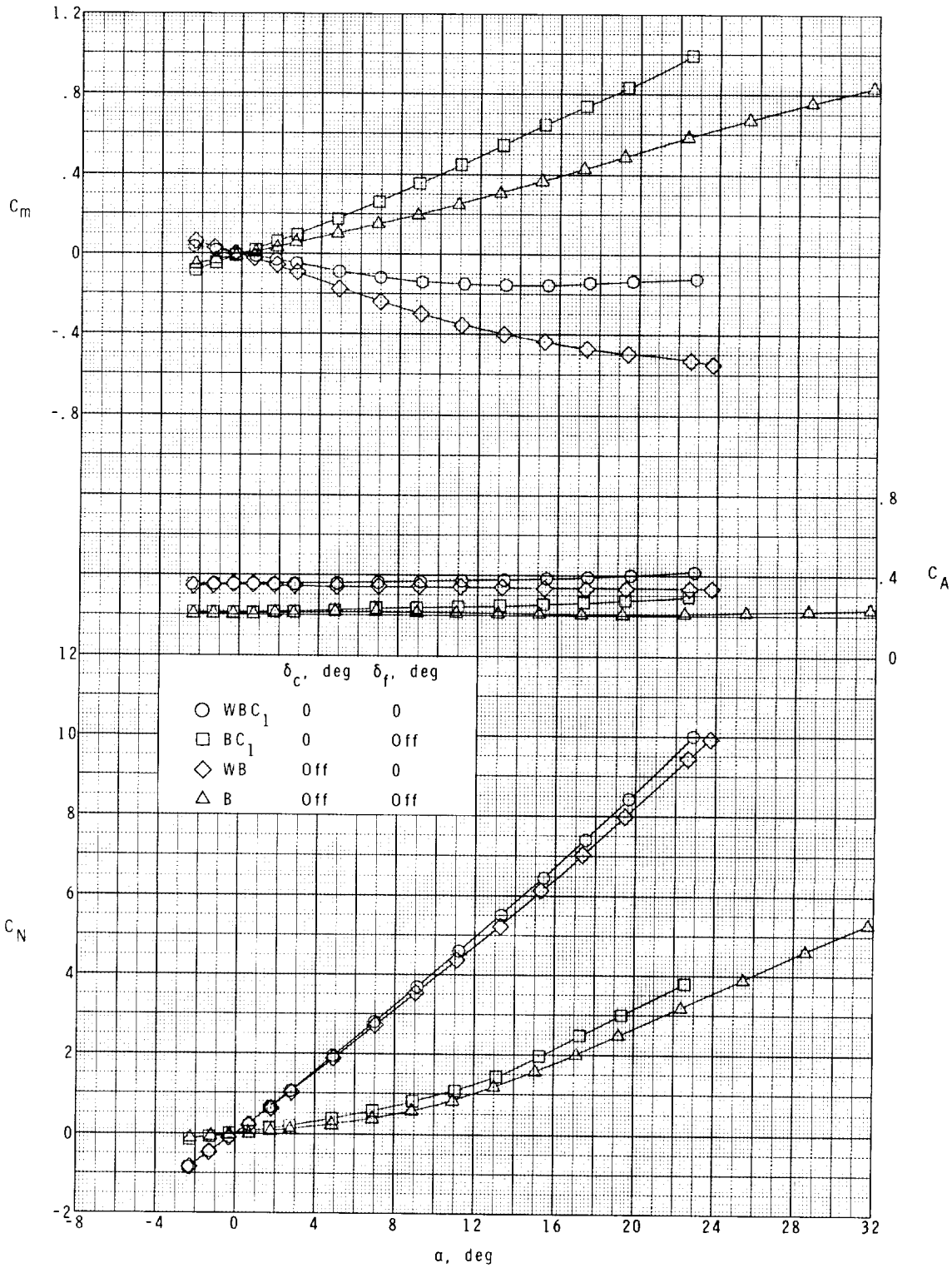

(b) M = 1.90.

Figure 4.- Continued.

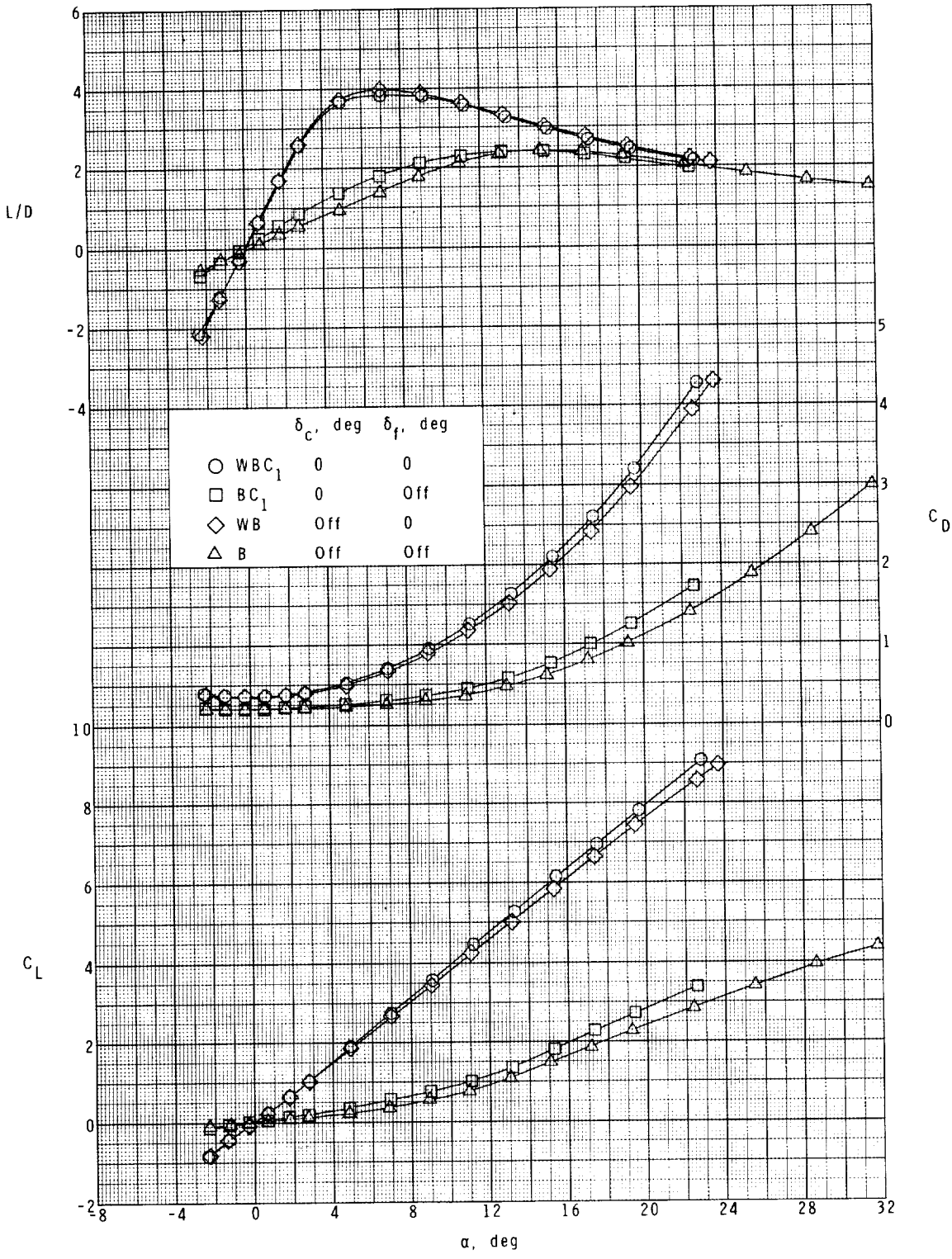

(b) Concluded.

Figure 4.- Continued.

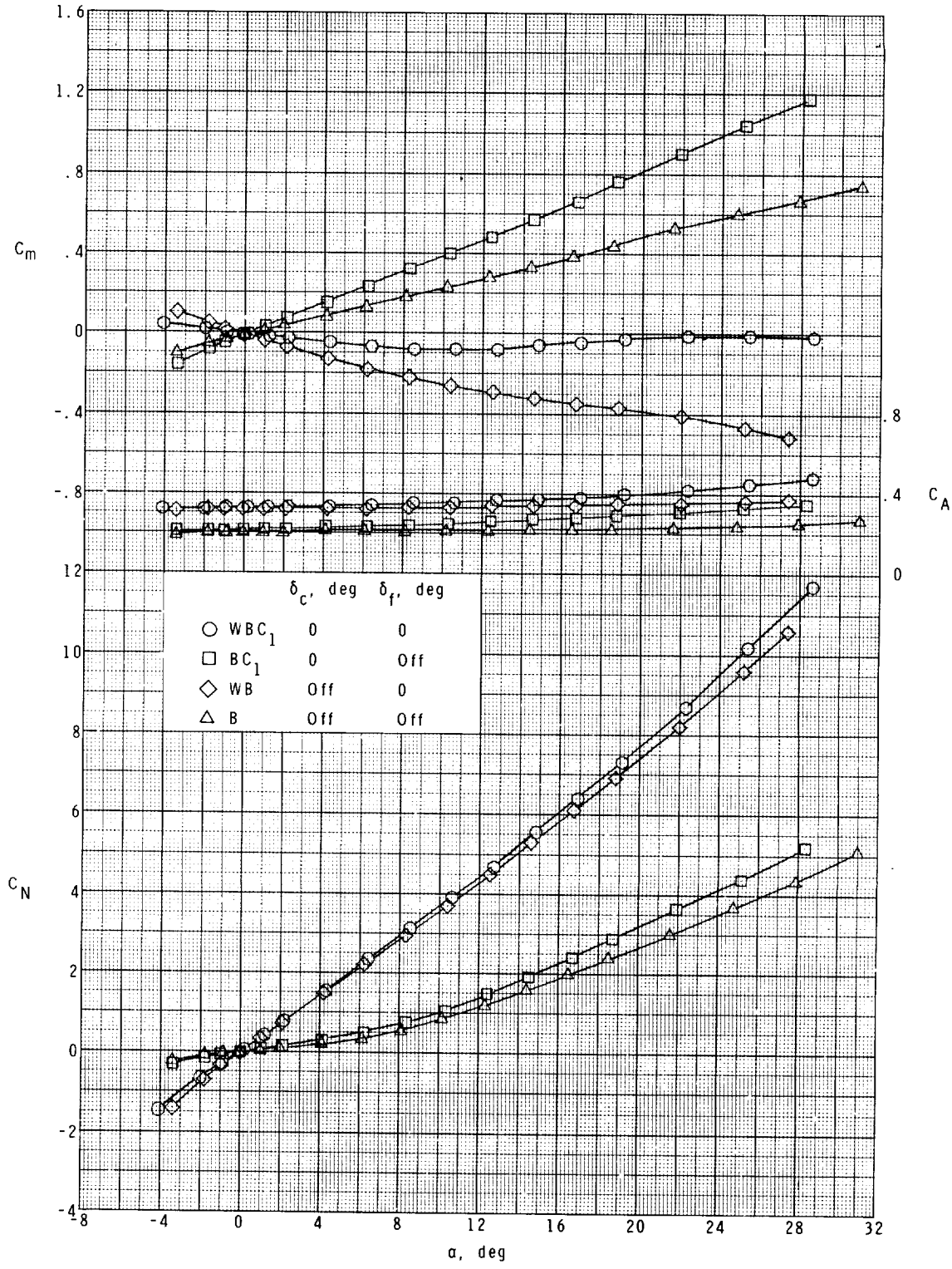

(c) M = 2.30.

Figure 4.- Continued.

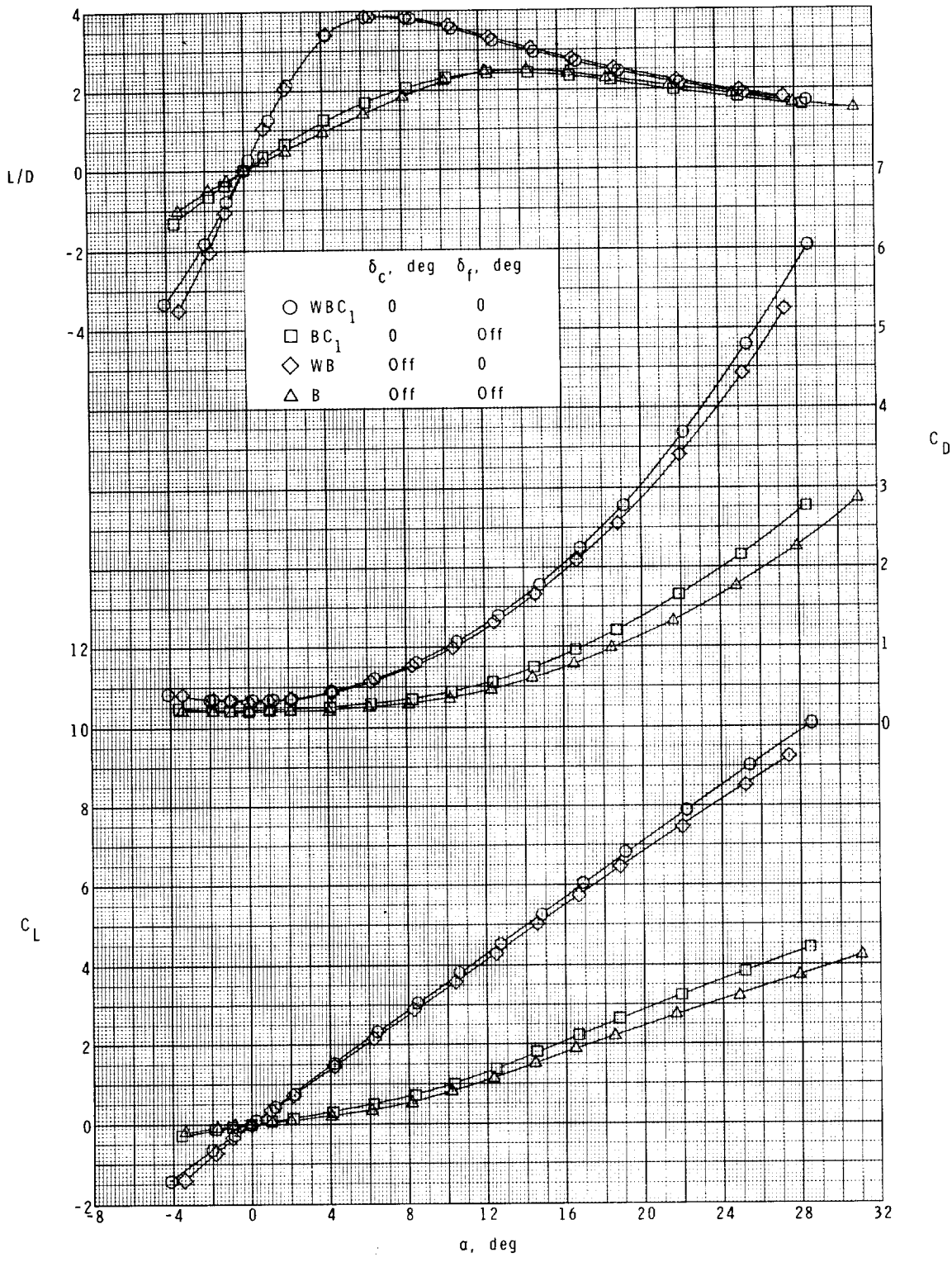

(c) Concluded.

Figure 4.- Continued.

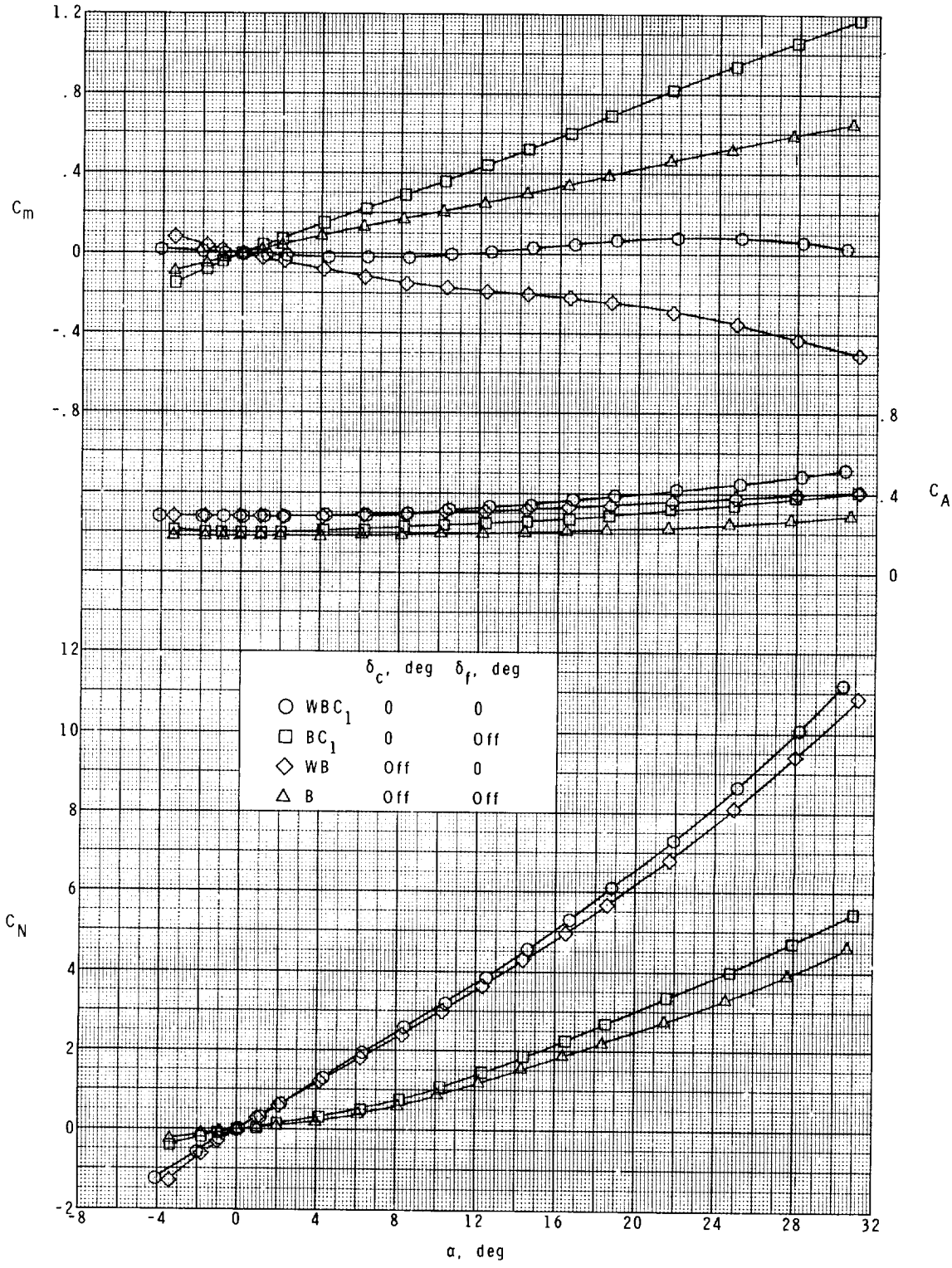

(d) M = 2.96.

Figure 4.- Continued.

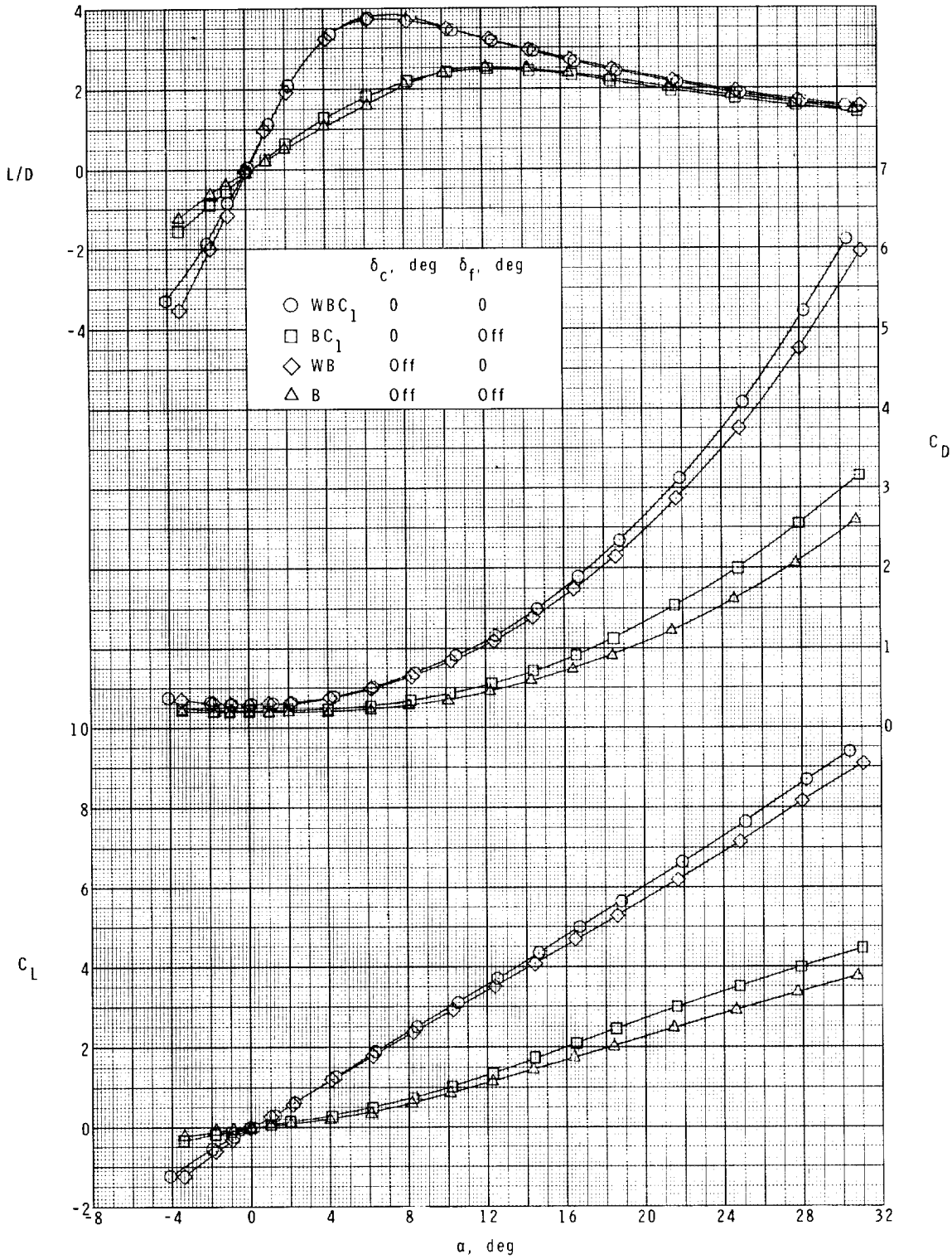

(d) Concluded.

Figure 4.- Continued.

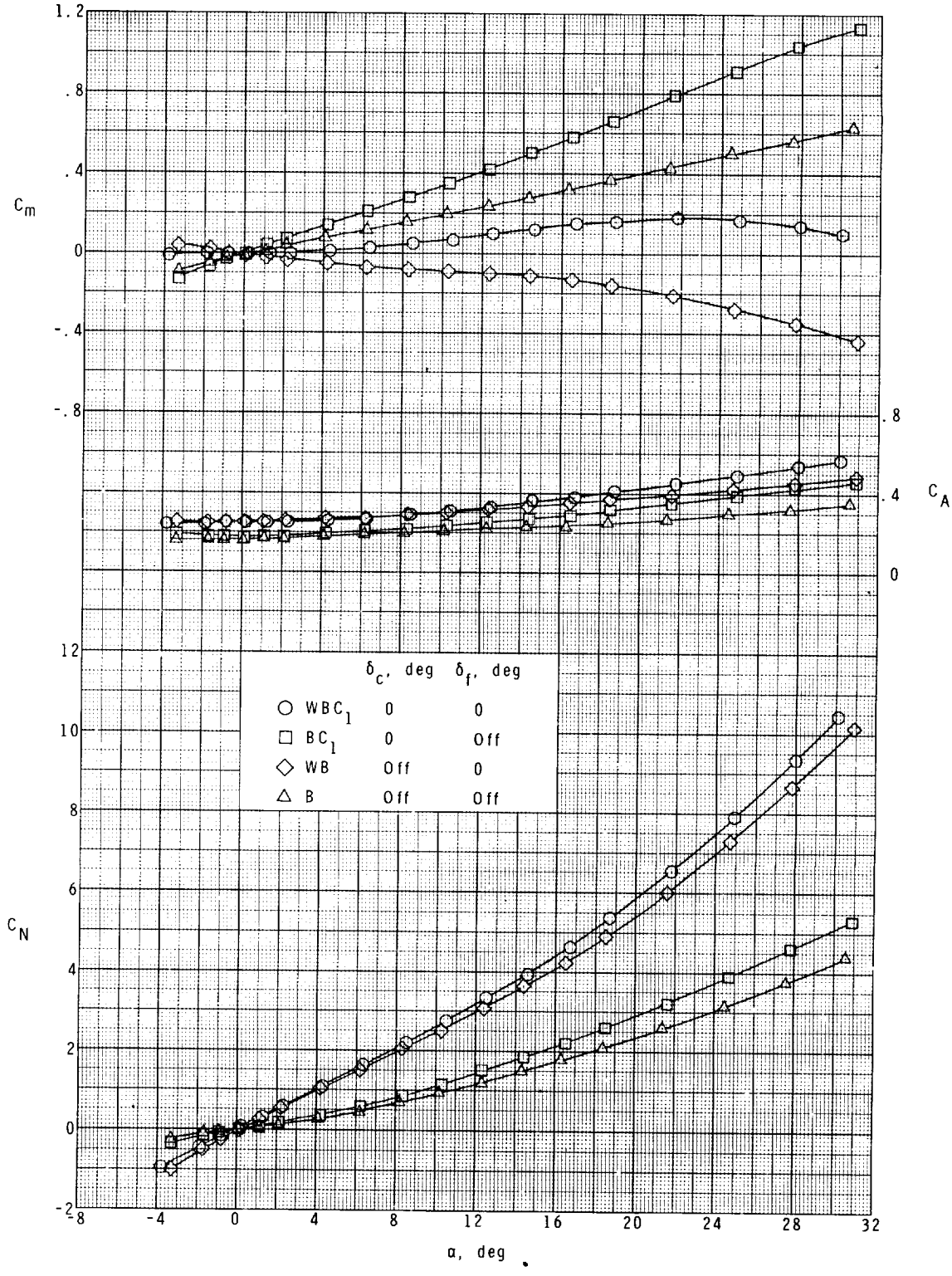

(e) M = 3.95.

Figure 4.- Continued.

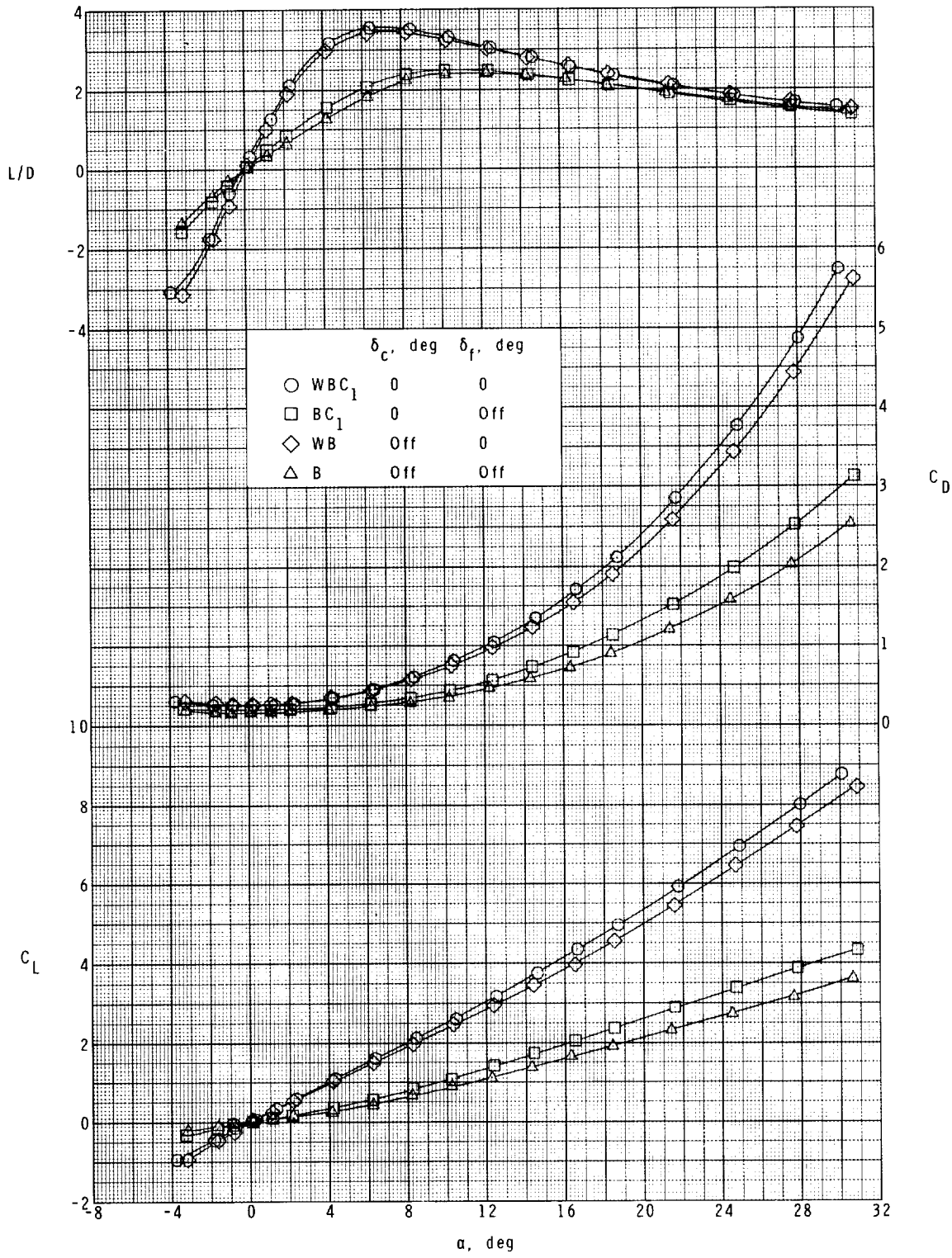

(e) Concluded.

Figure 4.- Continued.

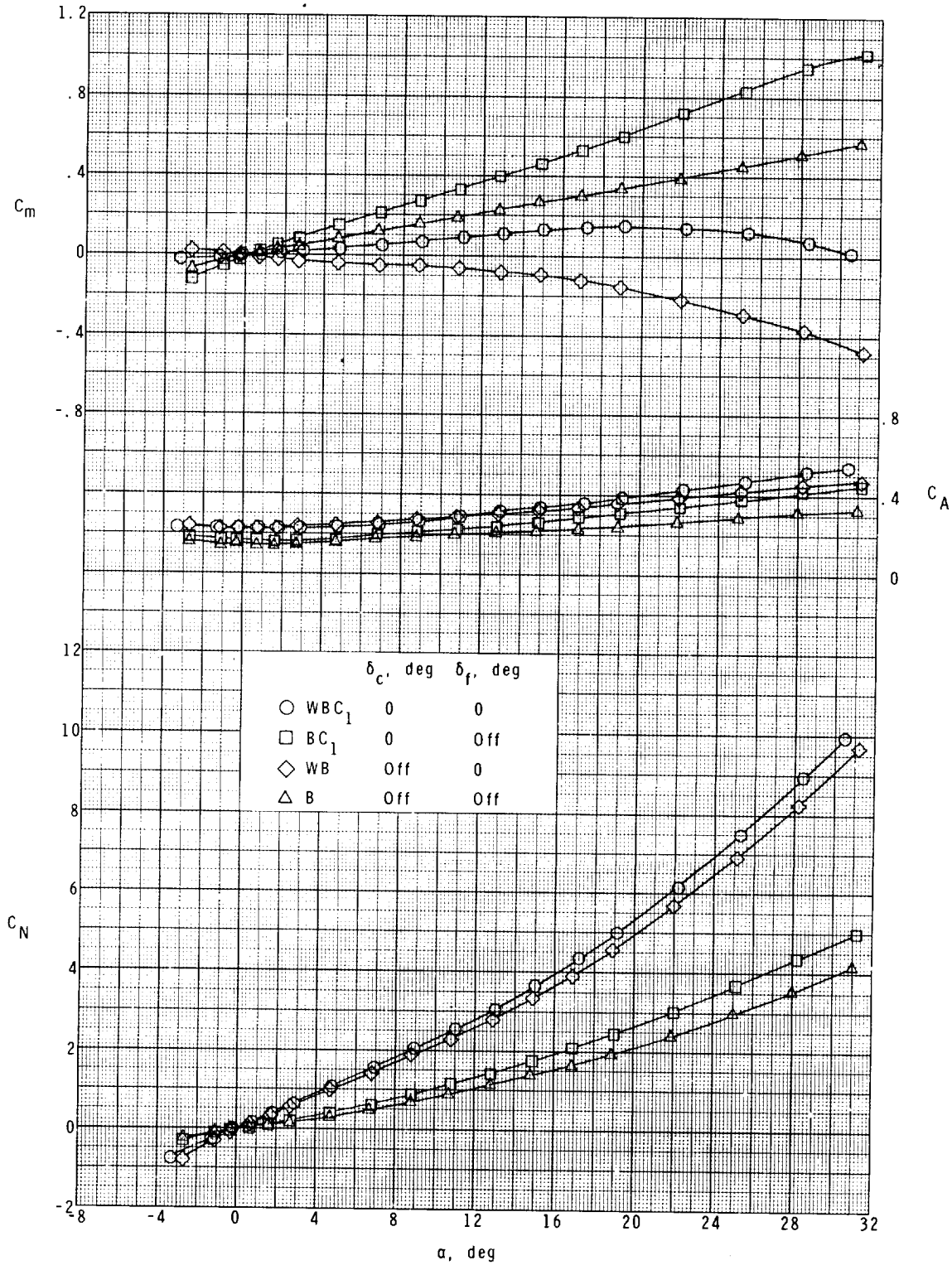

(f) M = 4.63.

Figure 4.- Continued.

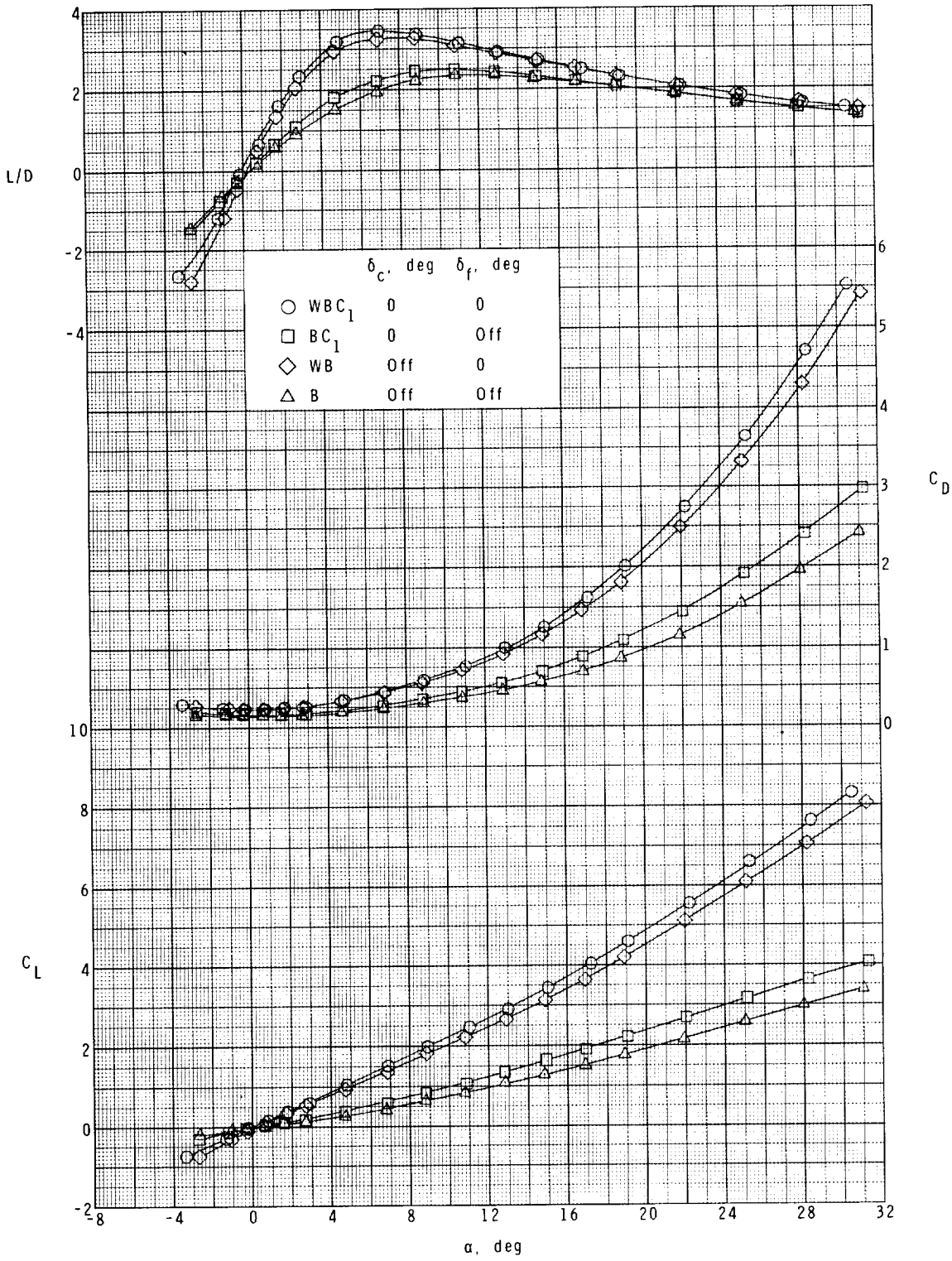

(f) Concluded.

Figure 4.- Concluded.

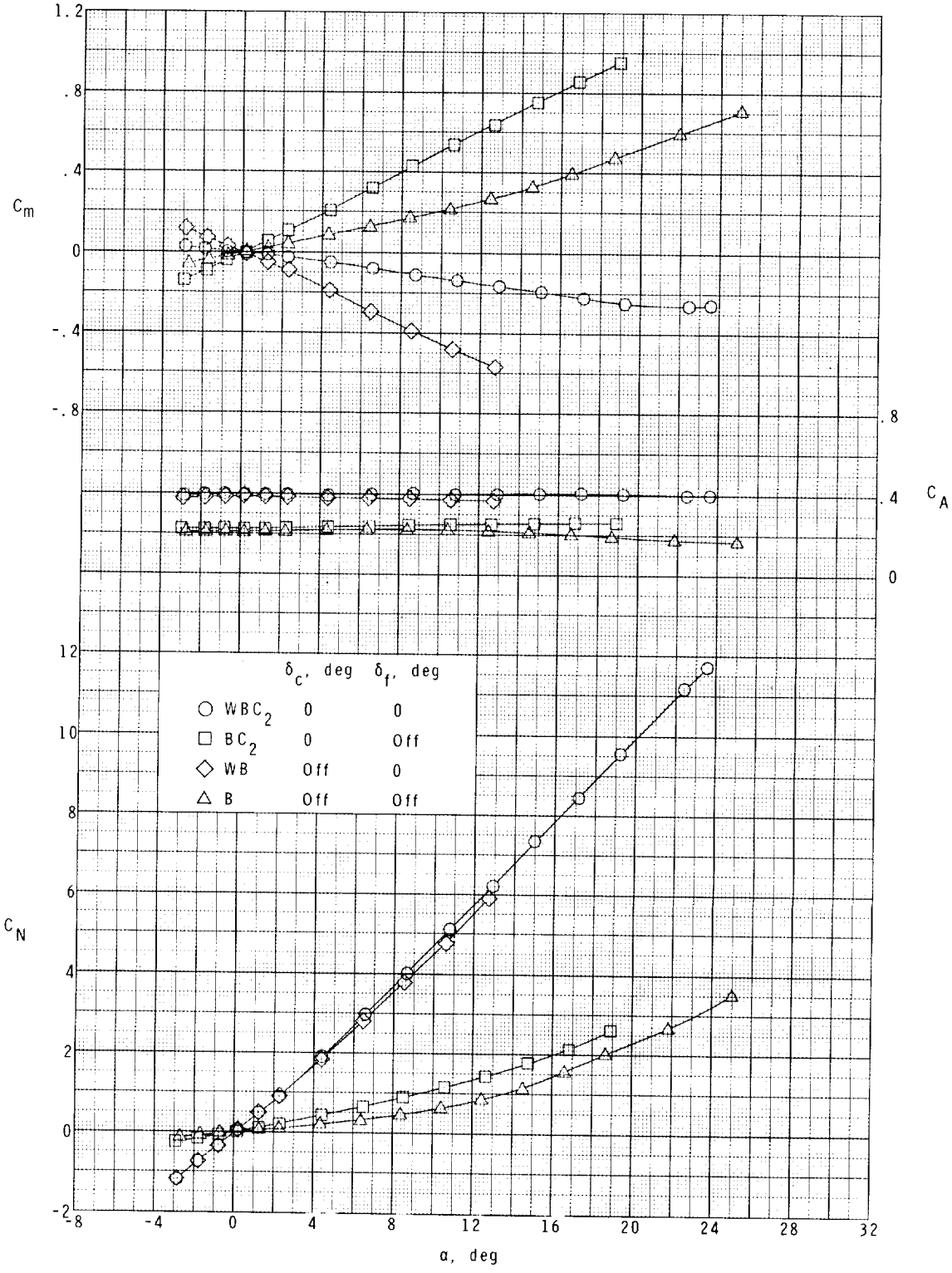

(a) M = 1.50.

Figure 5.- Effects of the wing and canard C_2 on the longitudinal aerodynamic characteristics of the model.

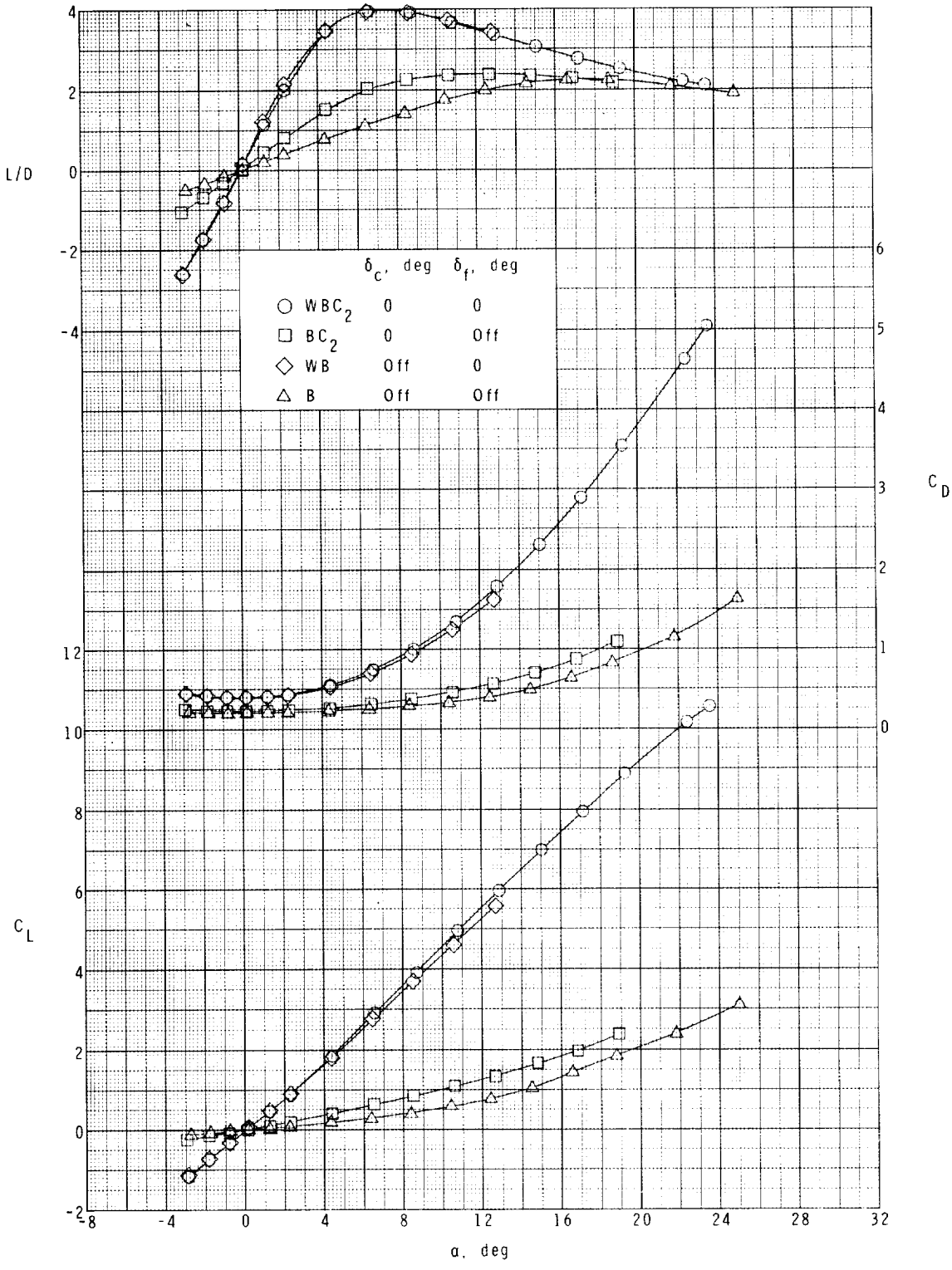

(a) Concluded.

Figure 5.- Continued.

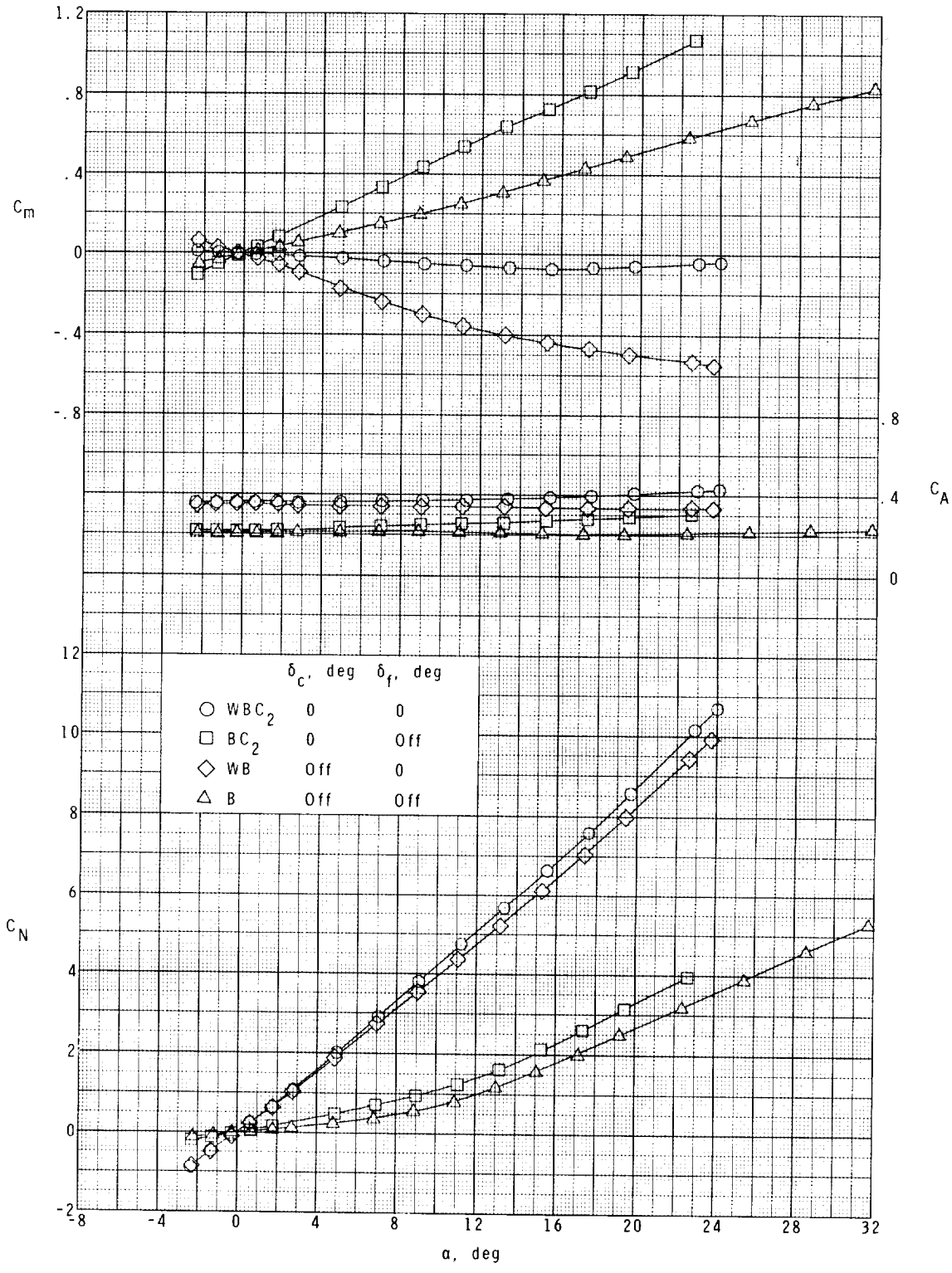

(b) M = 1.90.

Figure 5.- Continued.

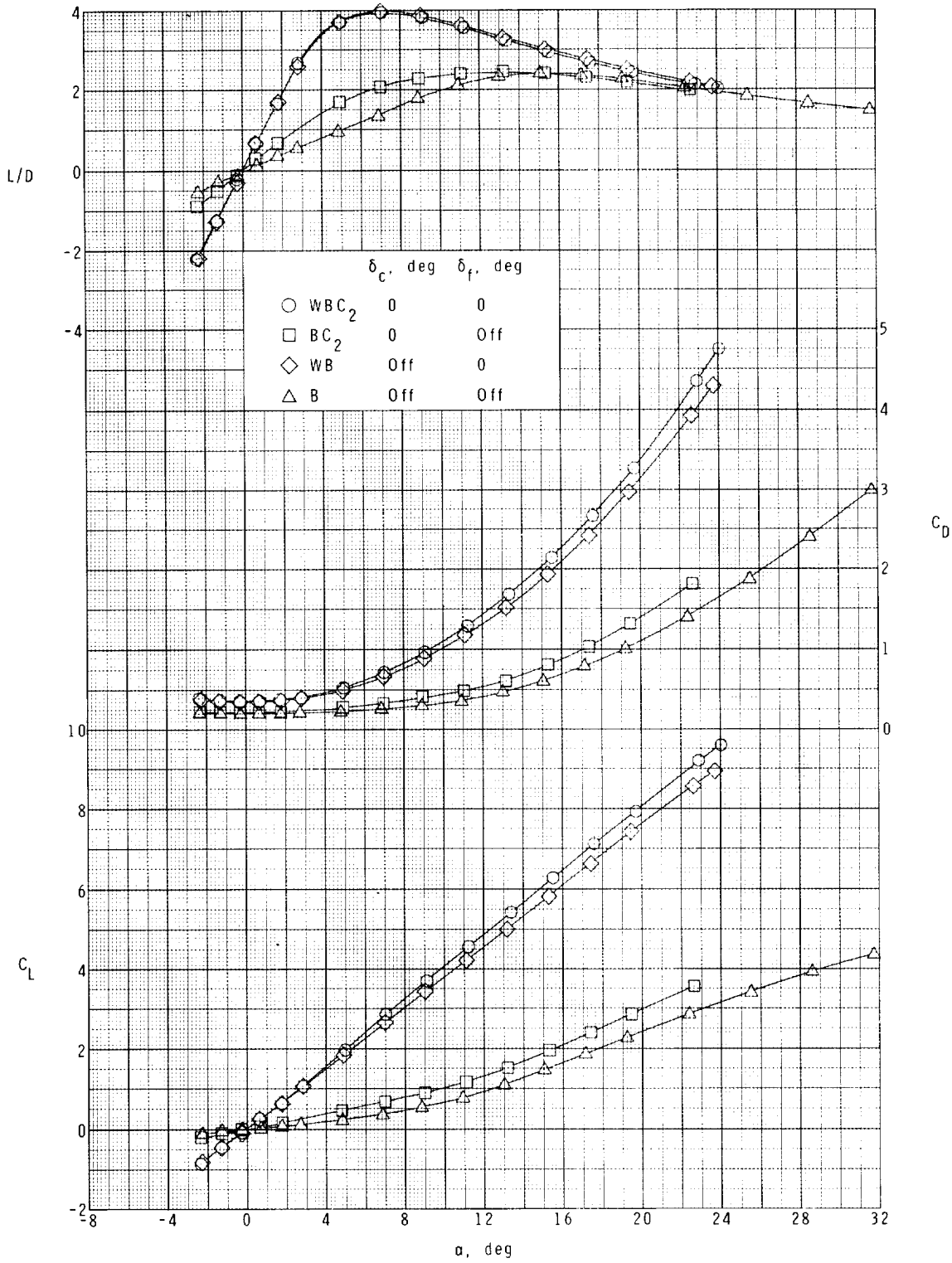

(b) Concluded.

Figure 5.- Continued.

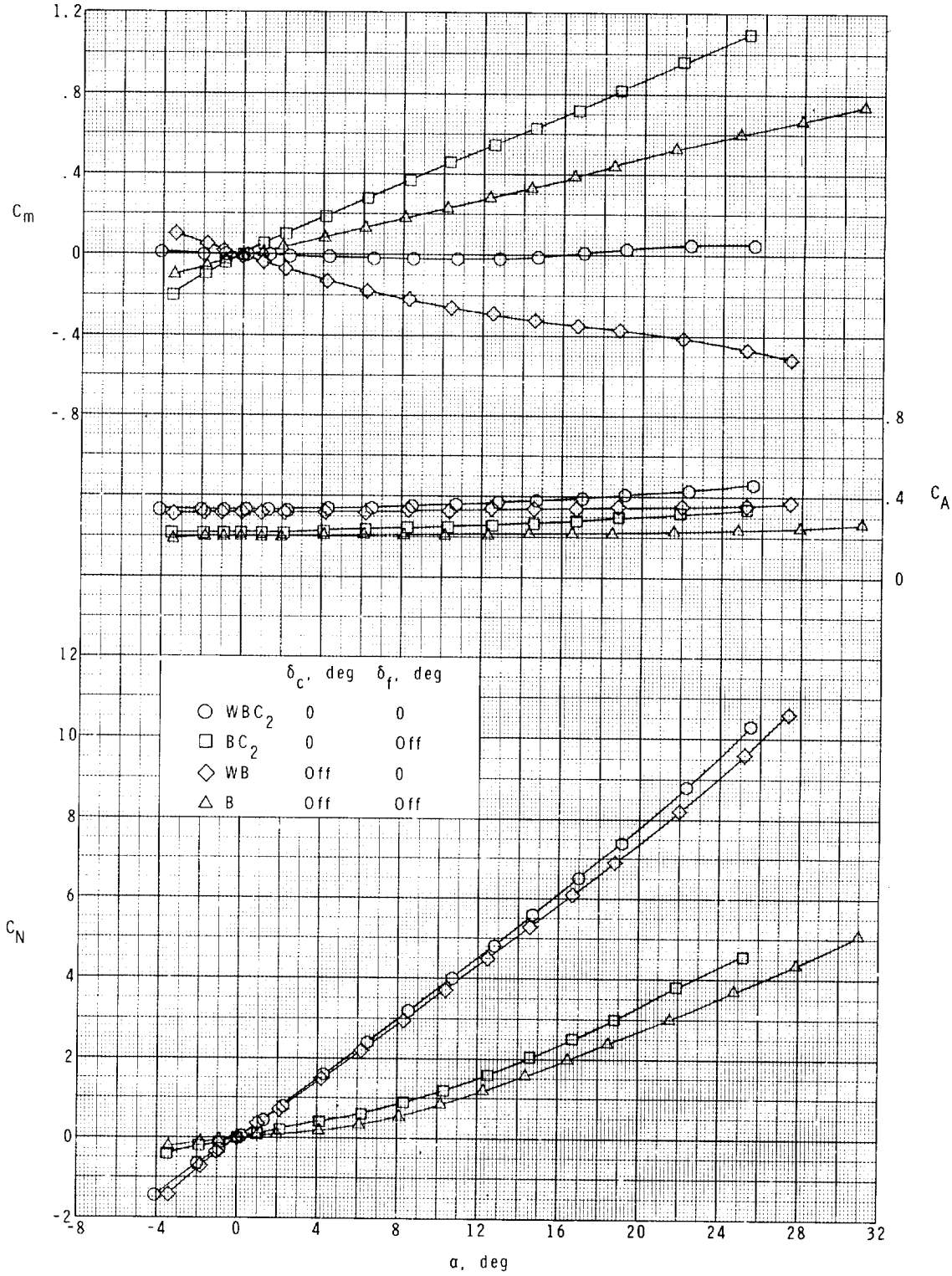

(c) M = 2.30.

Figure 5.- Continued.

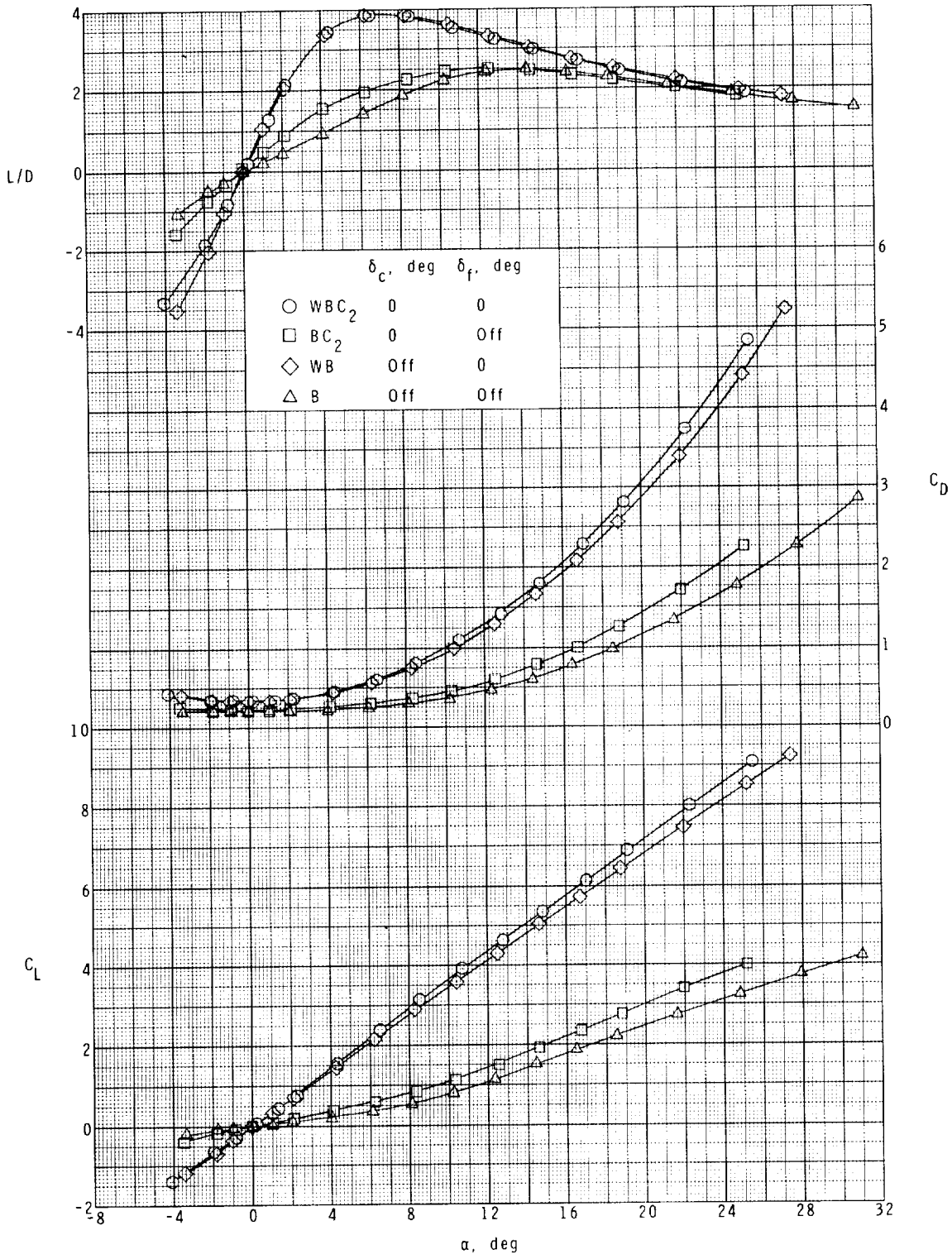

(c) Concluded.

Figure 5.- Continued.

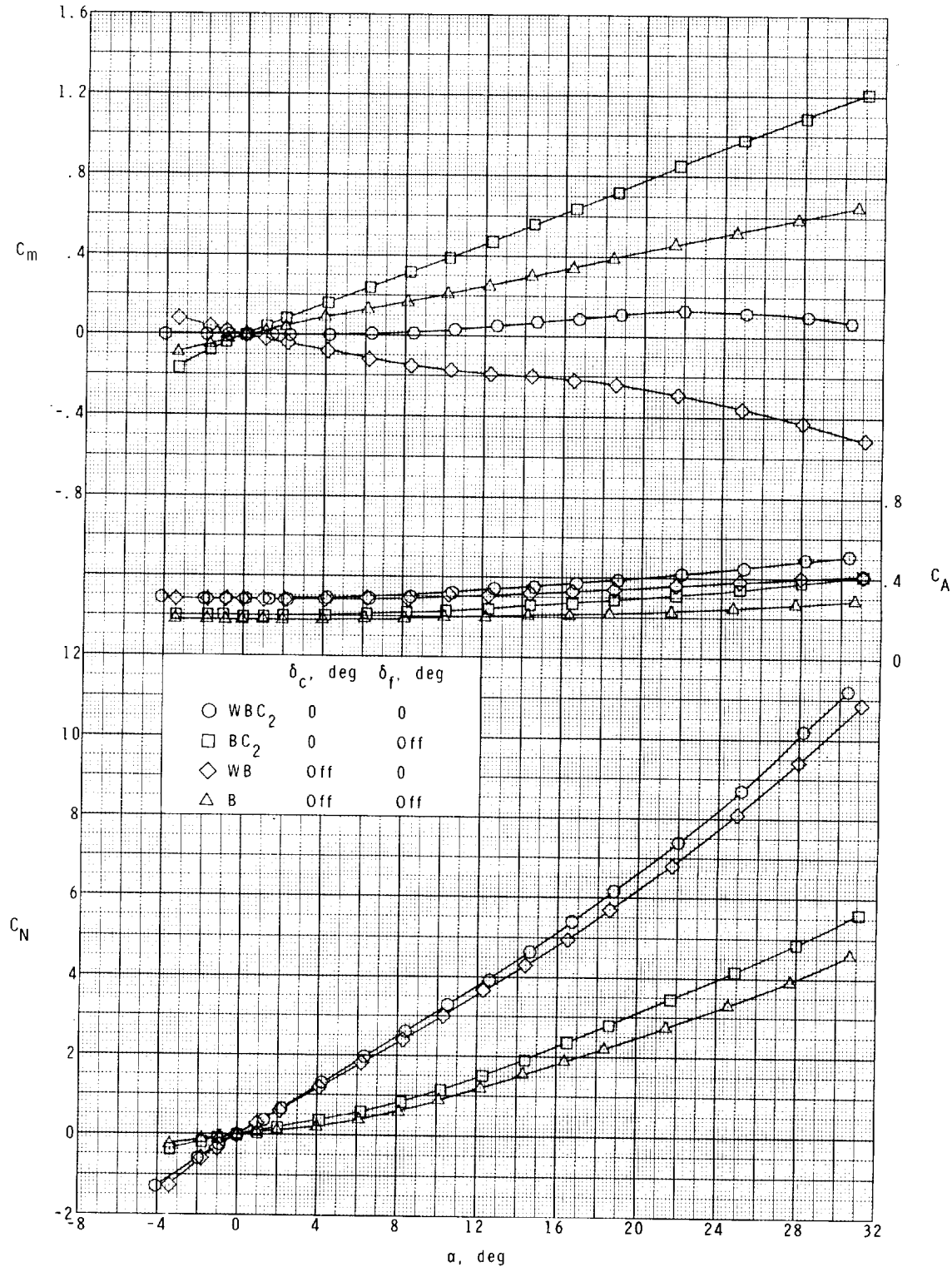

(d) M = 2.96.

Figure 5.- Continued.

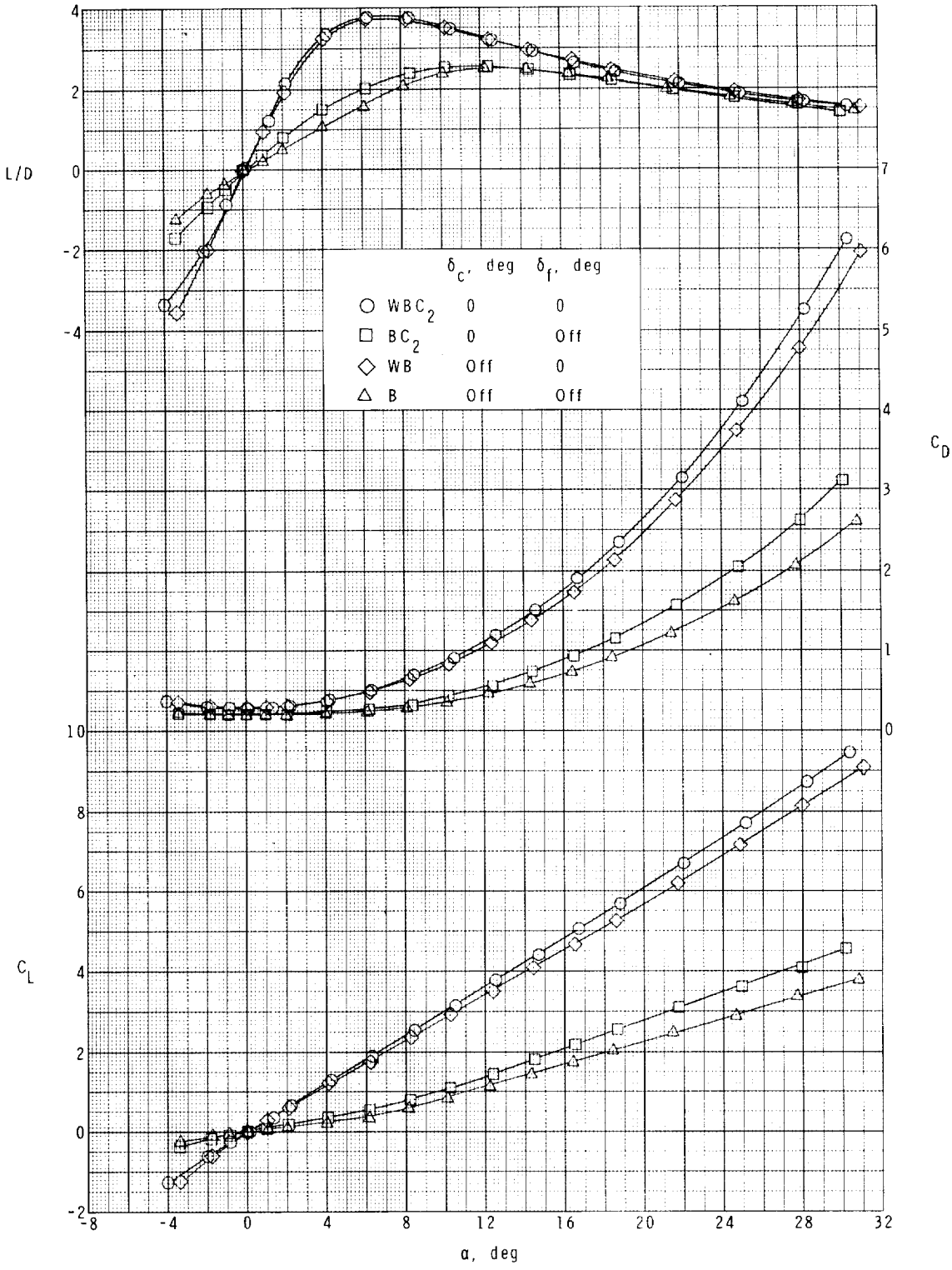

(d) Concluded.

Figure 5.- Continued.

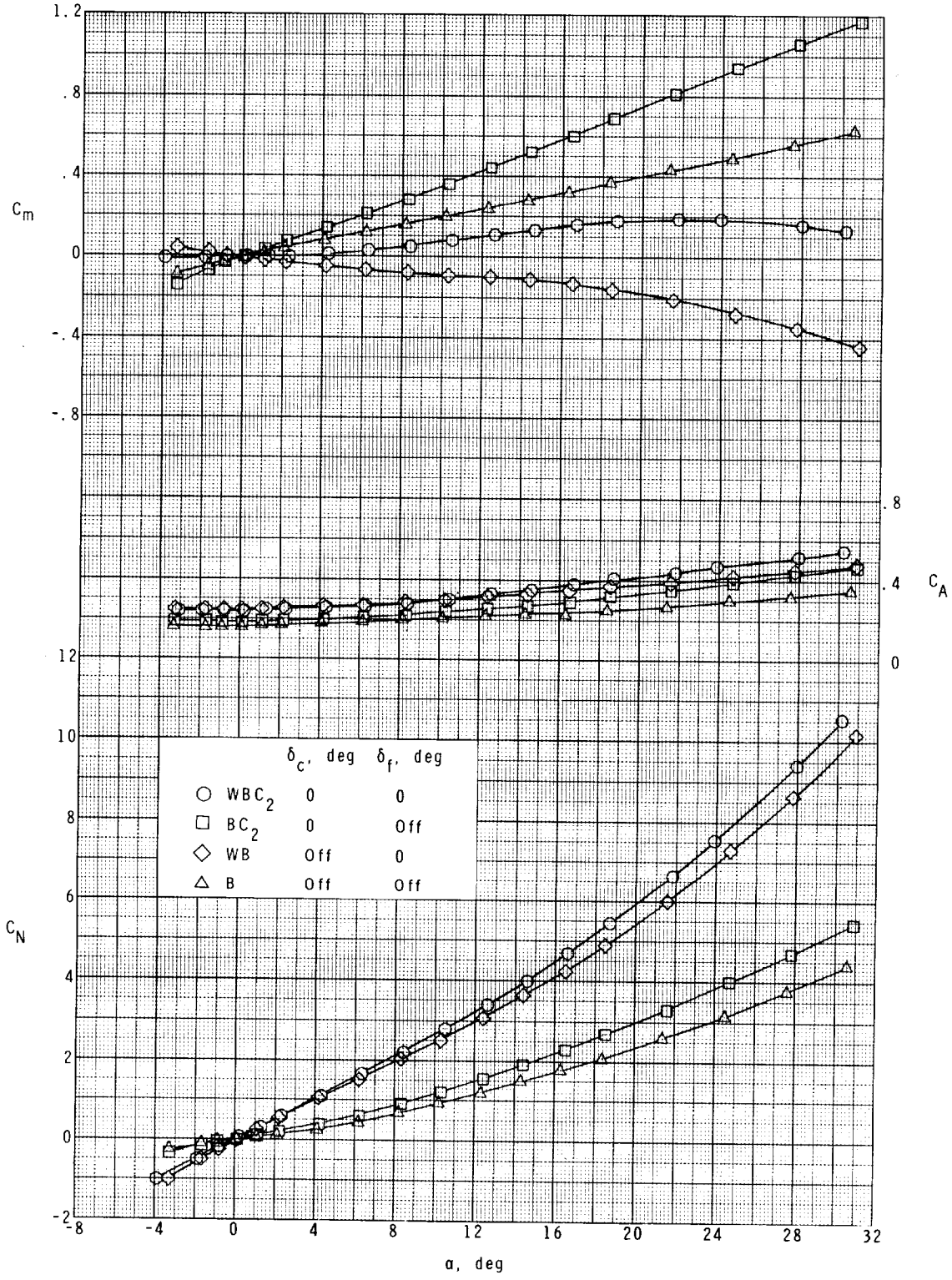

(e) M = 3.95.

Figure 5.- Continued.

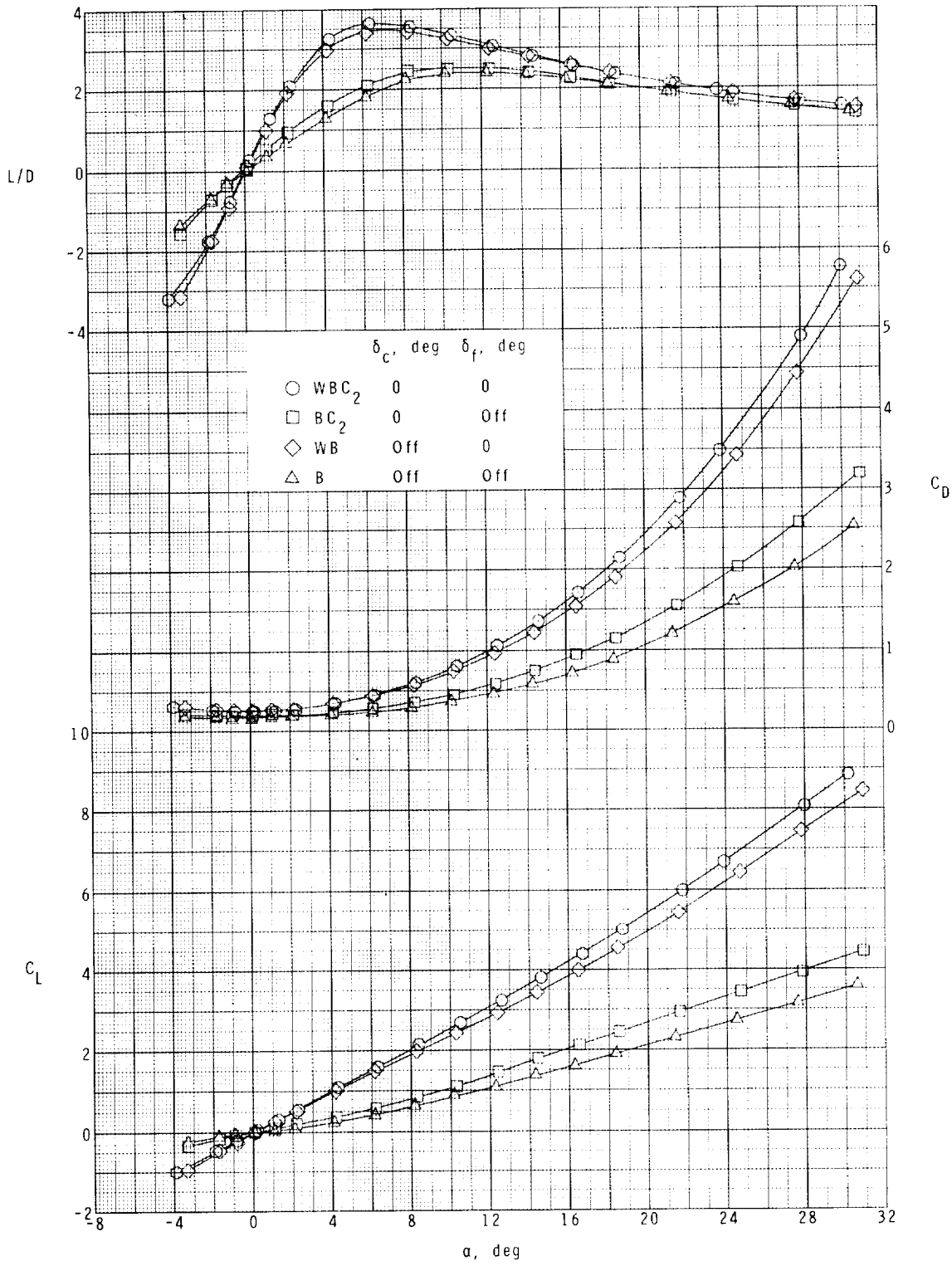

(e) Concluded.

Figure 5.- Continued.

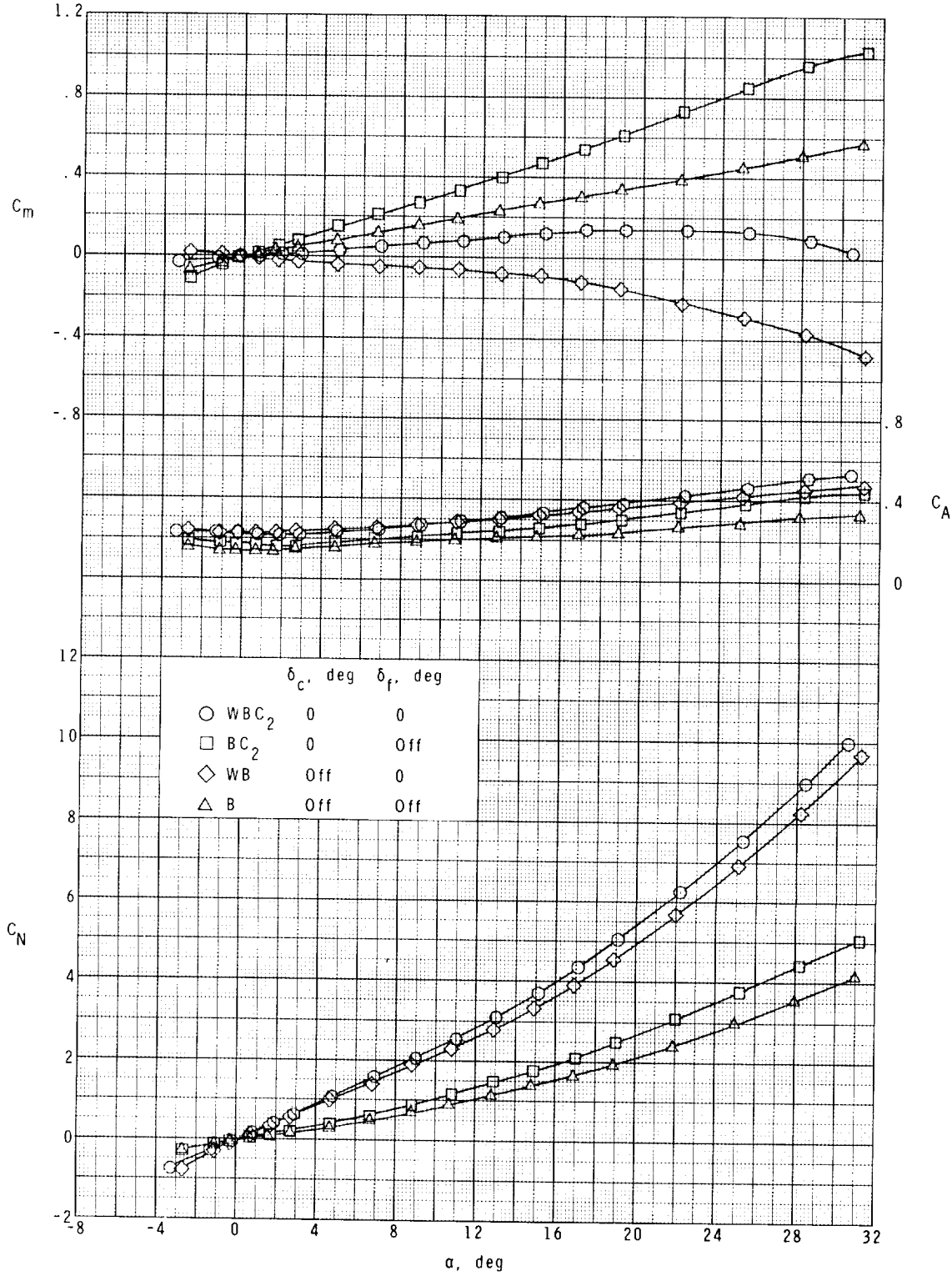

(f) M = 4.63.

Figure 5.- Continued.

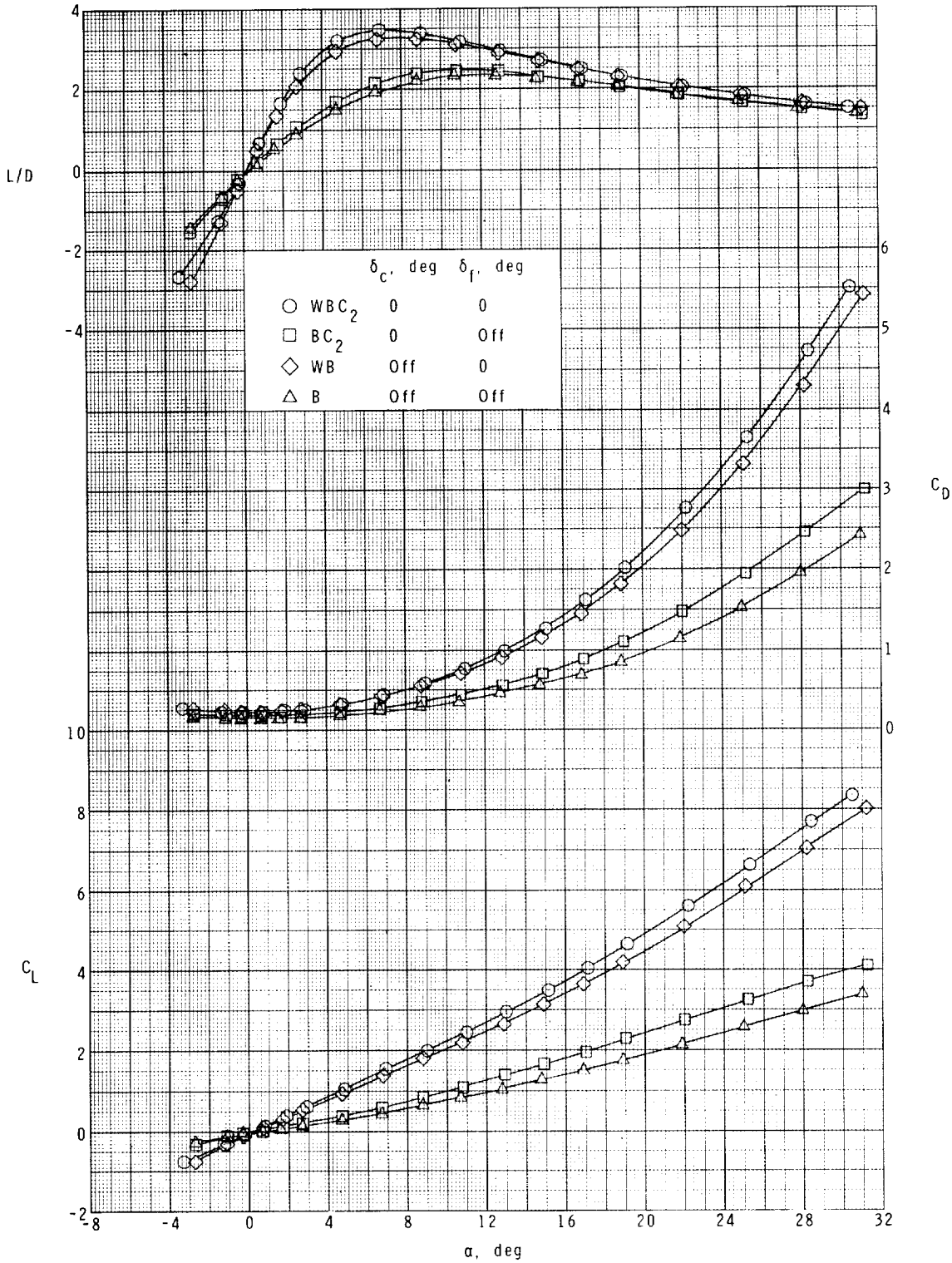

(f) Concluded.

Figure 5.- Concluded.

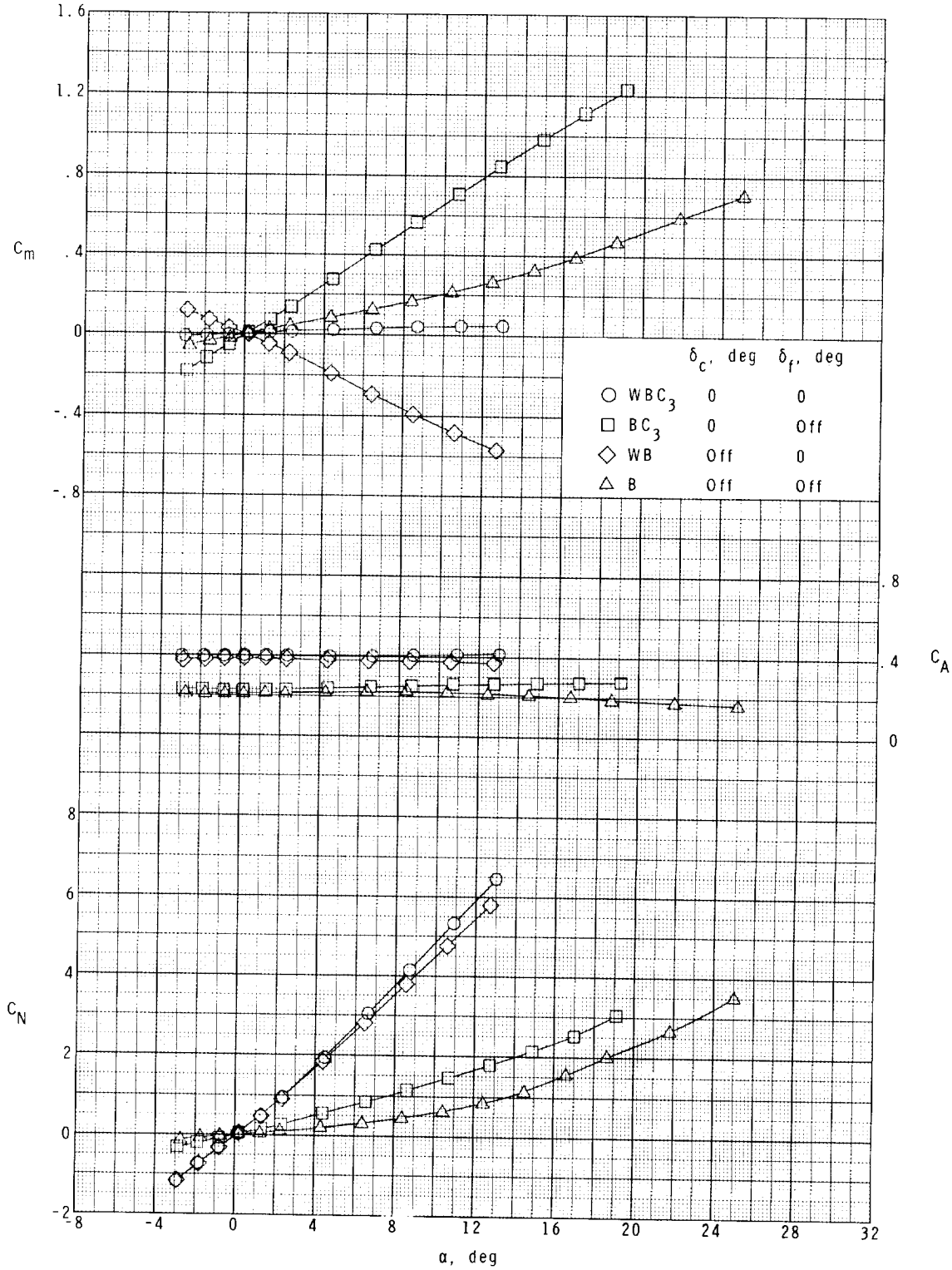

(a) M = 1.50.

Figure 6.- Effects of the wing and canard C_3 on the longitudinal aerodynamic characteristics of the model.

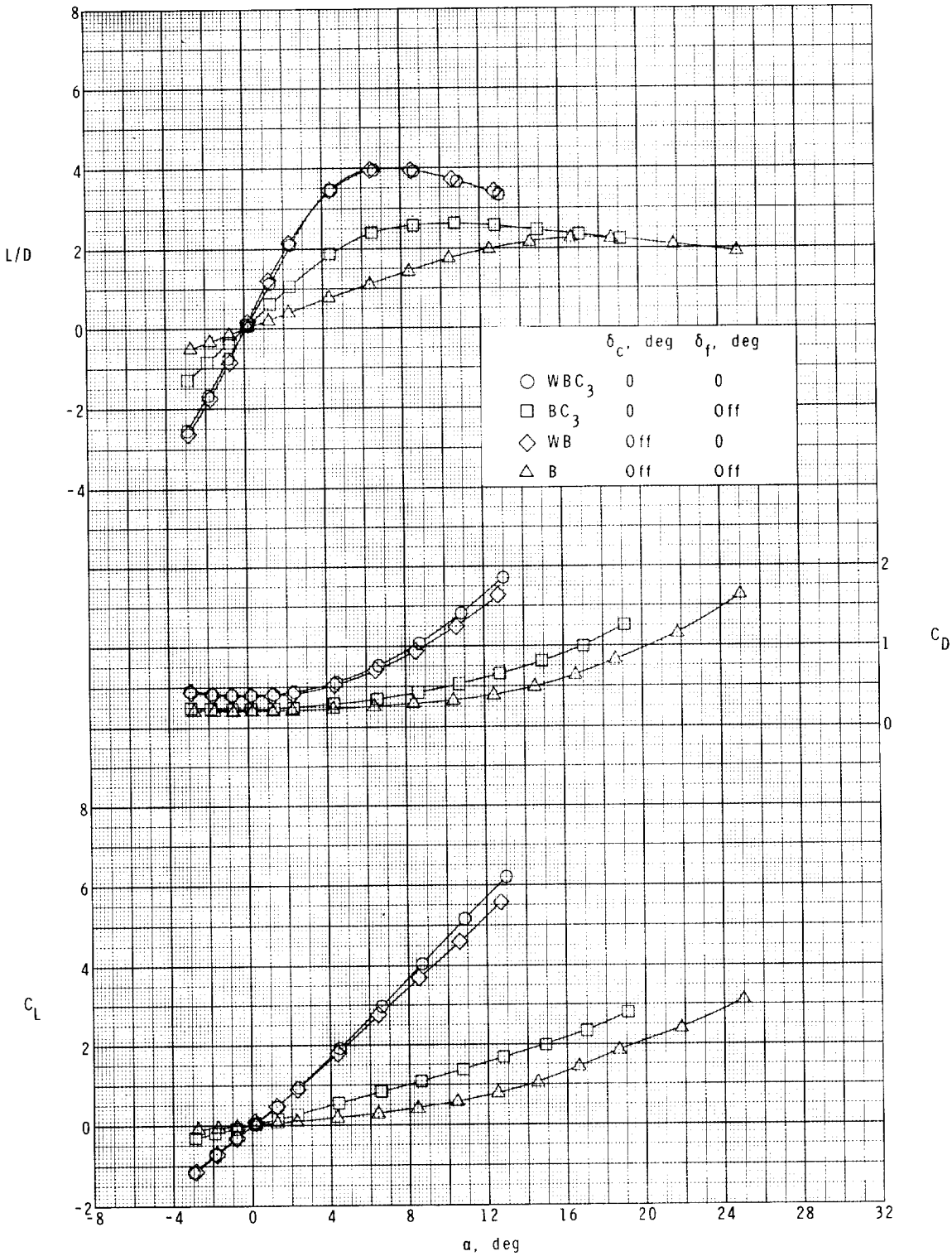

(a) Concluded.

Figure 6.- Continued.

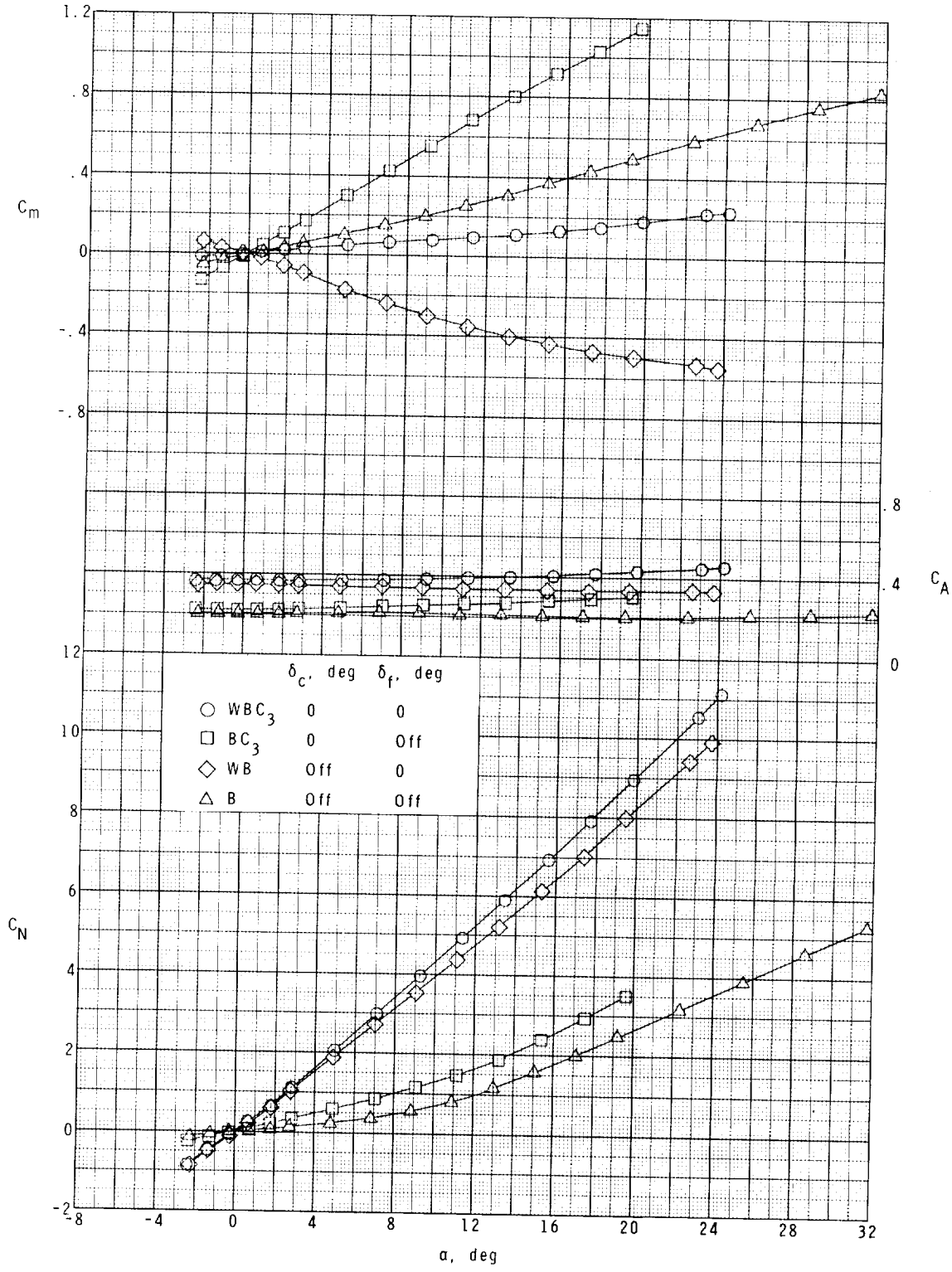

(b) M = 1.90.

Figure 6.- Continued.

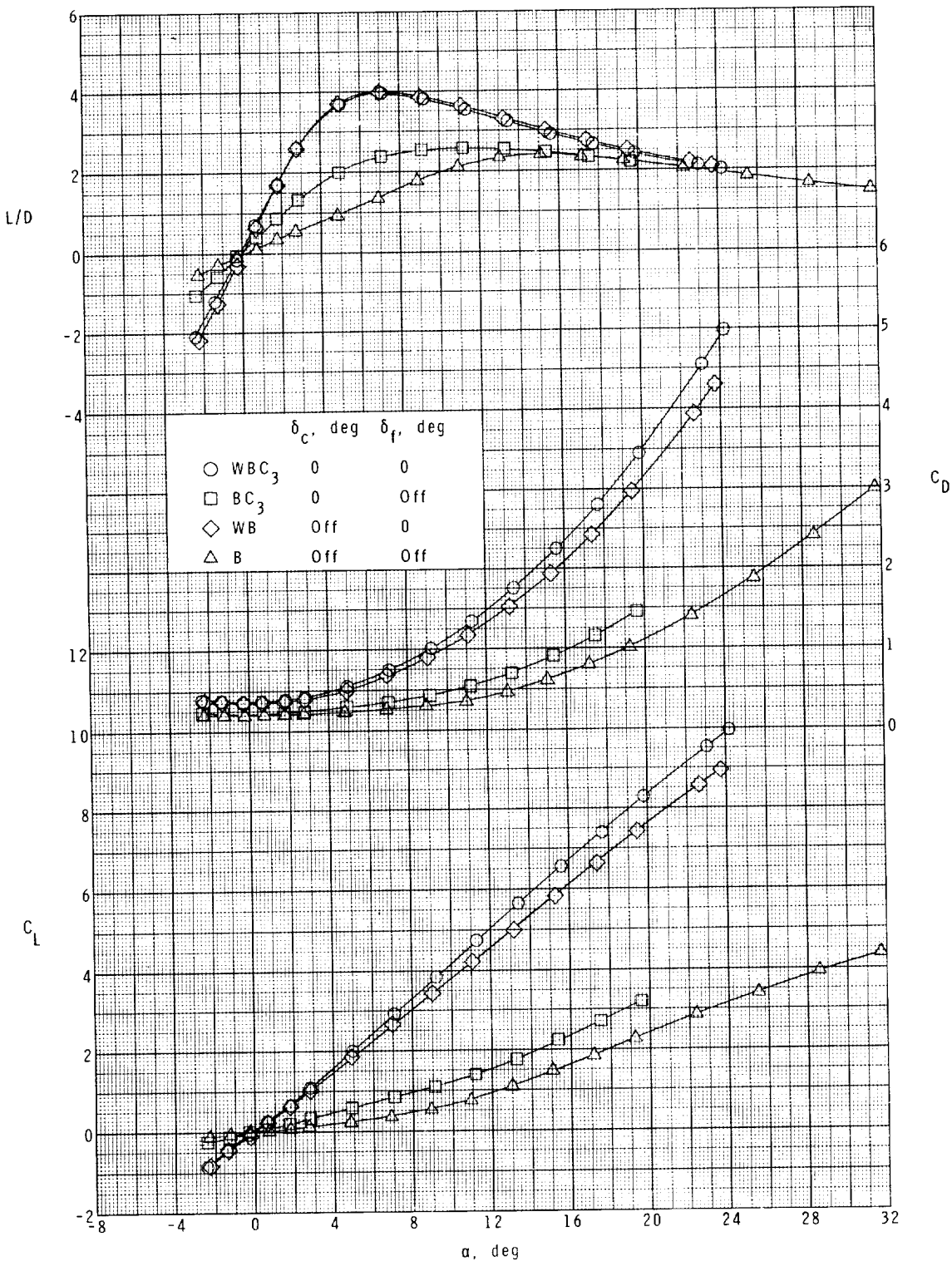

(b) Concluded.

Figure 6.- Continued.

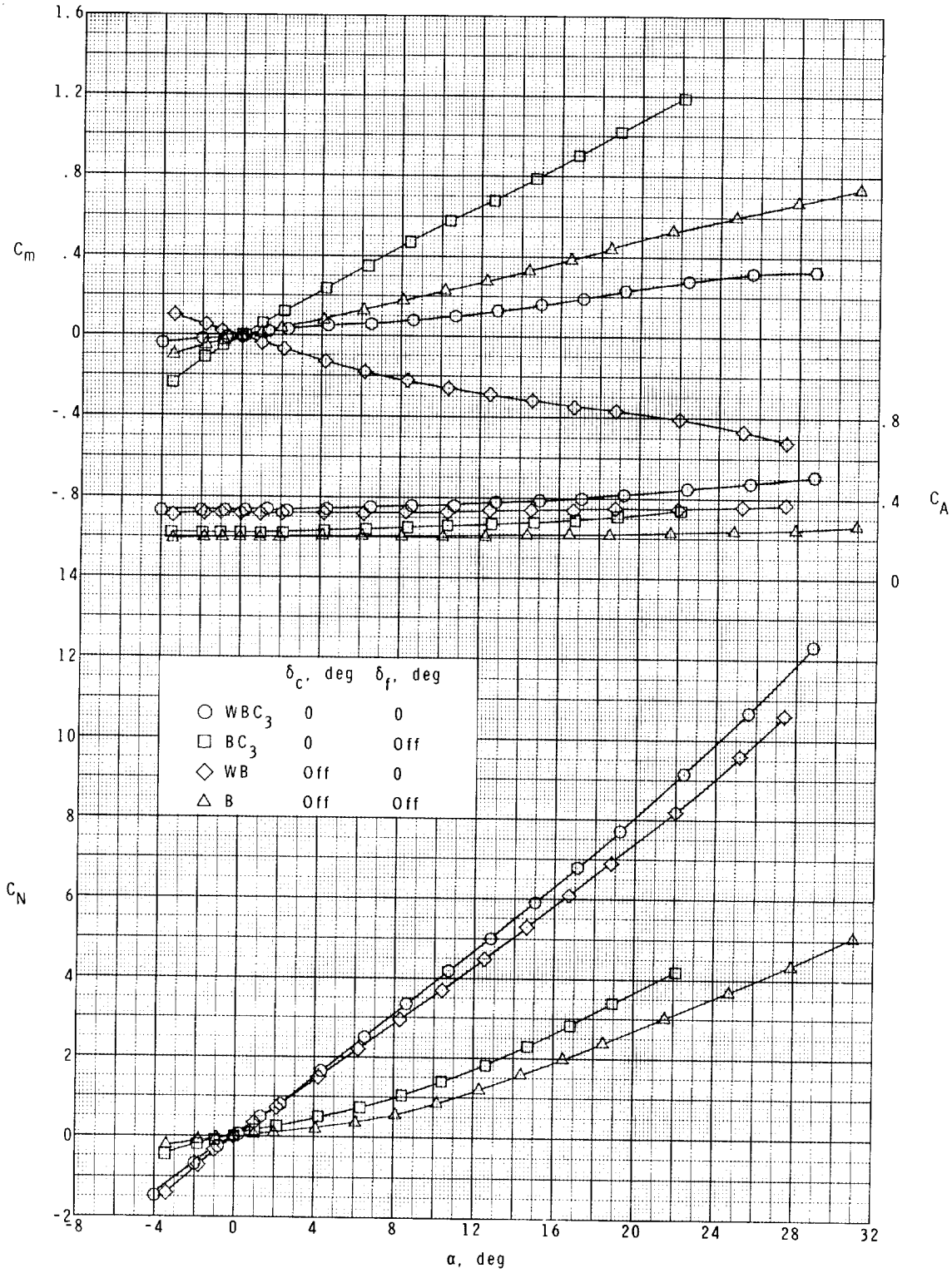

(c) M = 2.30.

Figure 6.- Continued.

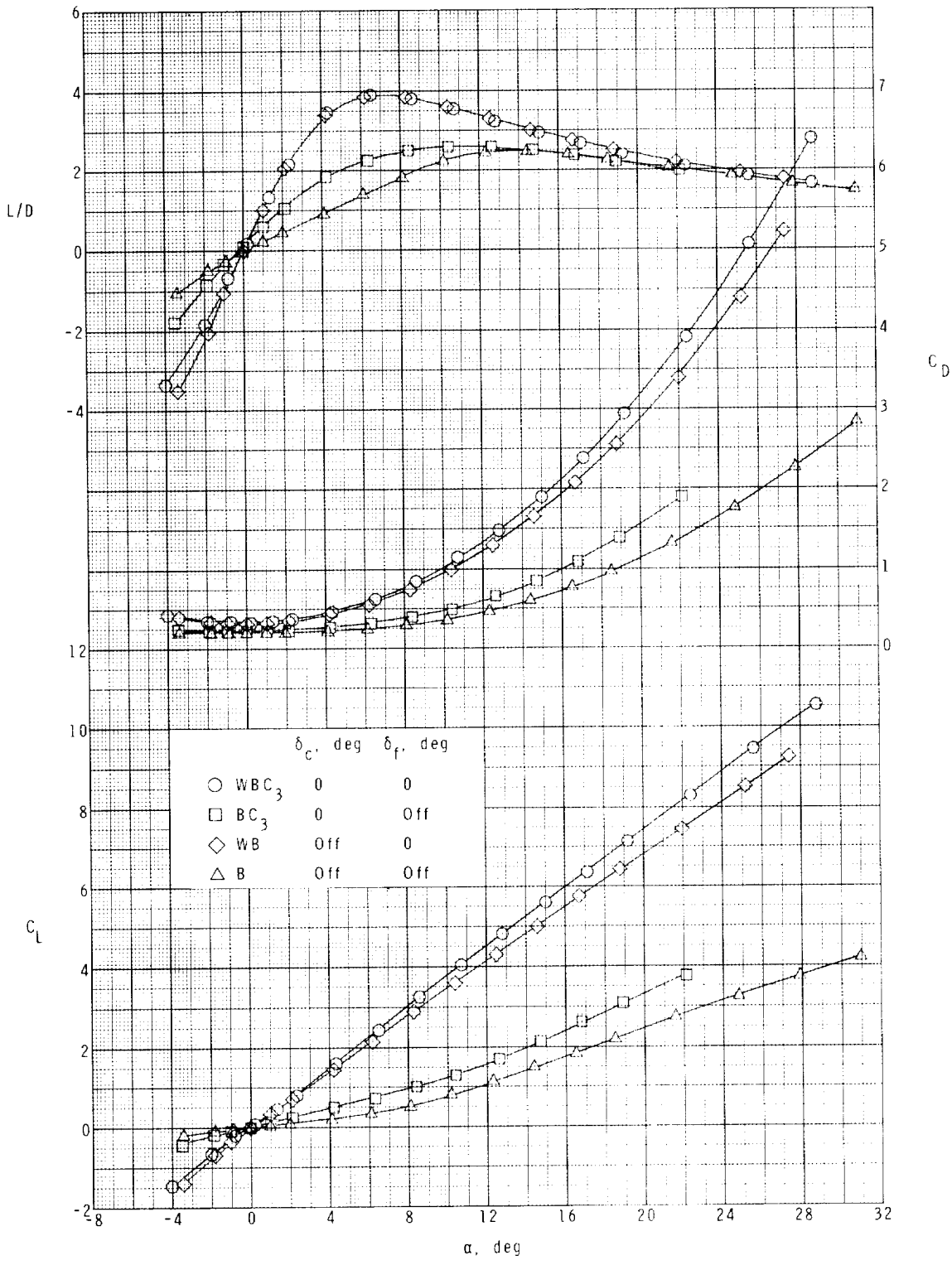

(c) Concluded.

Figure 6.- Continued.

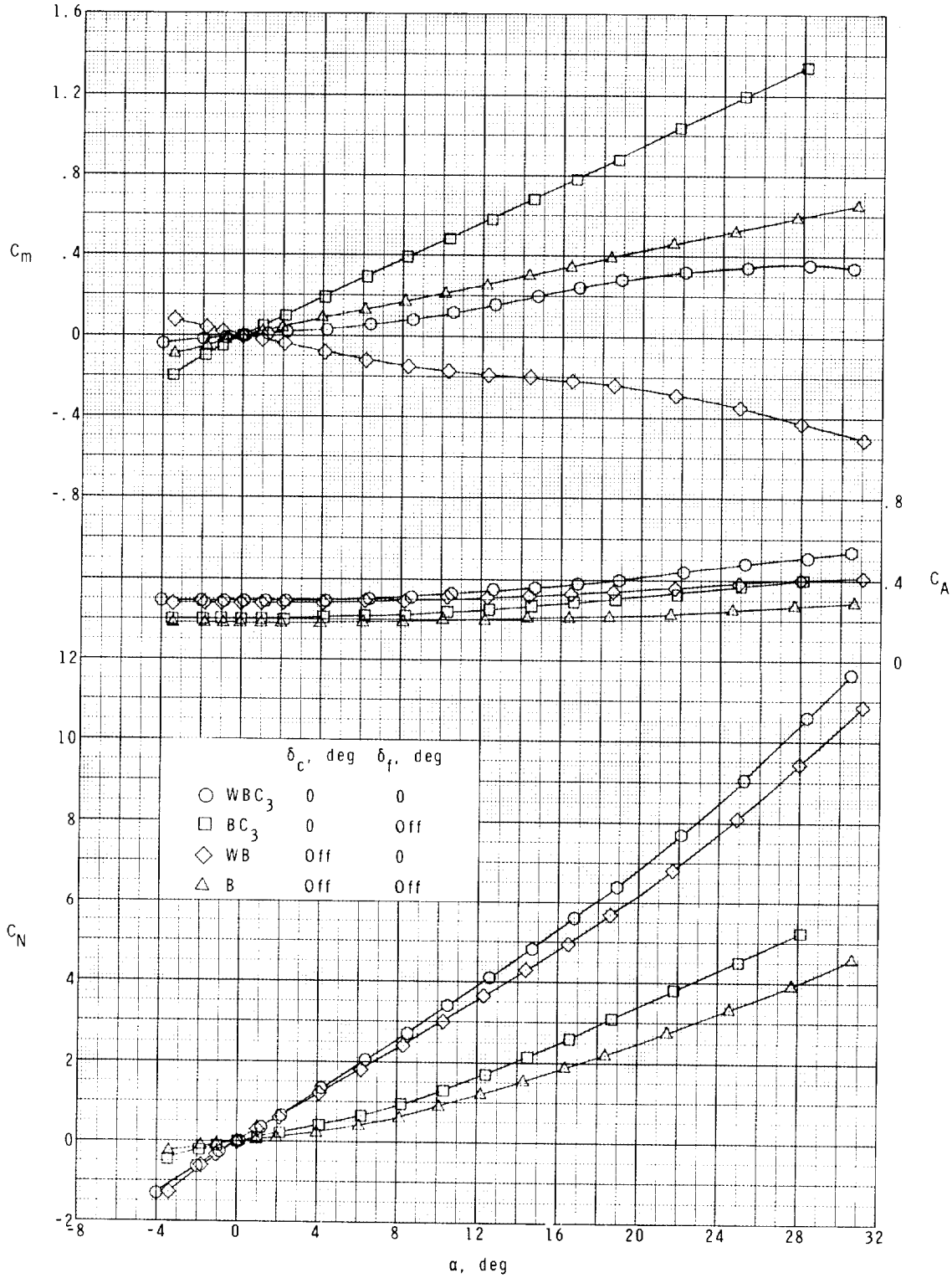

(d) M = 2.96.

Figure 6.- Continued.

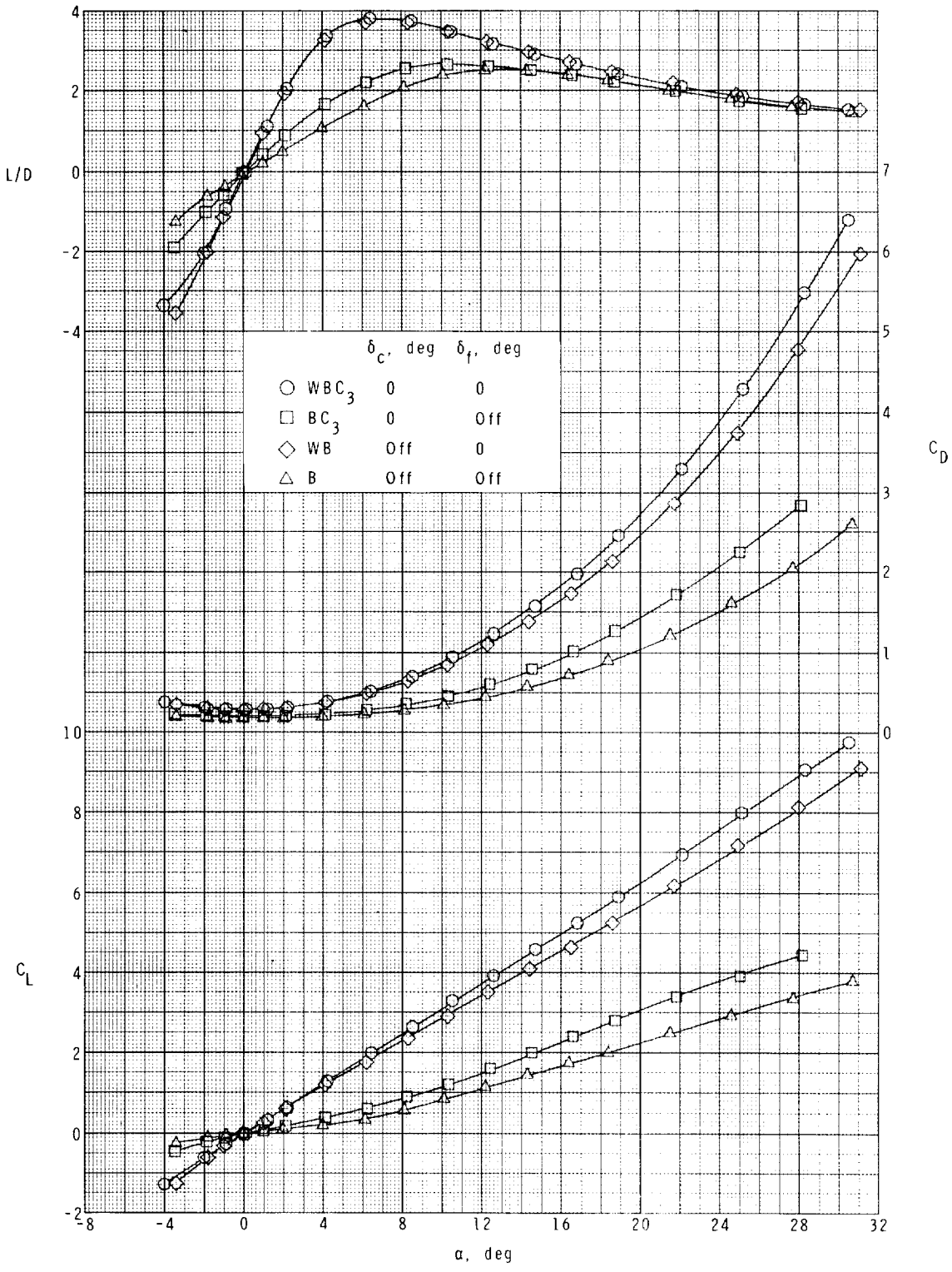

(d) Concluded.

Figure 6.- Continued.

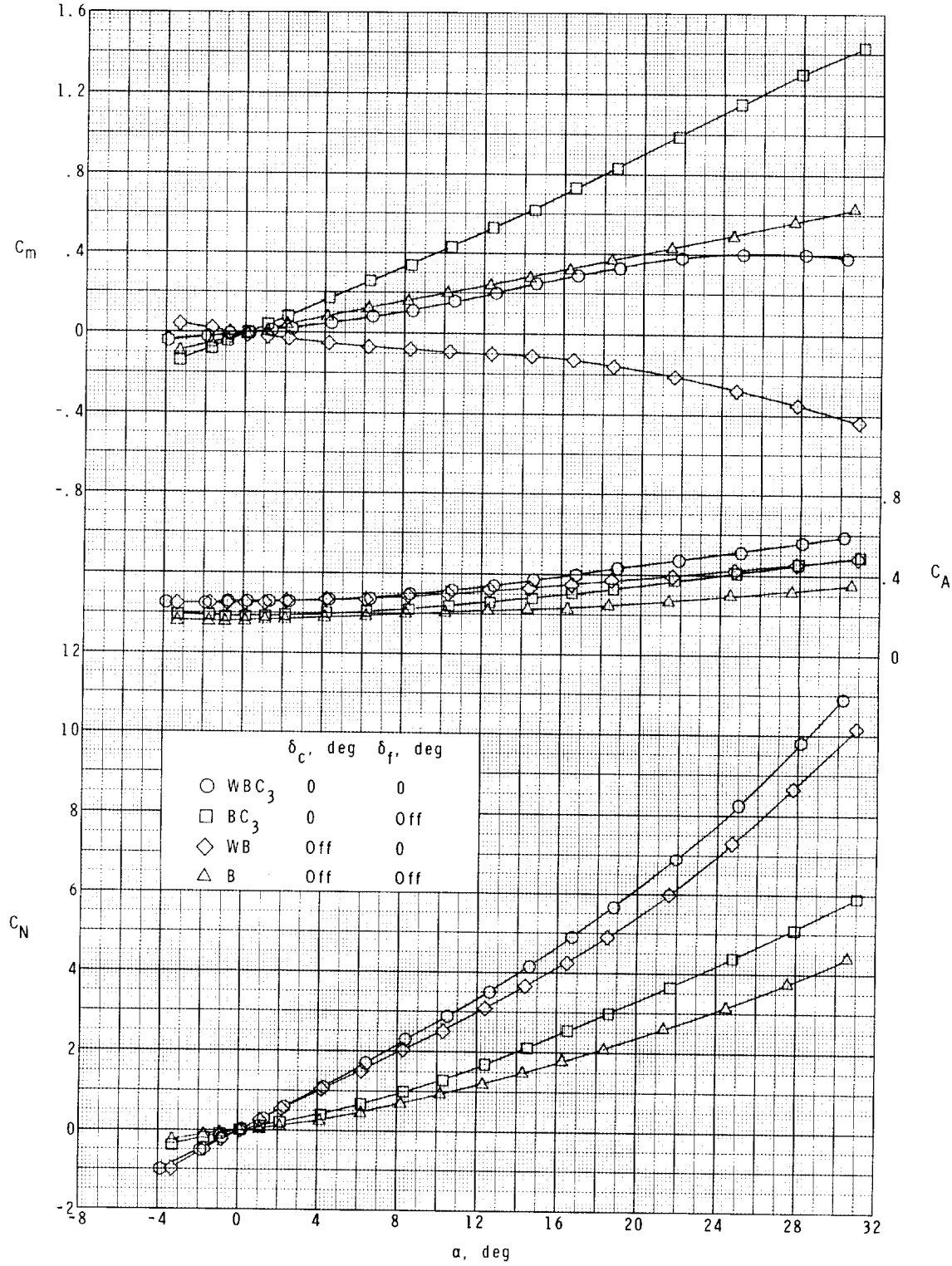

(e) M = 3.95.

Figure 6.- Continued.

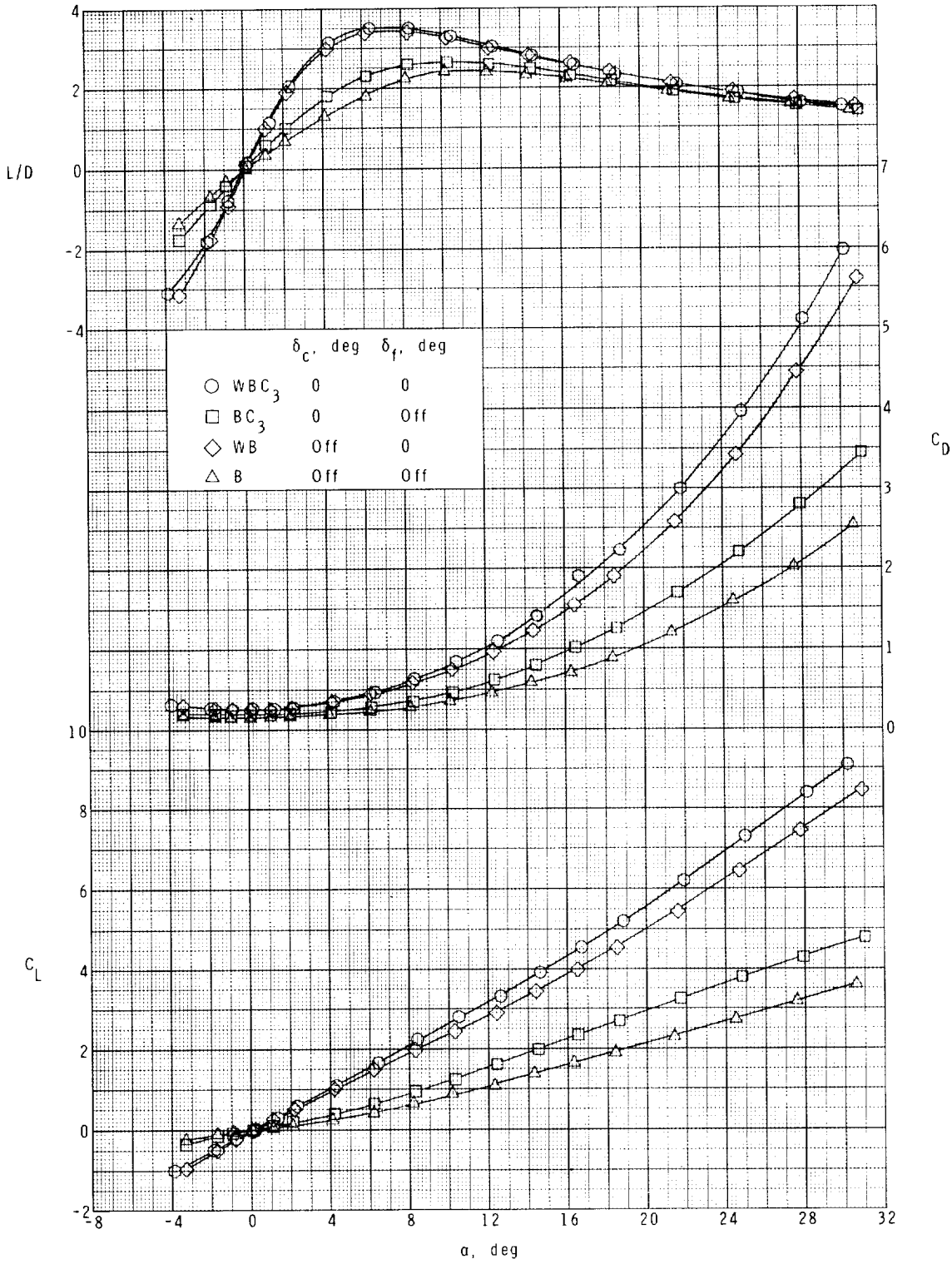

(e) Concluded.

Figure 6.- Continued.

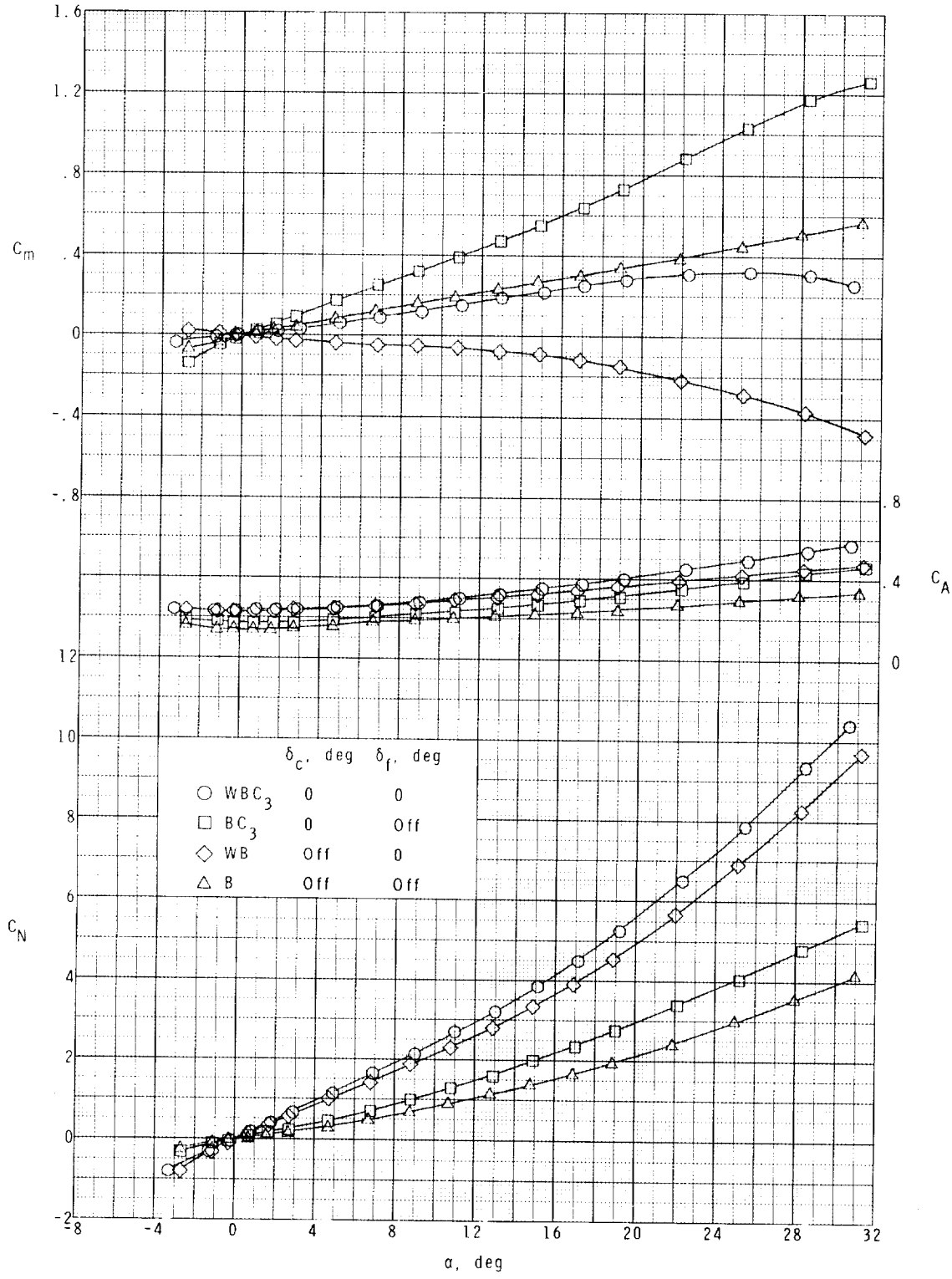

(f) M = 4.63.

Figure 6.- Continued.

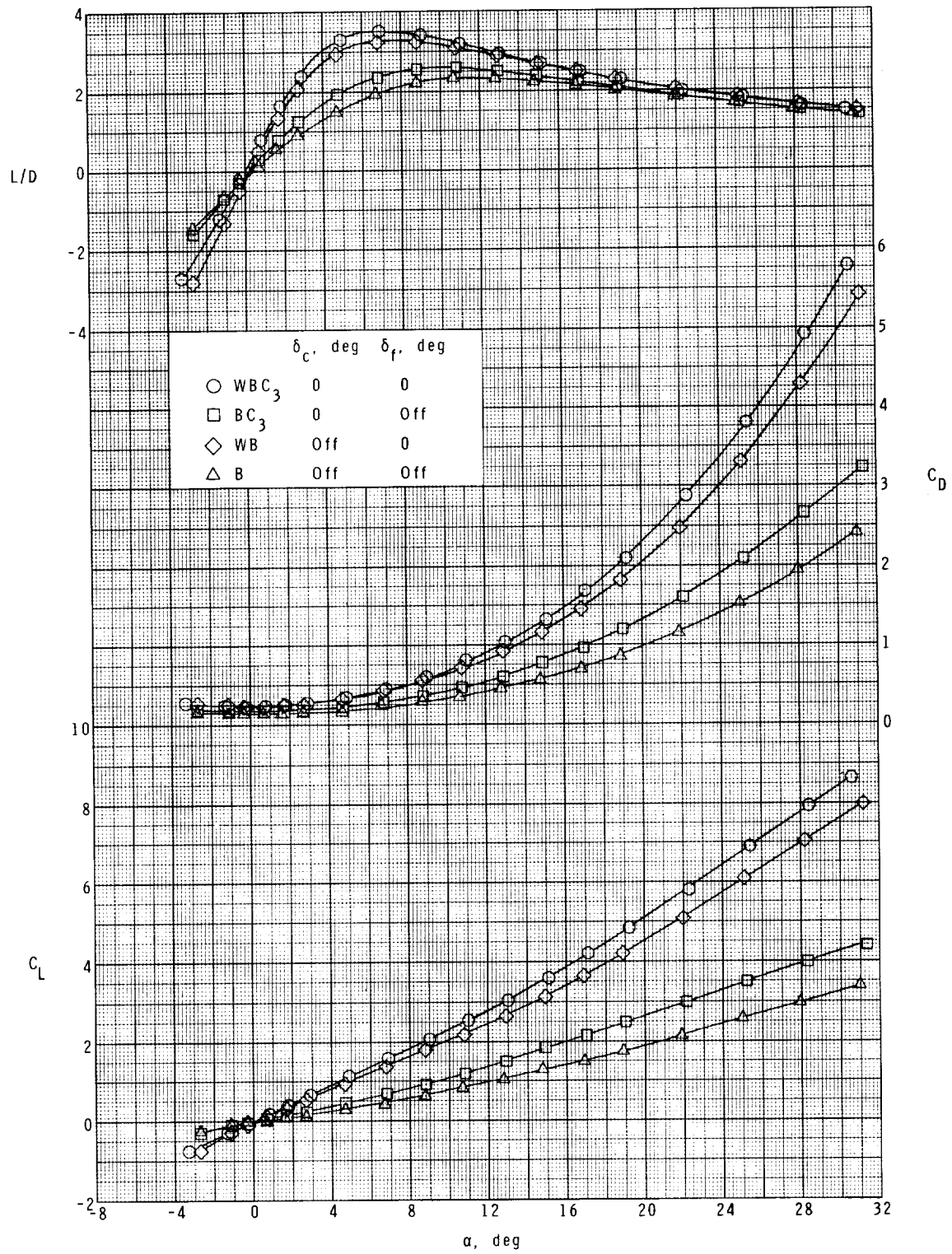

(f) Concluded.

Figure 6.- Concluded.

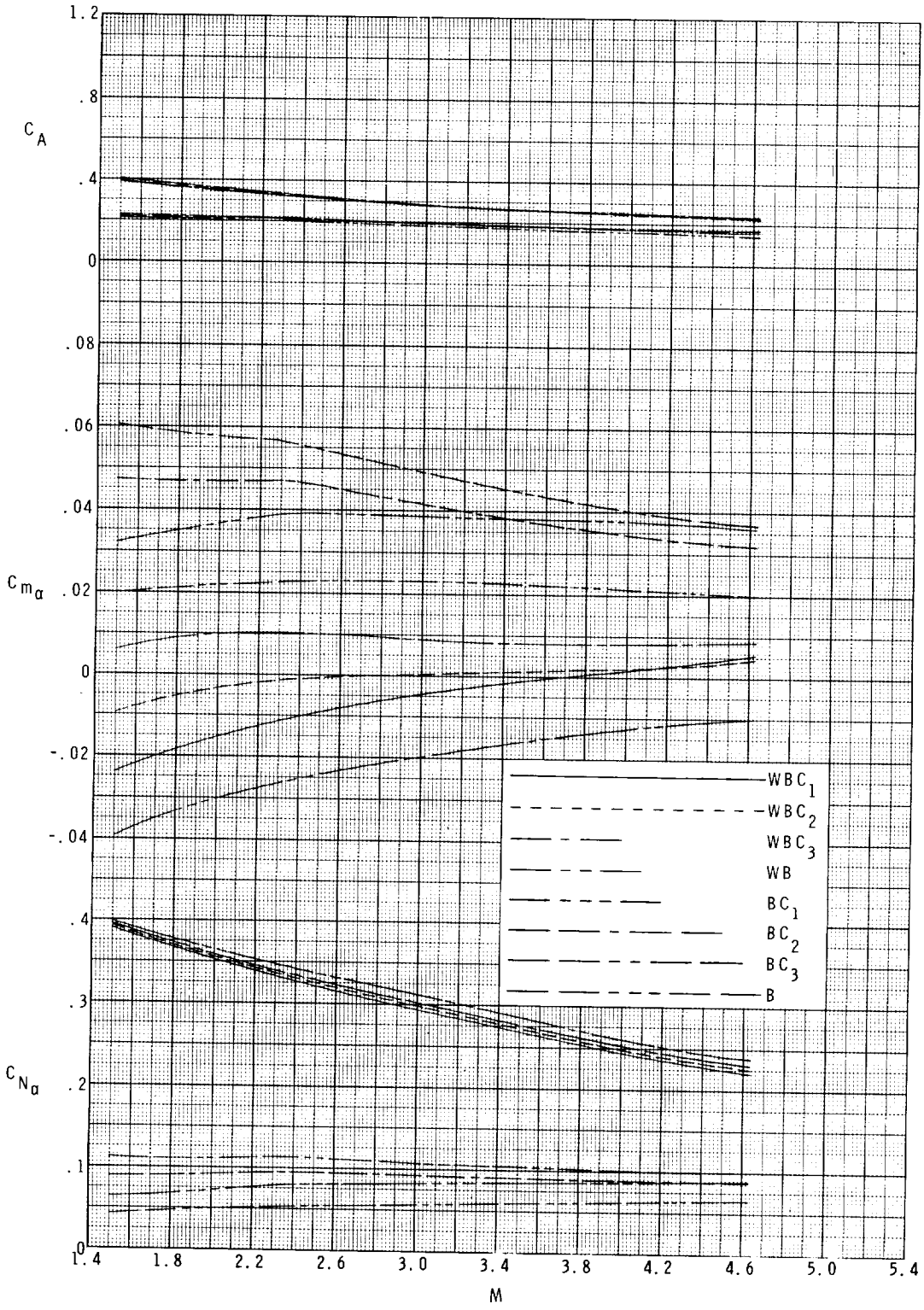

(a) C_A, C_{m_α}, and C_{N_α} as functions of Mach number.

Figure 7.- Summary of longitudinal characteristics.

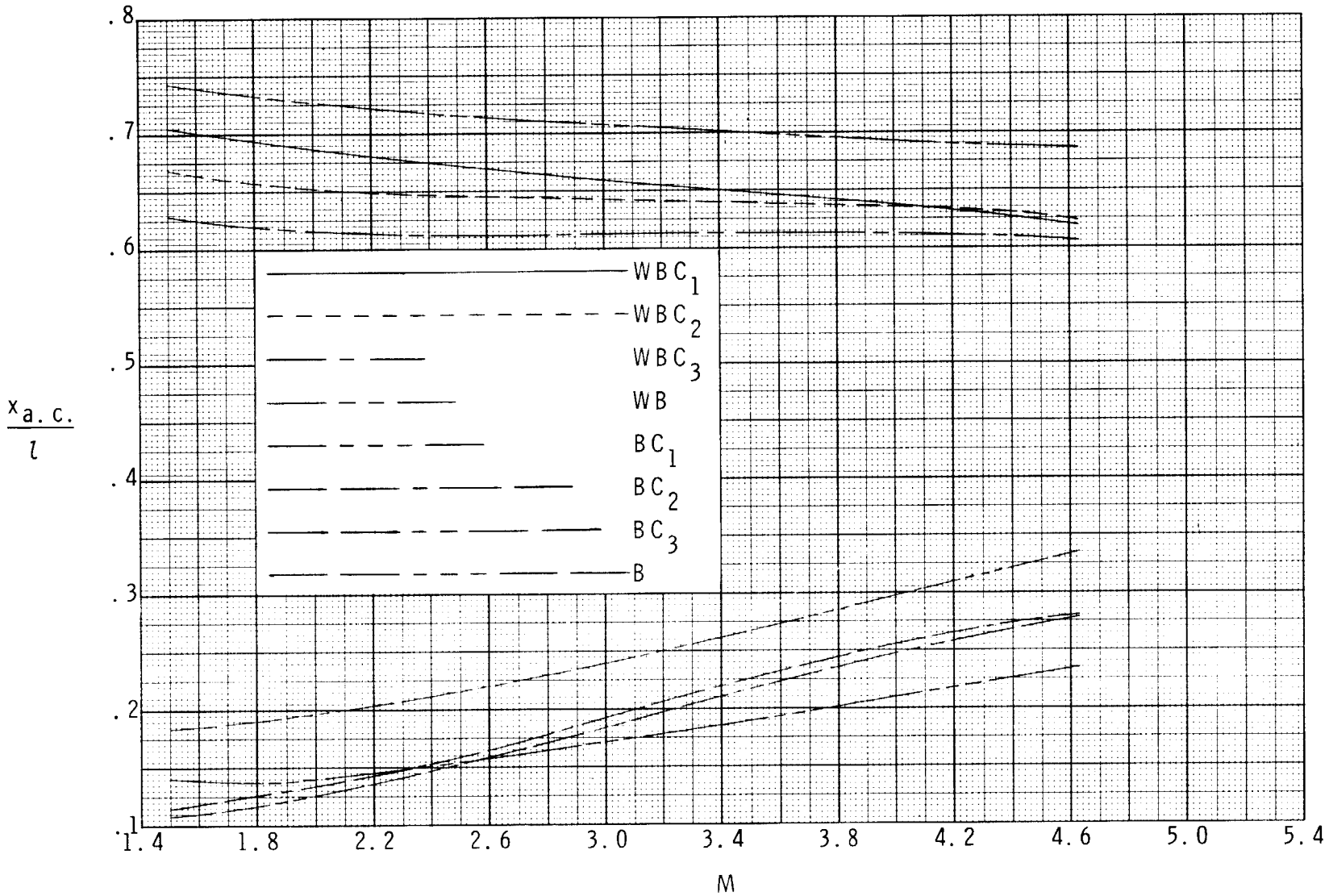

(b) $\frac{x_{a.c.}}{l}$ as a function of Mach number.

Figure 7.- Concluded.

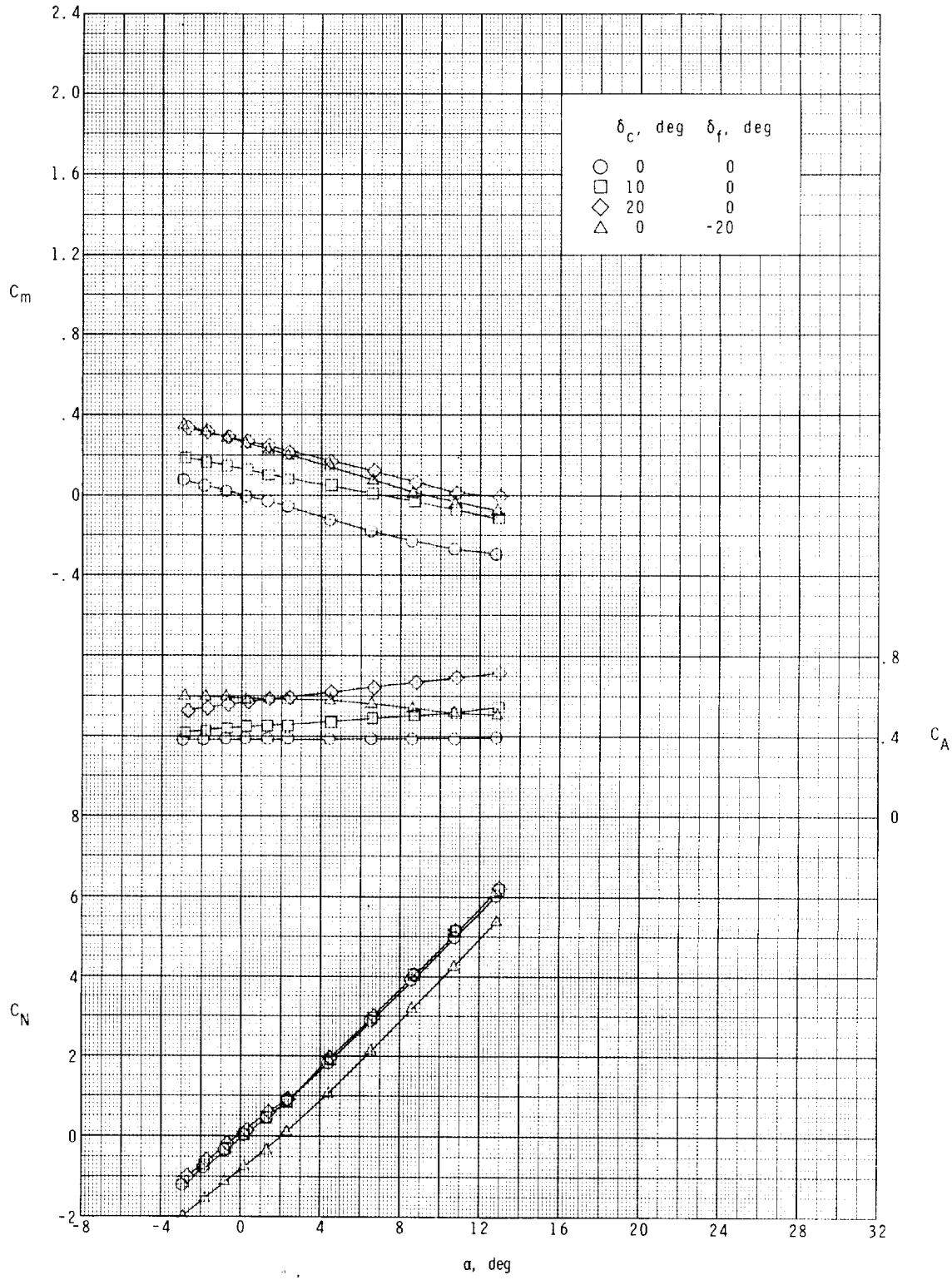

(a) M = 1.50.

Figure 8.- Effects of deflection of the canard C_1 and the wing flap on the longitudinal aerodynamic characteristics of the model. Configuration WBC_1.

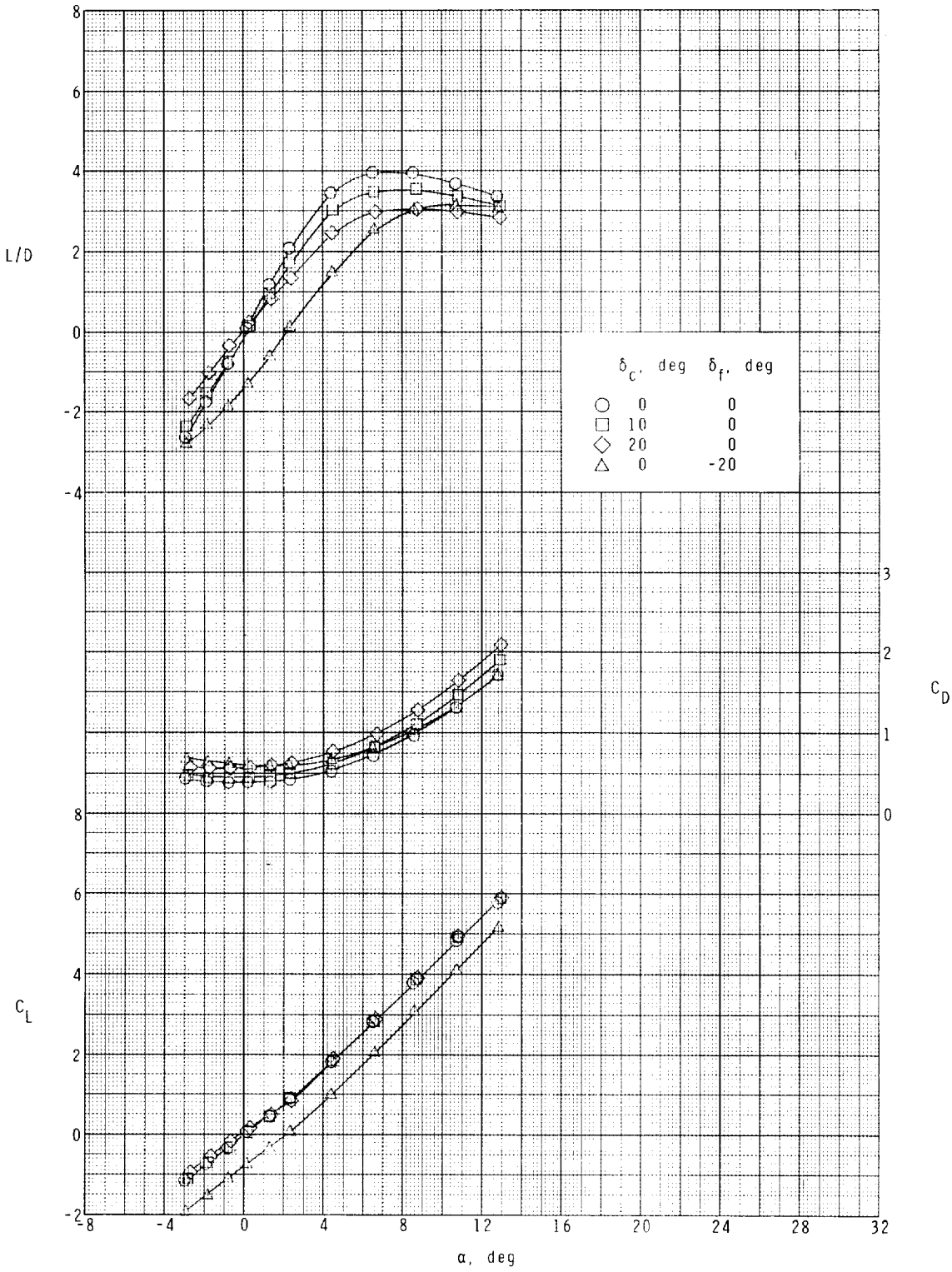

(a) Concluded.

Figure 8.- Continued.

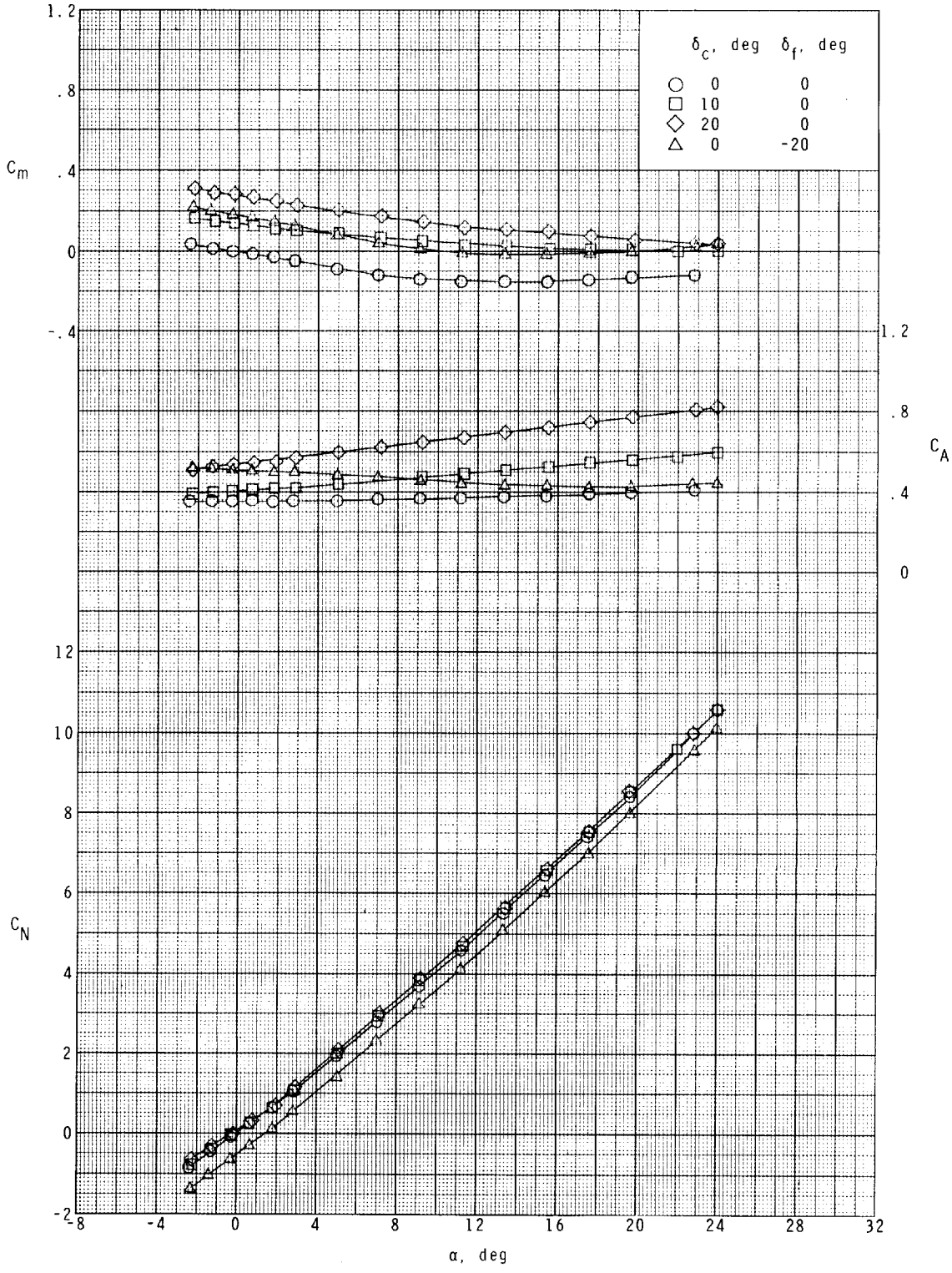

(b) M = 1.90.

Figure 8.- Continued.

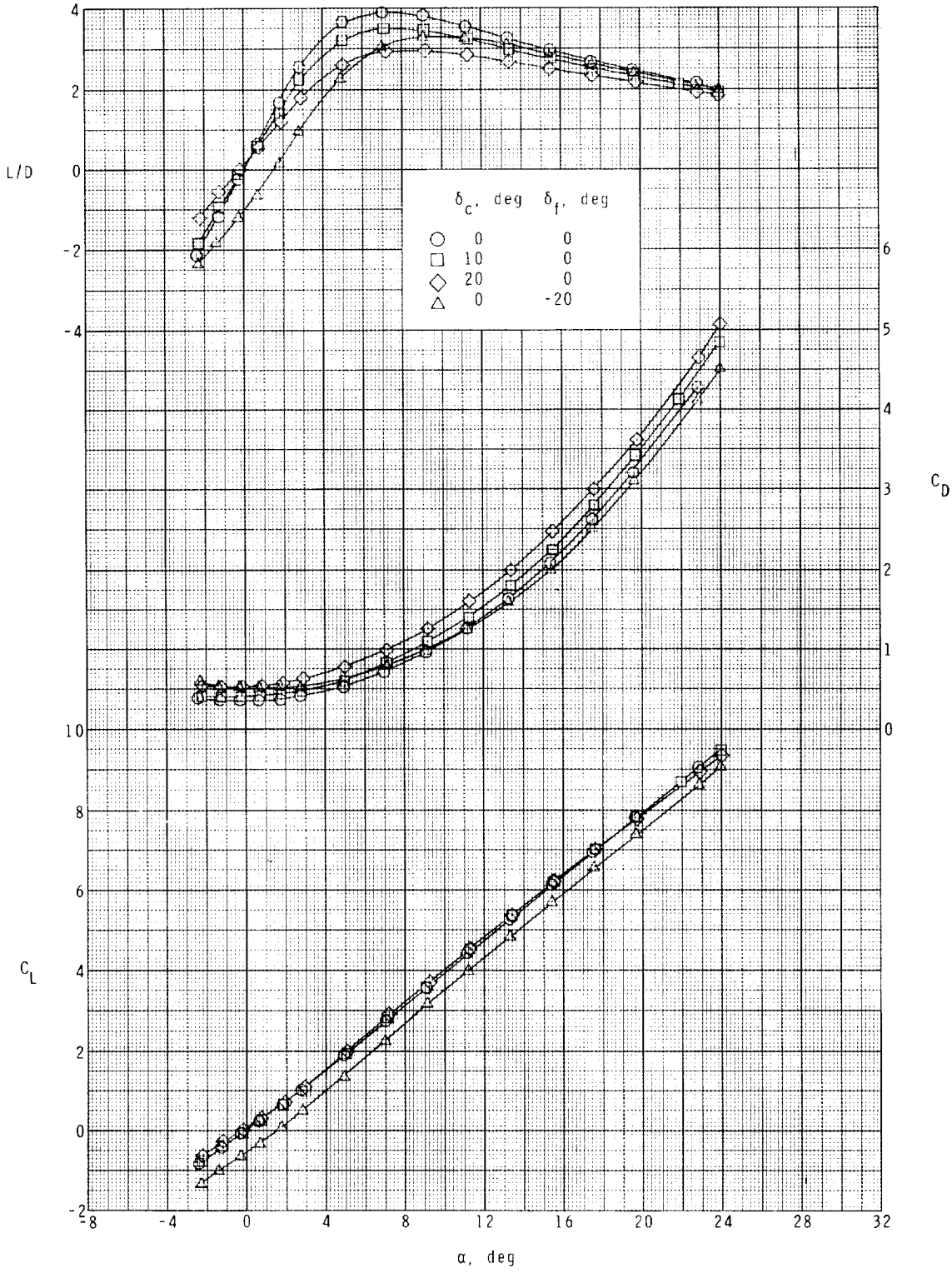

(b) Concluded.

Figure 8.- Continued.

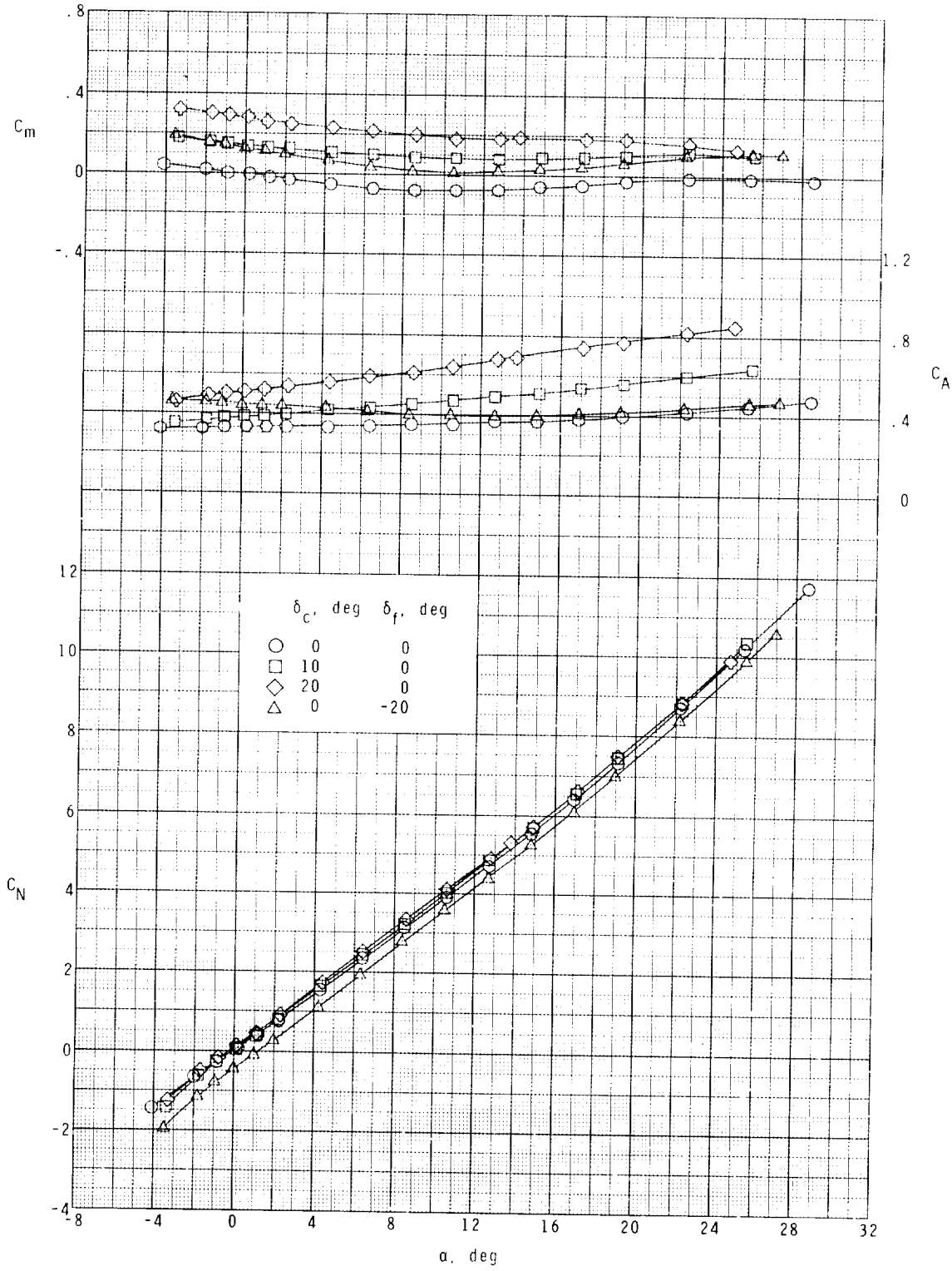

(c) M = 2.30.

Figure 8.- Continued.

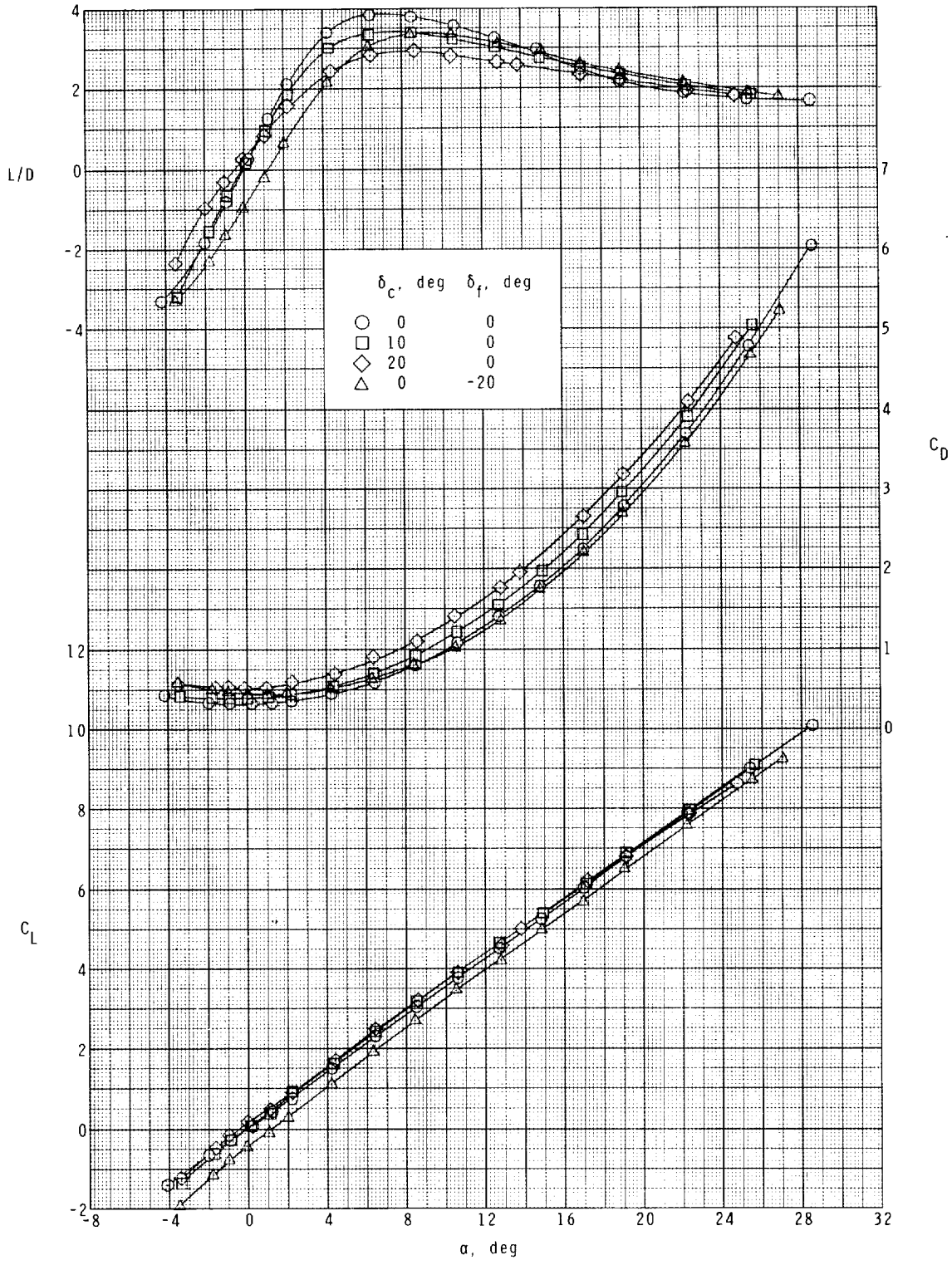

(c) Concluded.

Figure 8.- Continued.

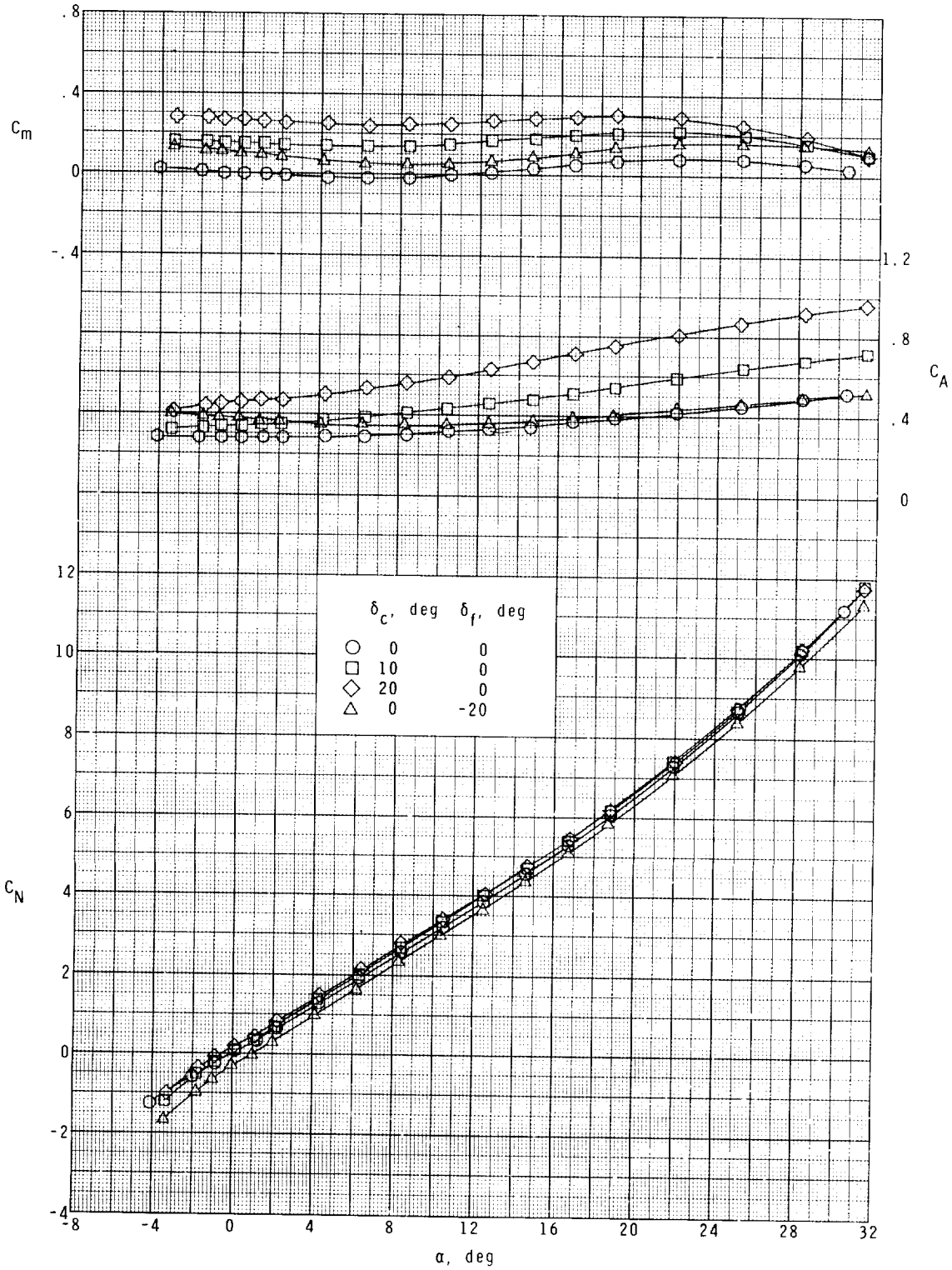

(d) M = 2.96.

Figure 8.- Continued.

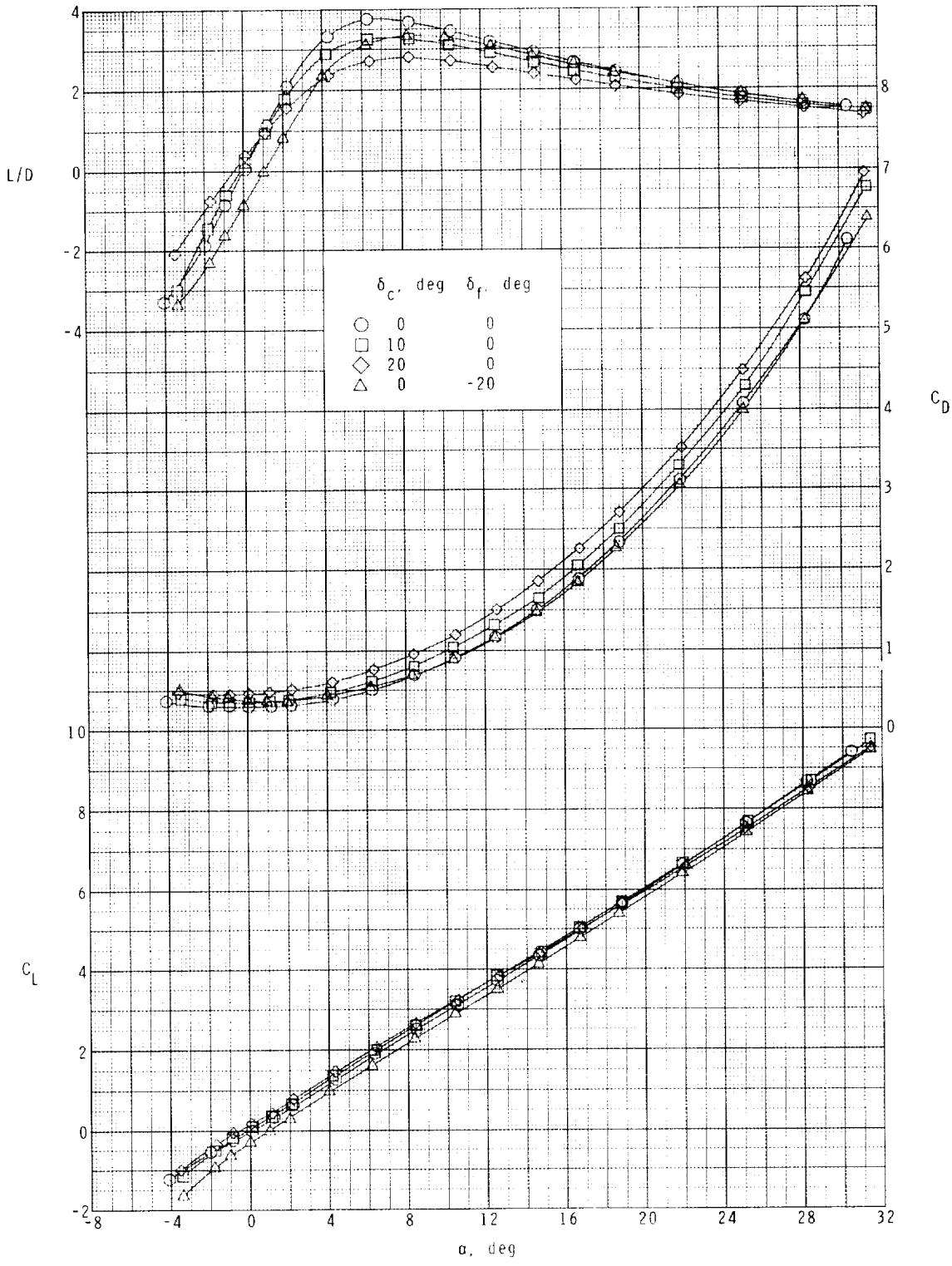

(d) Concluded.

Figure 8.- Continued.

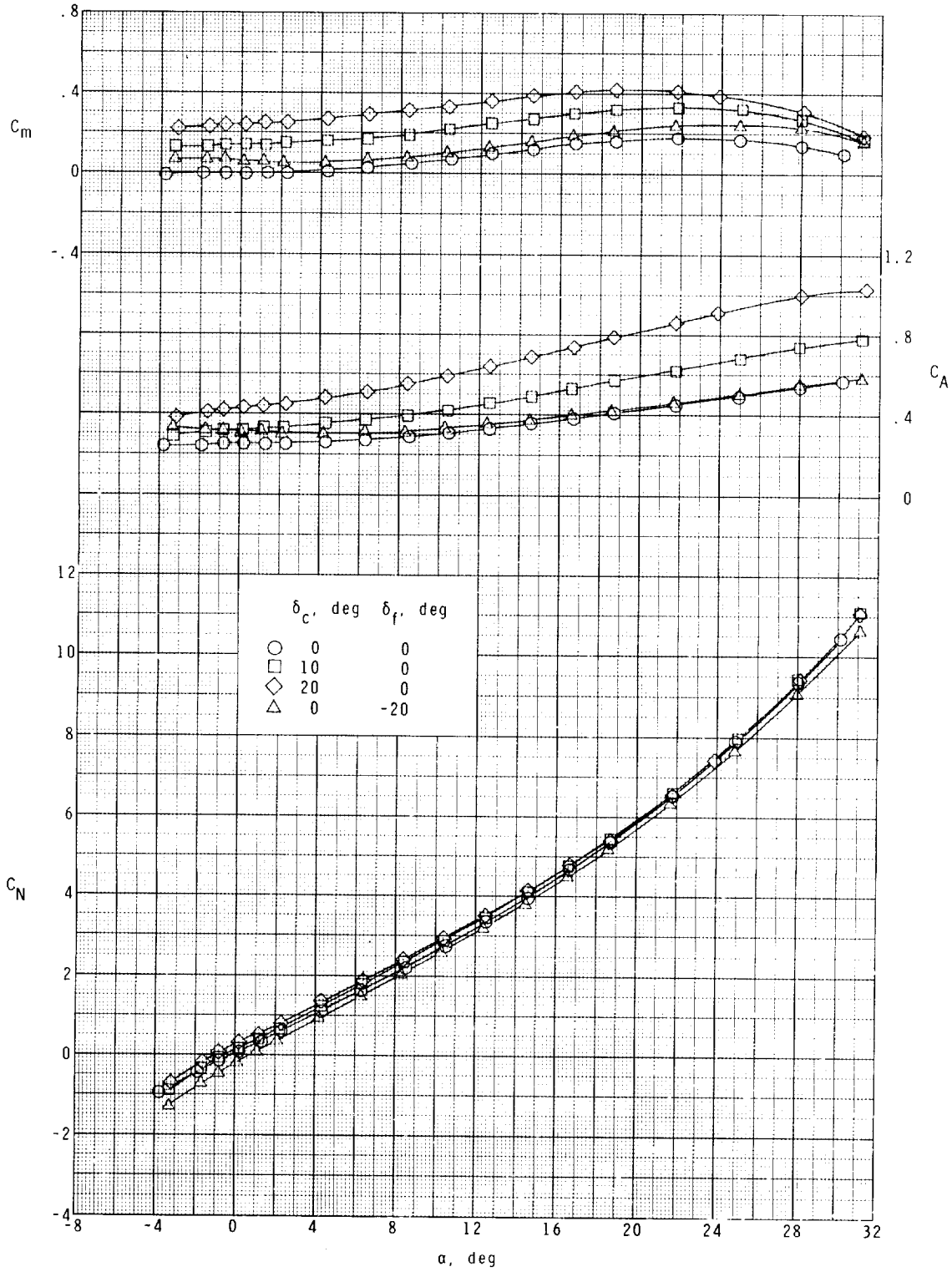

(e) M = 3.95.

Figure 8.- Continued.

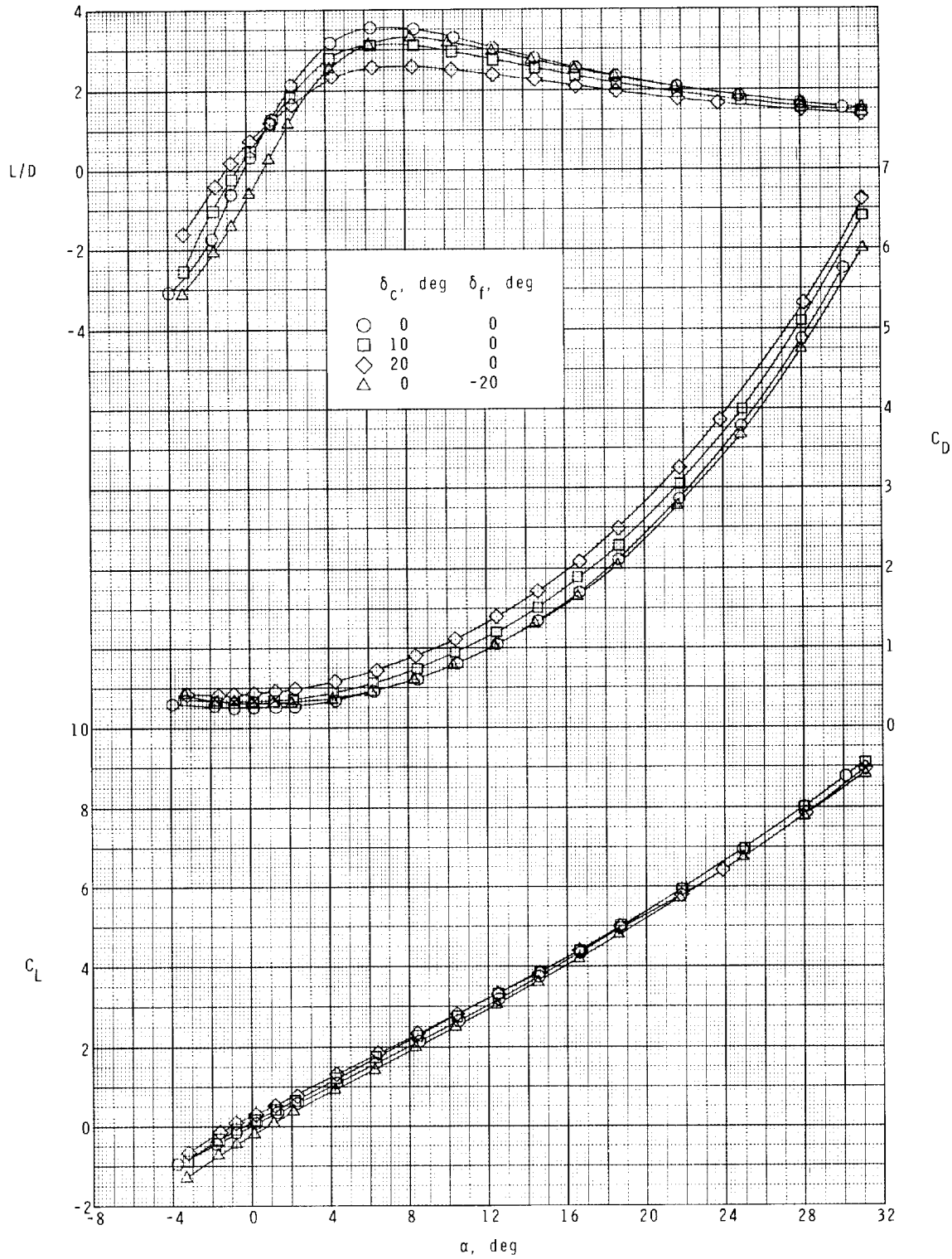

(e) Concluded.

Figure 8.- Continued.

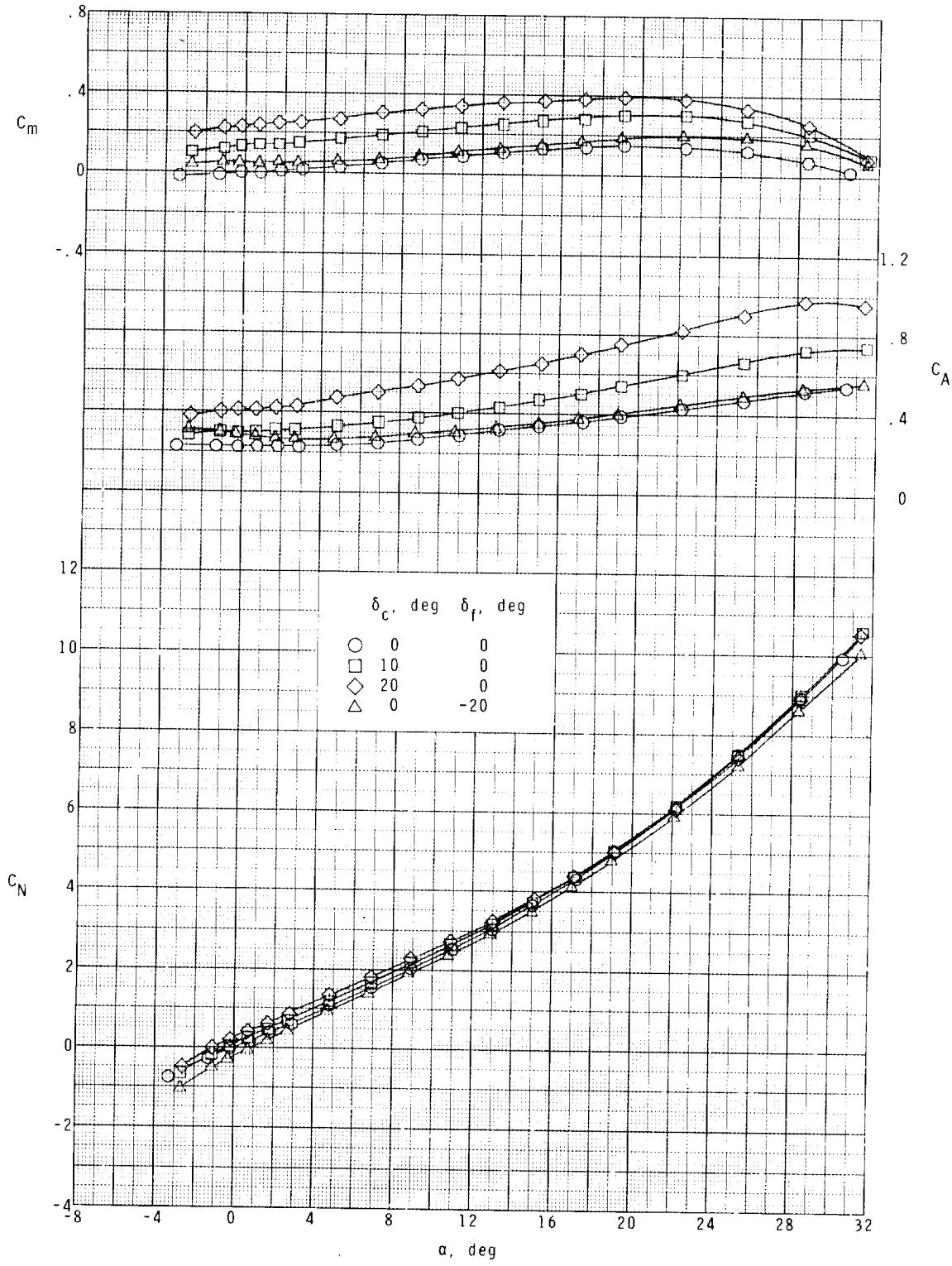

(f) M = 4.63.

Figure 8.- Continued.

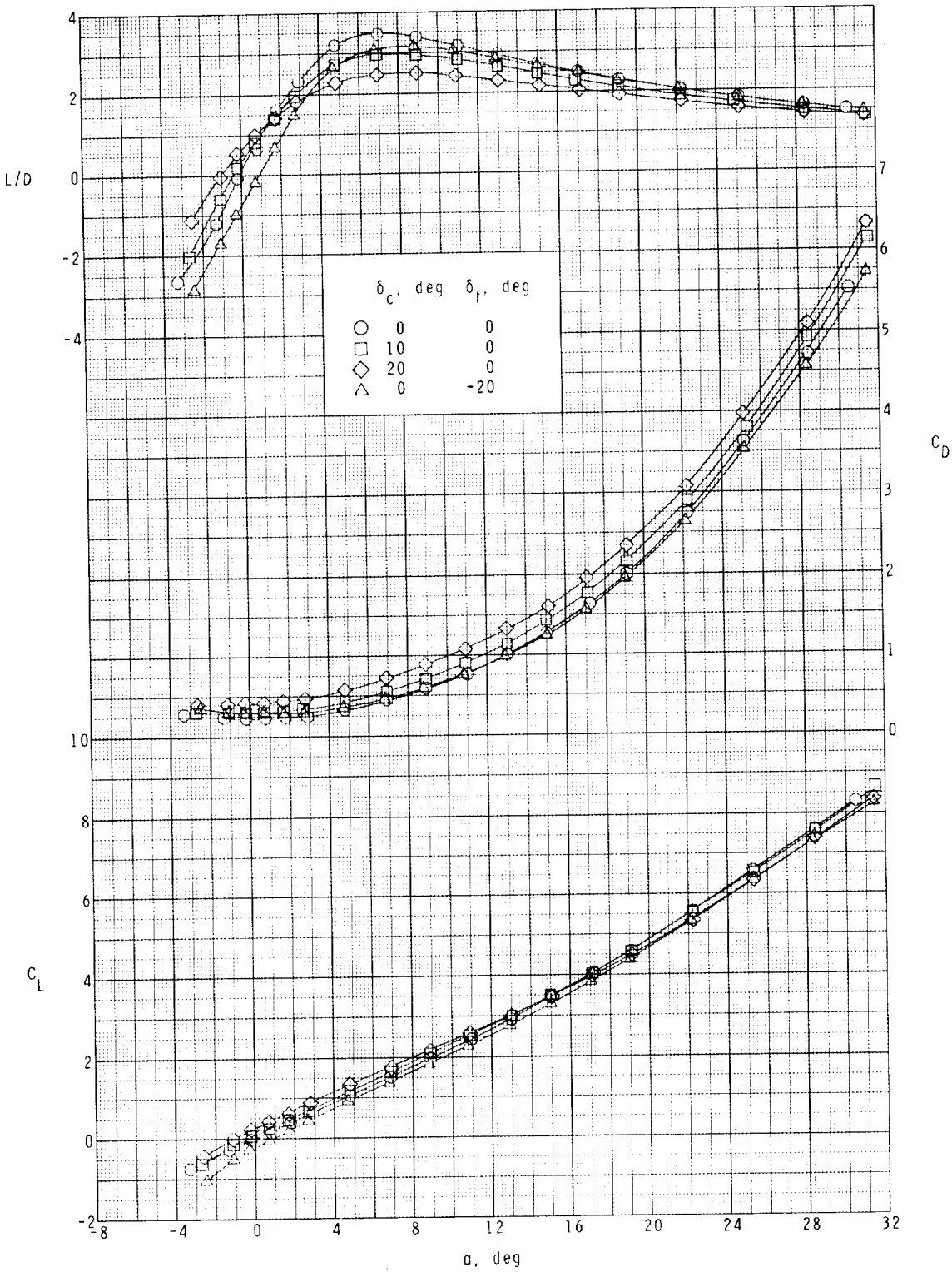

(f) Concluded.

Figure 8.- Concluded.

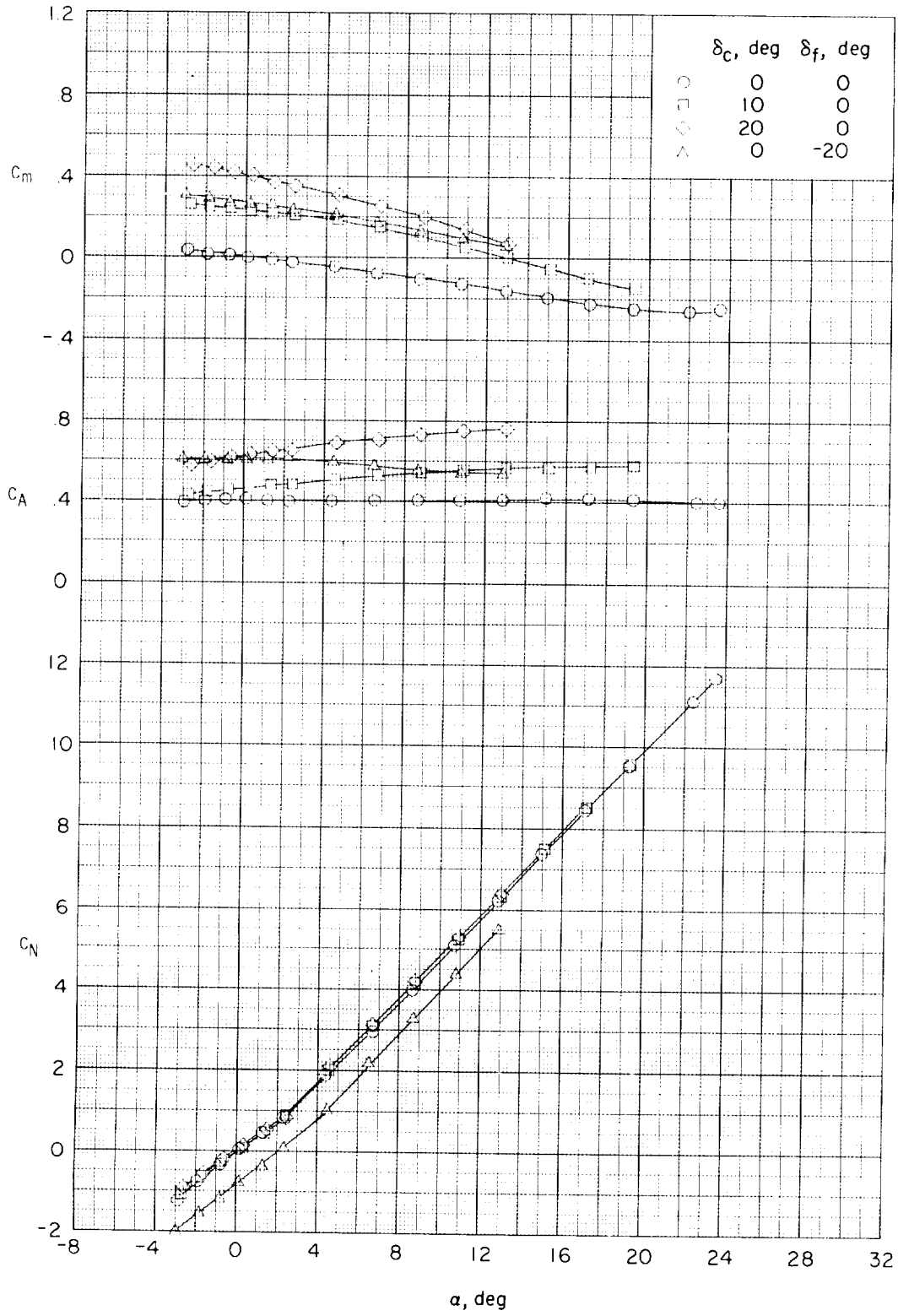

(a) M = 1.50.

Figure 9.- Effects of deflection of the canard C_2 and the wing flap on the longitudinal aerodynamic characteristics of the model. Configuration WBC_2.

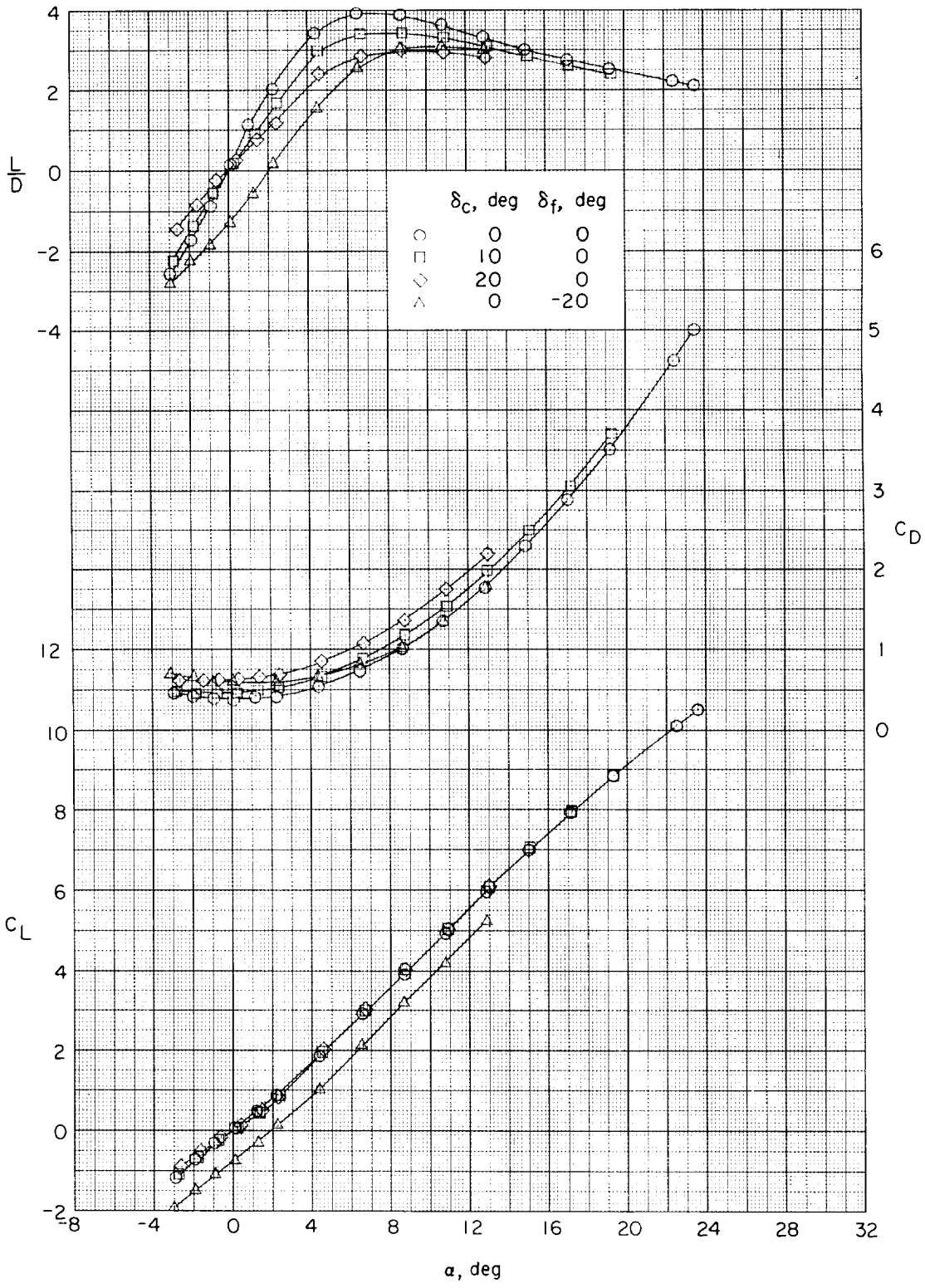

(a) Concluded.

Figure 9.- Continued.

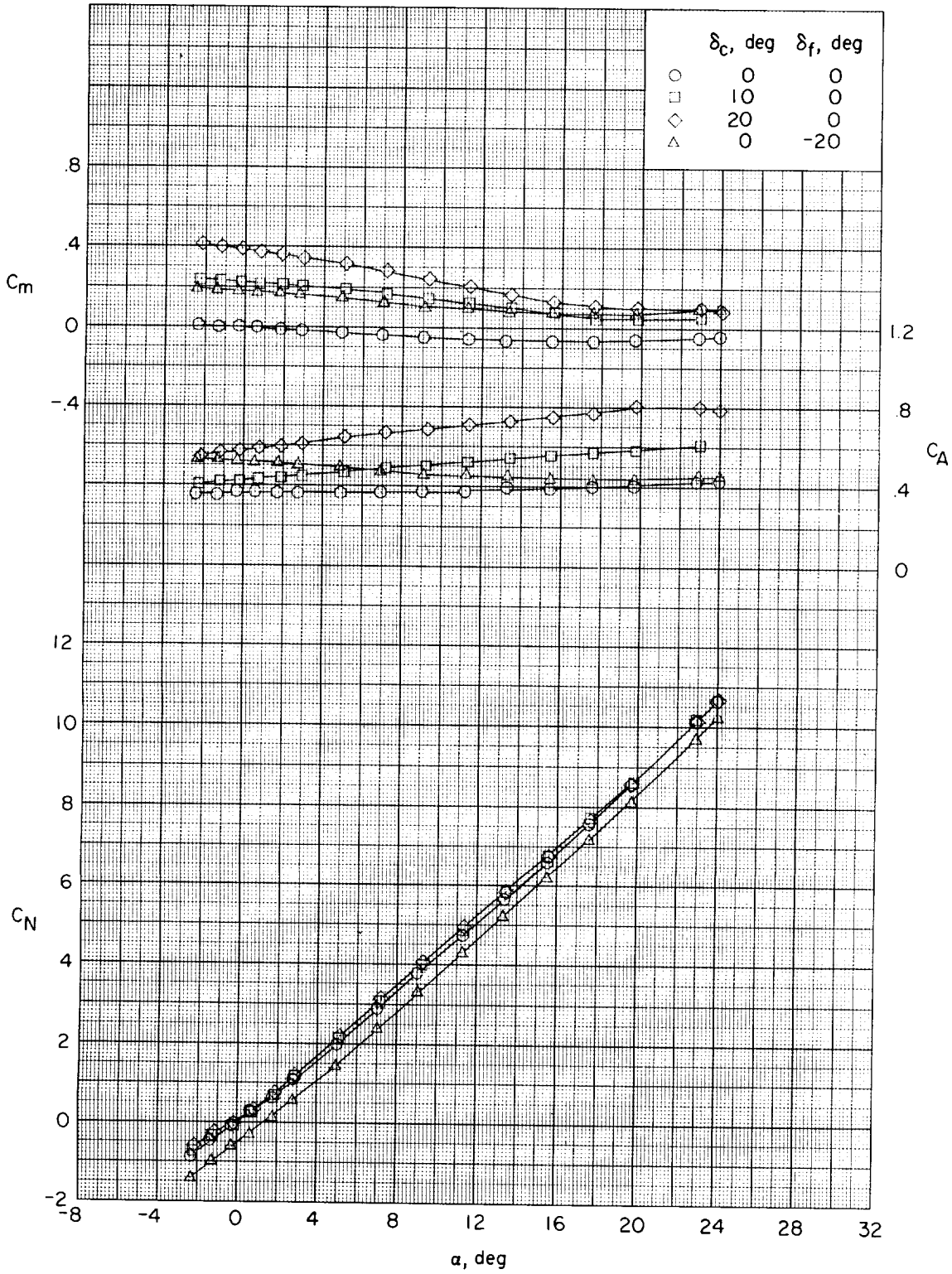

(b) M = 1.90.

Figure 9.- Continued.

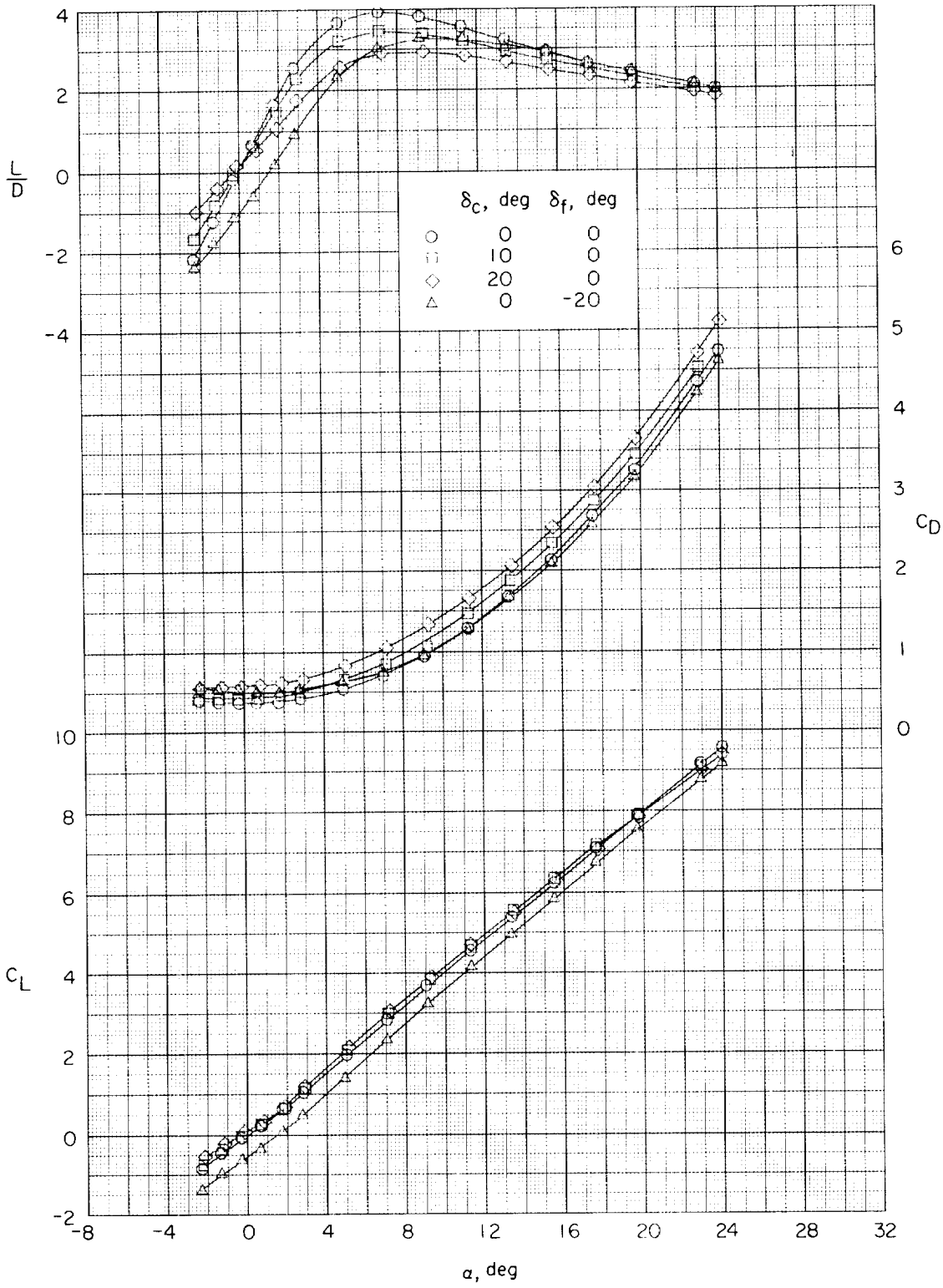

(b) Concluded.

Figure 9.- Continued.

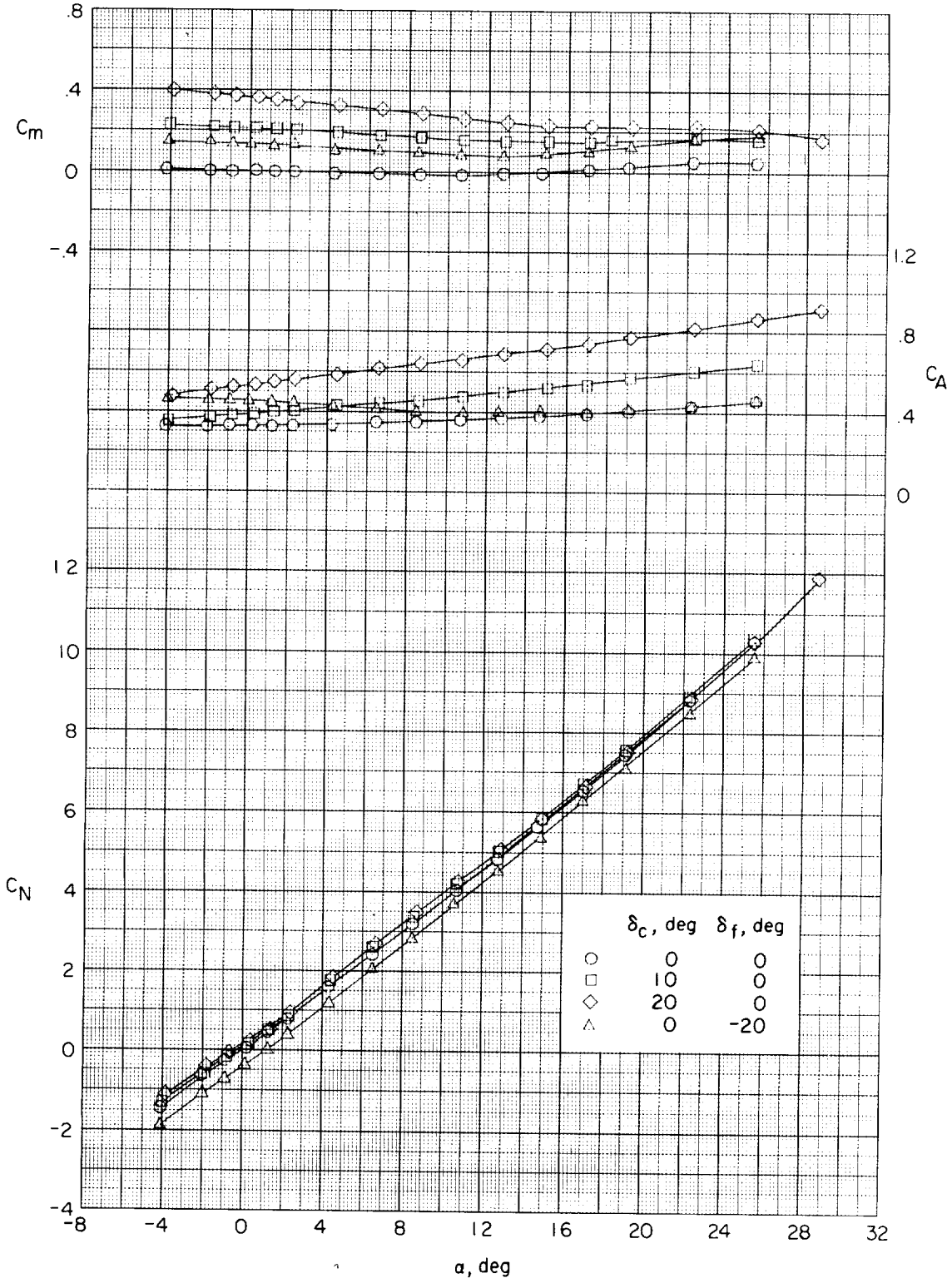

(c) M = 2.30.

Figure 9.- Continued.

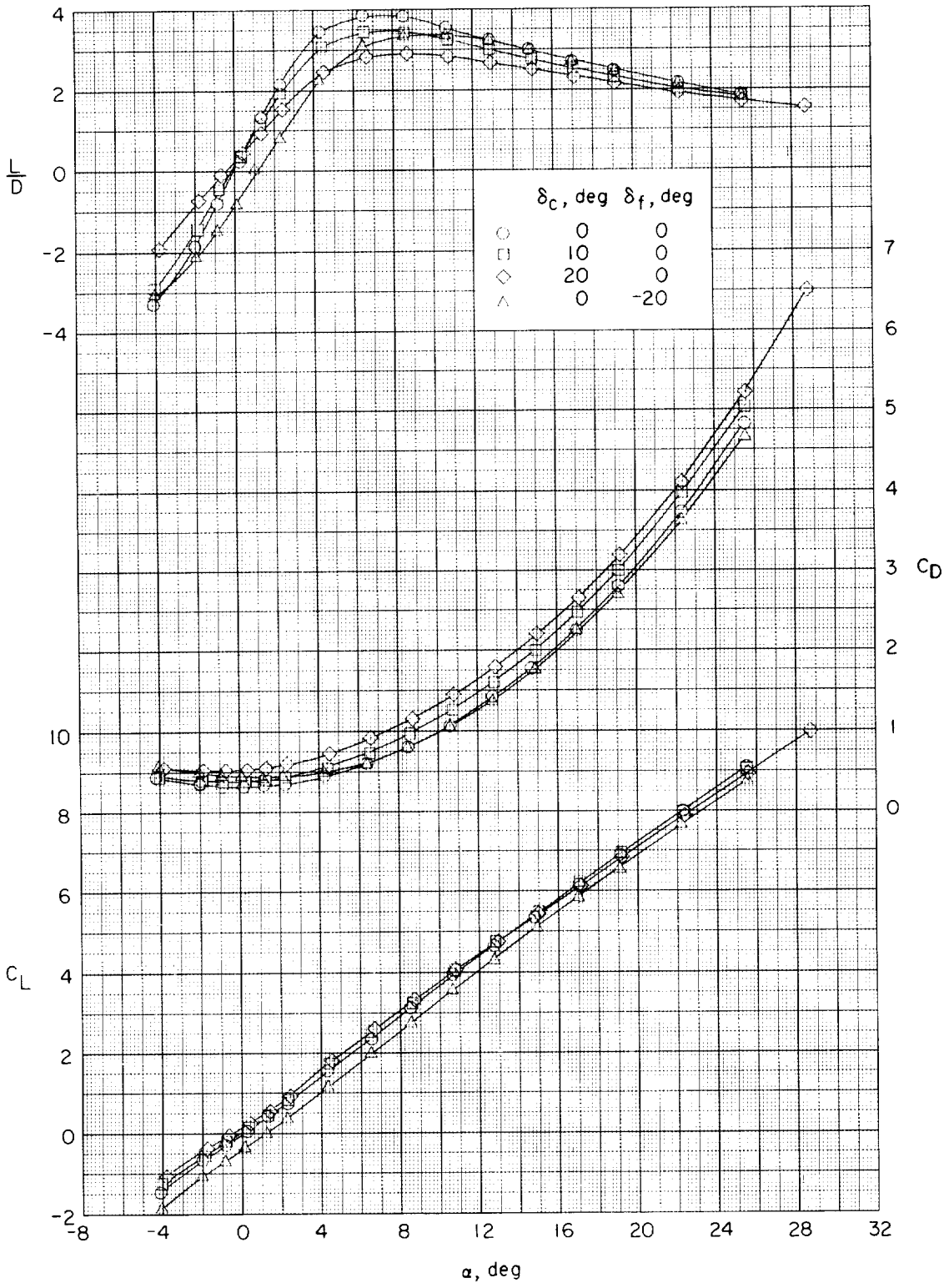

(c) Concluded.

Figure 9.- Continued.

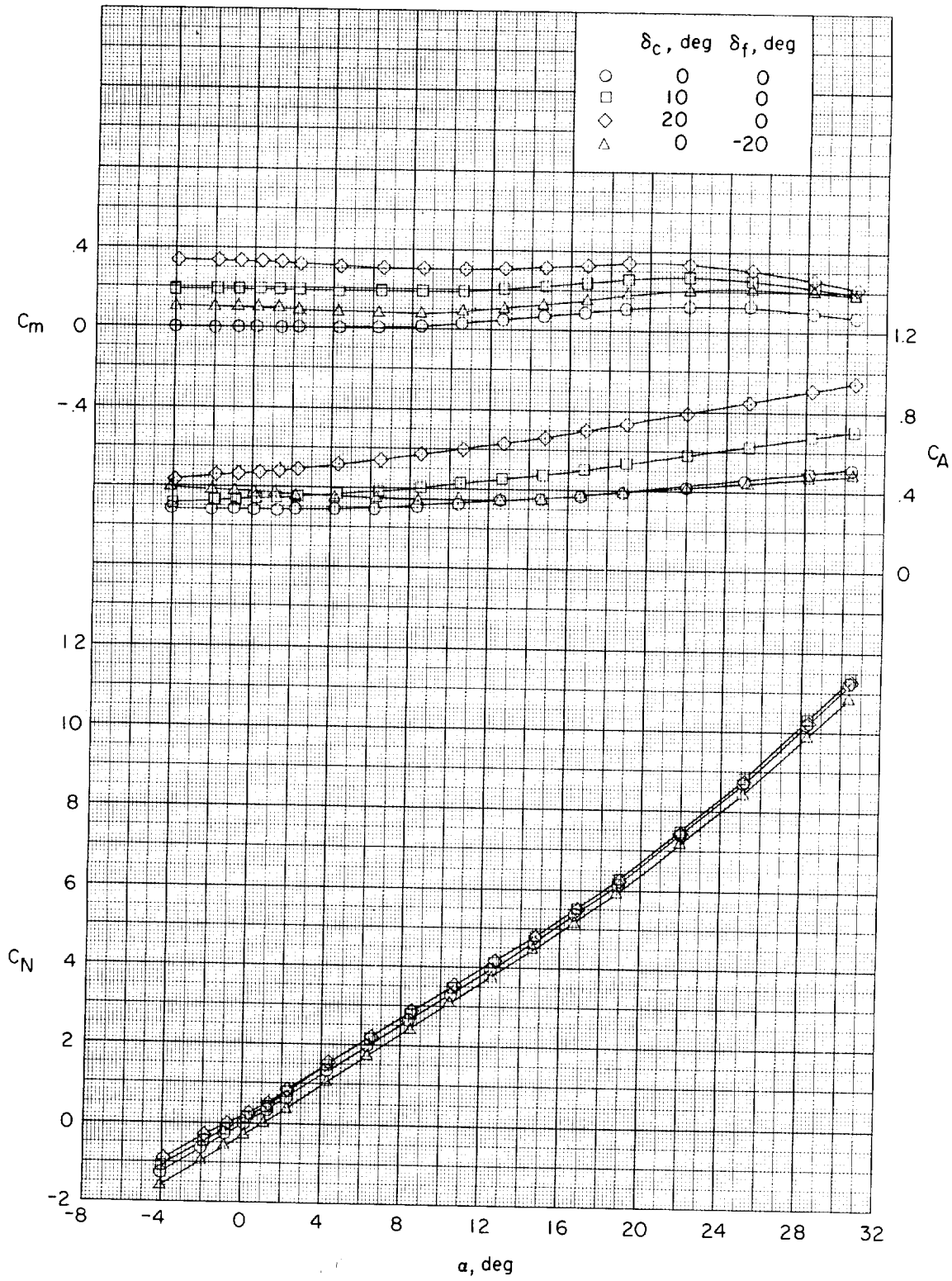

(d) M = 2.96.

Figure 9.- Continued.

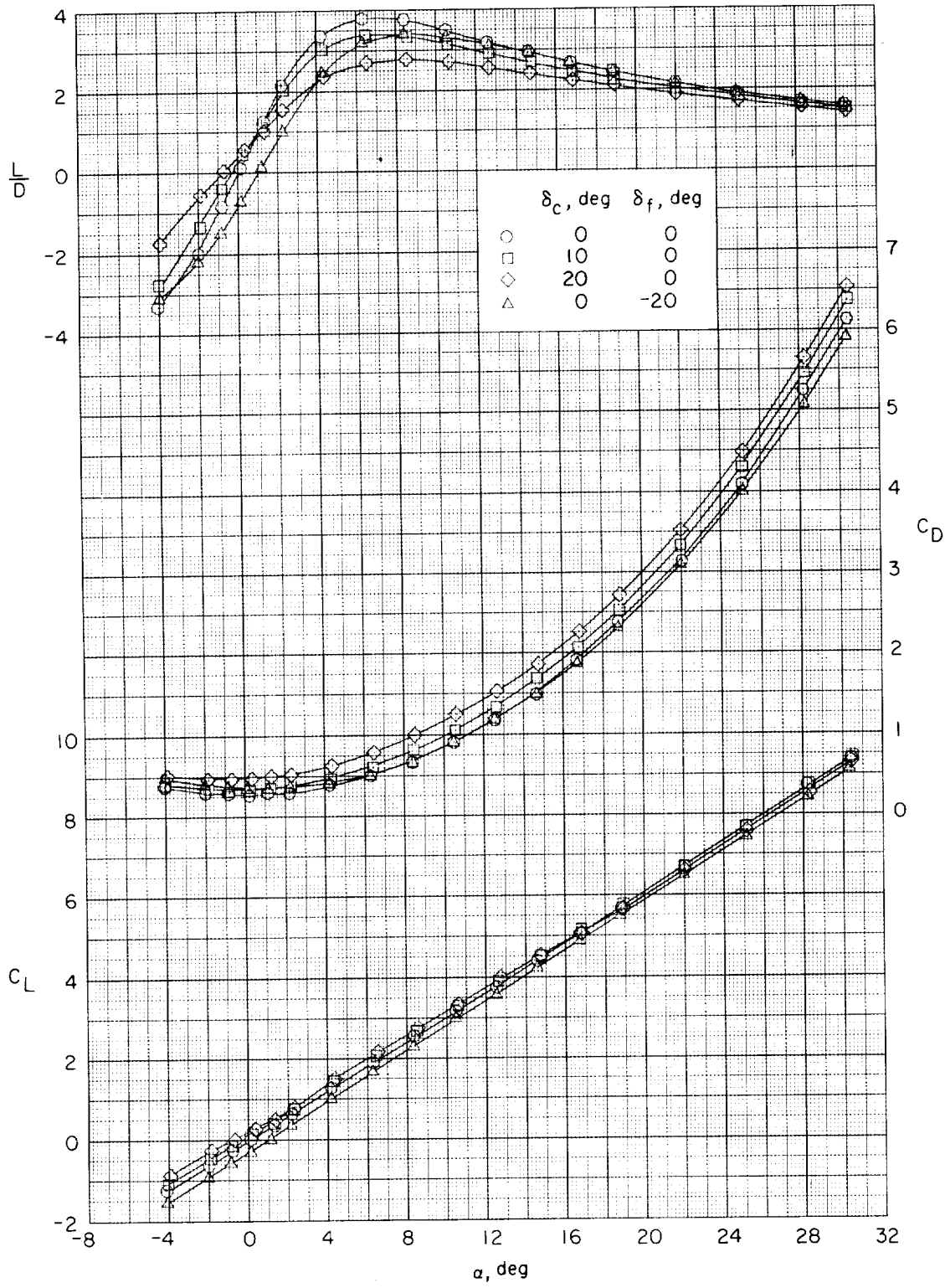

(d) Concluded.

Figure 9.- Continued.

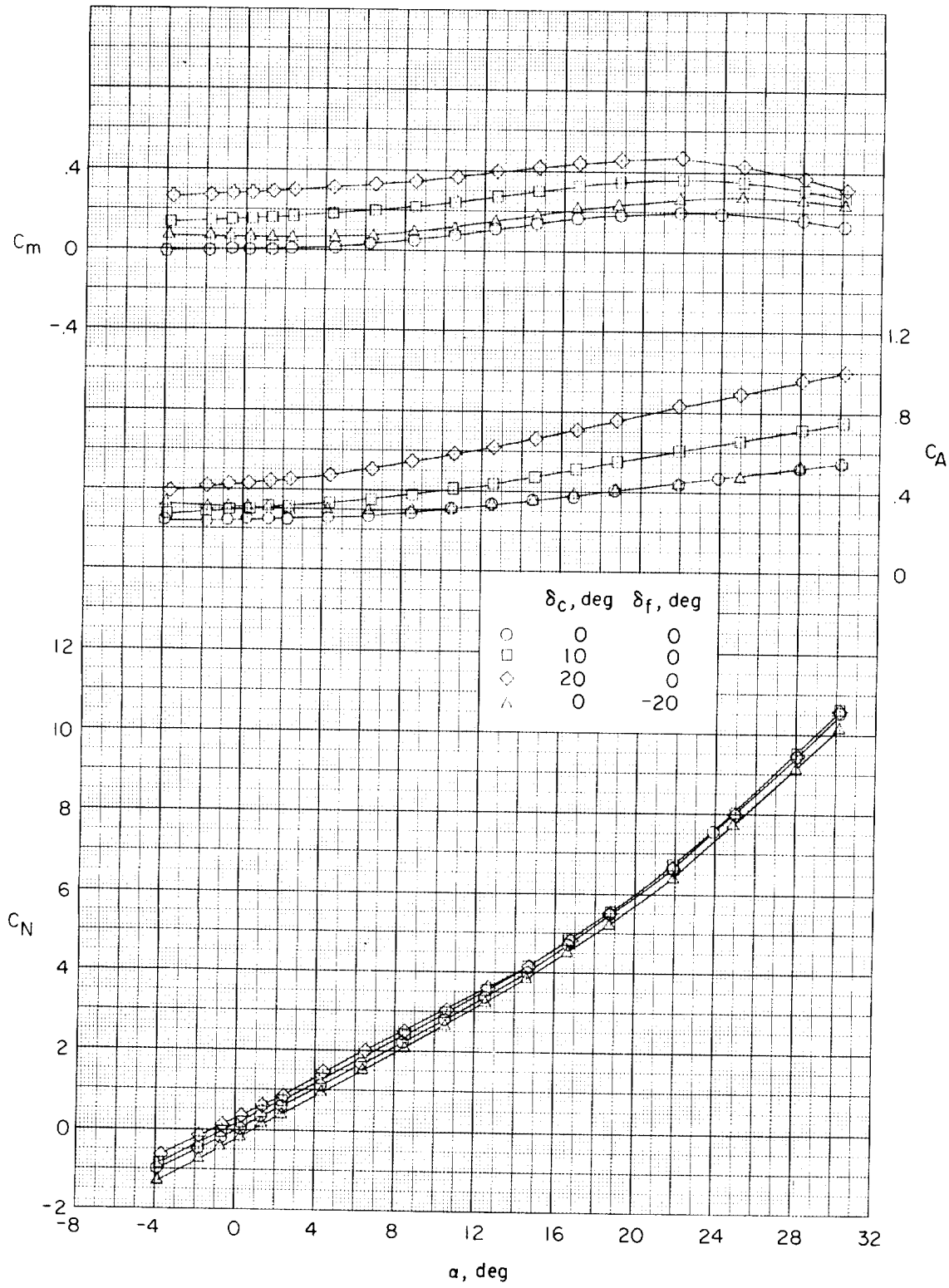

(e) M = 3.95.

Figure 9.- Continued.

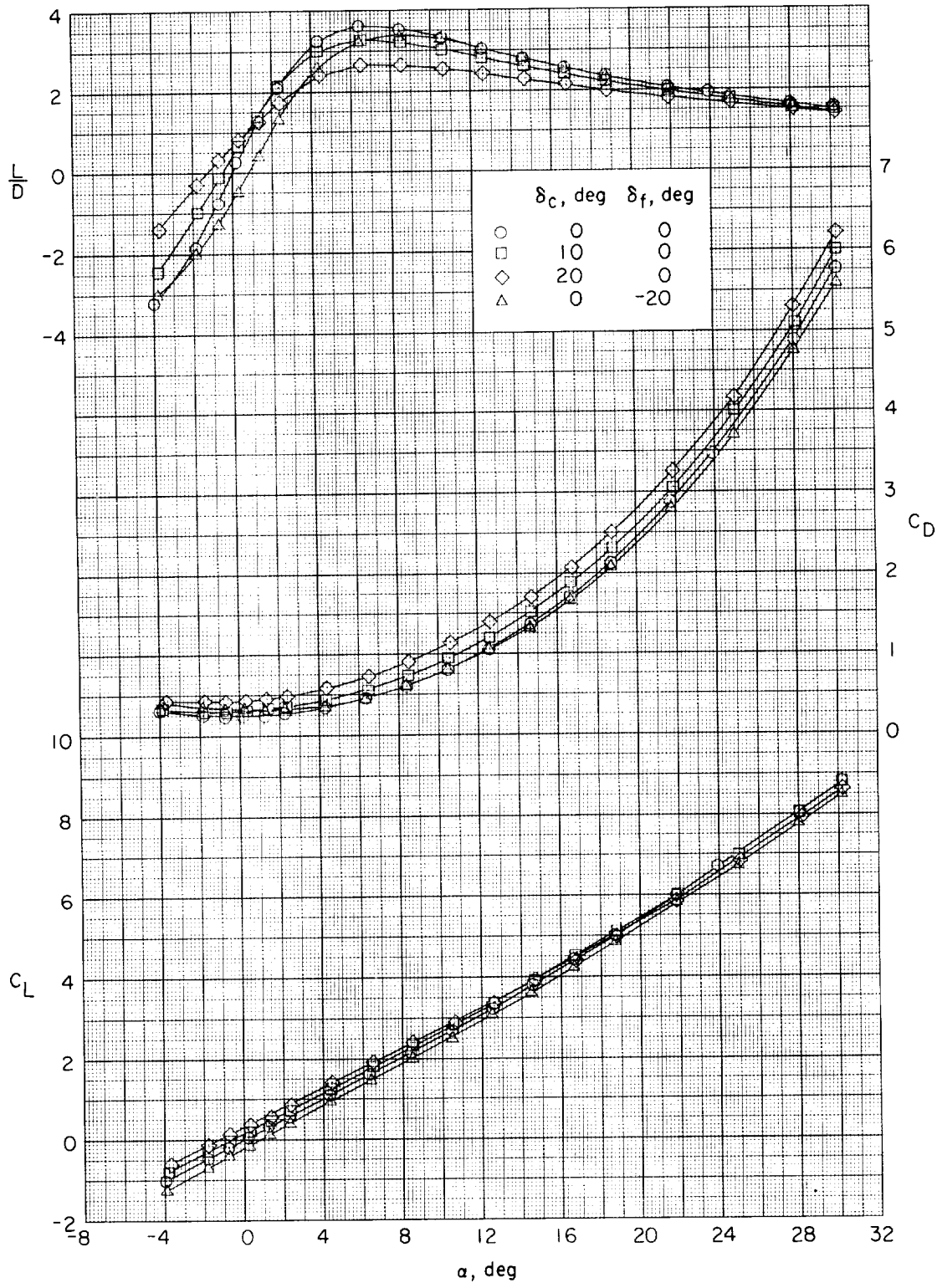

(e) Concluded.

Figure 9.- Continued.

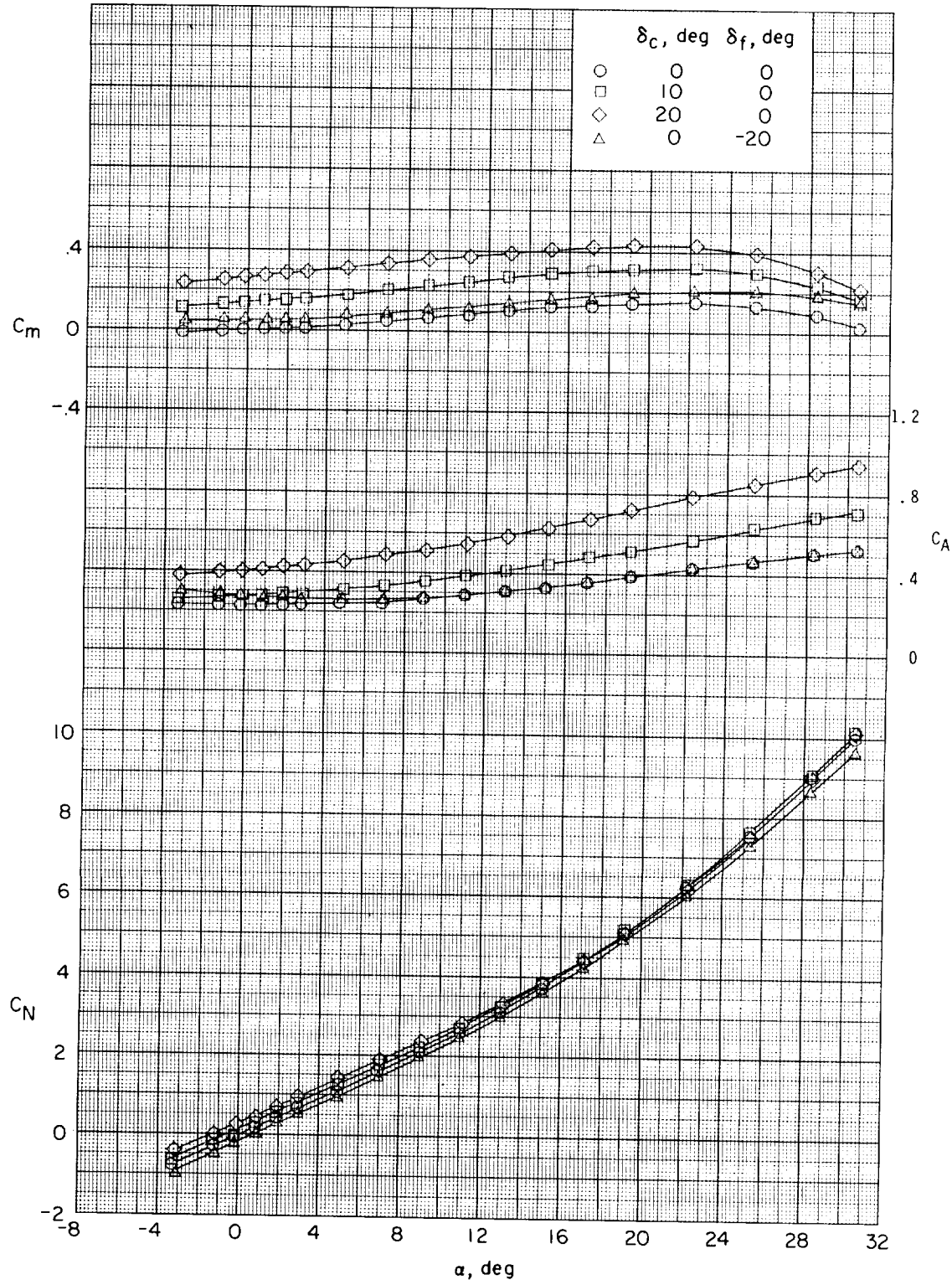

(f) M = 4.63.

Figure 9.- Continued.

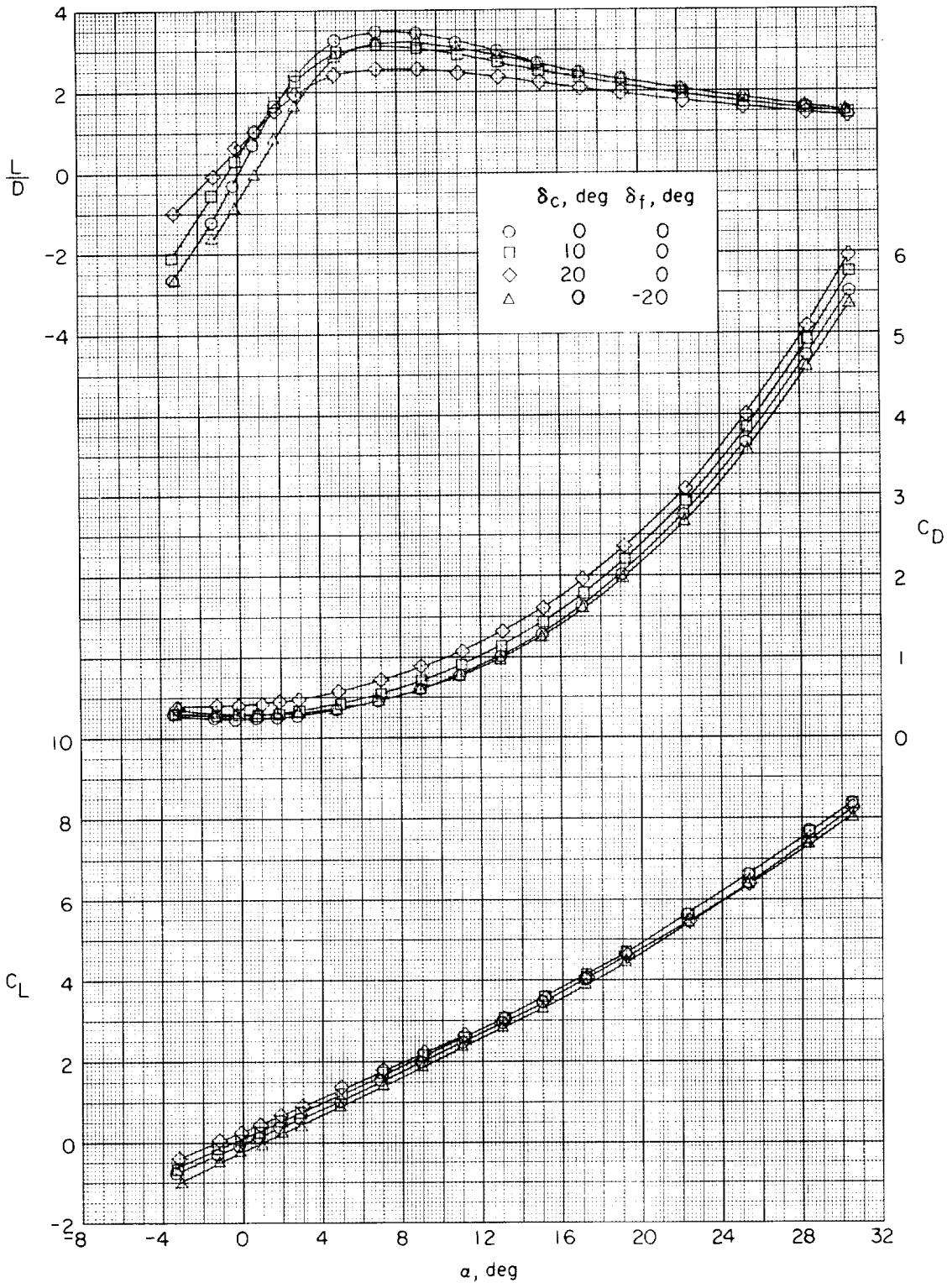

(f) Concluded.

Figure 9.- Concluded.

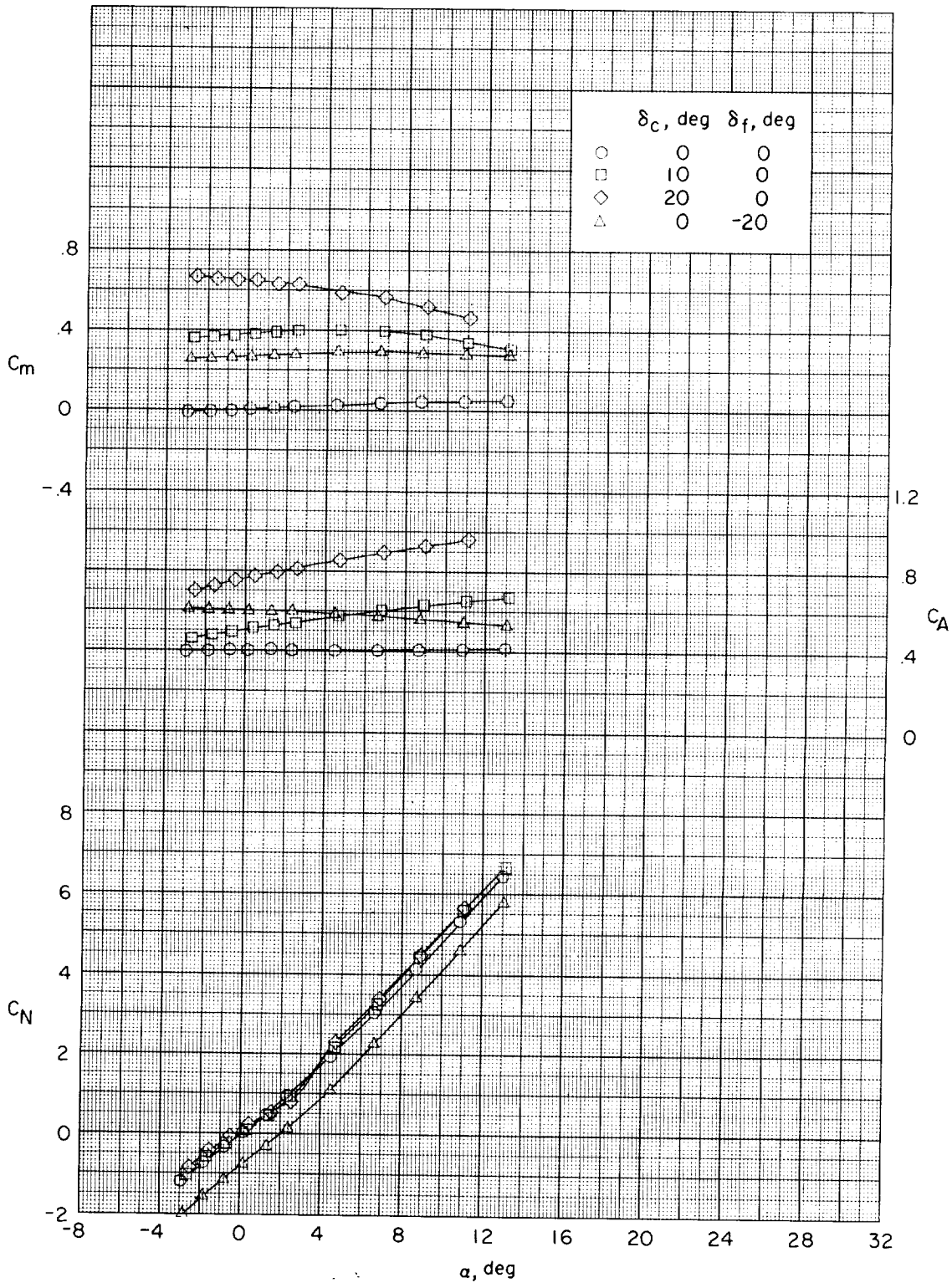

(a) M = 1.50.

Figure 10.- Effects of deflection of the canard C_3 and the wing flap on the longitudinal aerodynamic characteristics of the model. Configuration WBC_3.

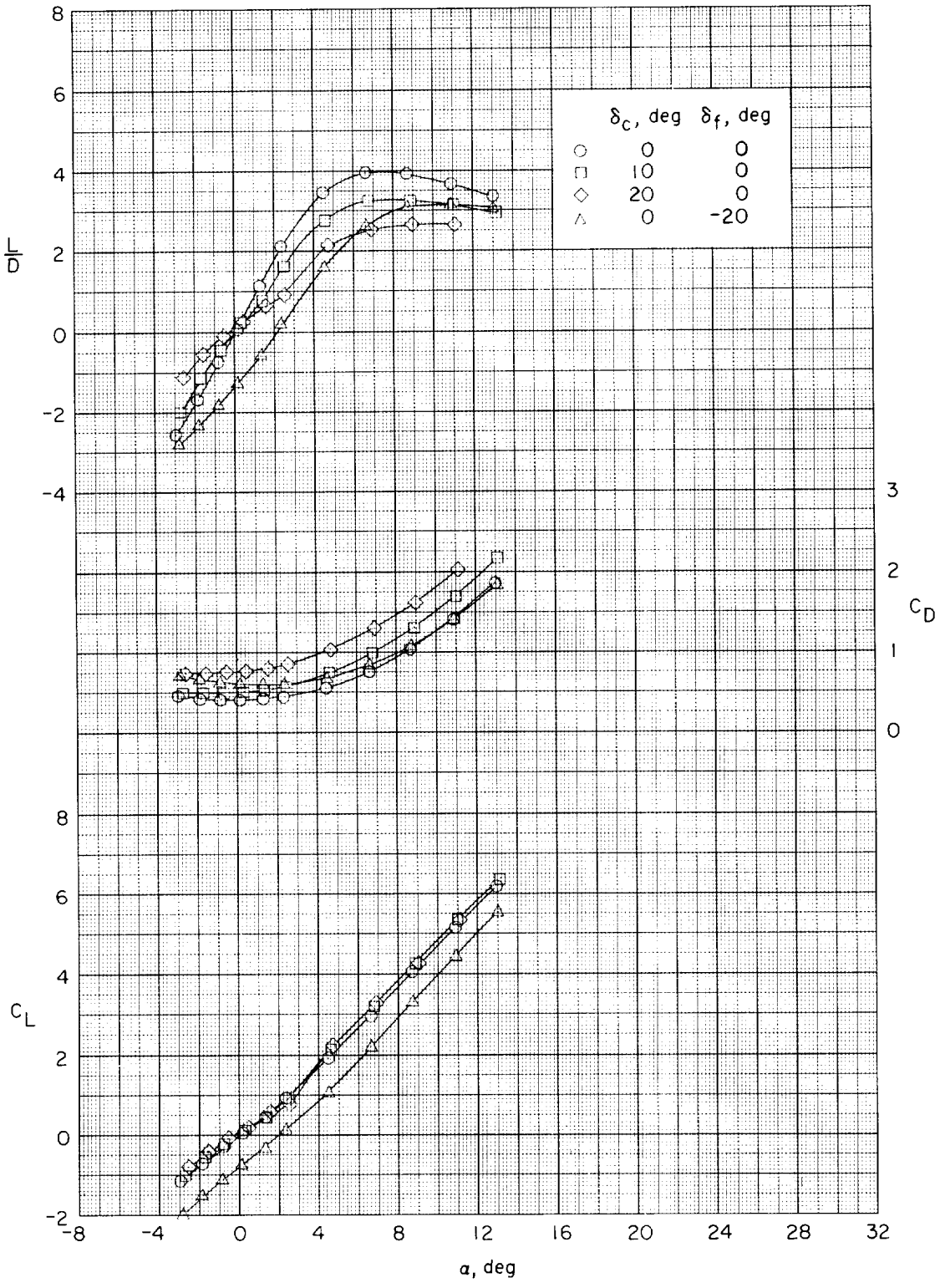

(a) Concluded.

Figure 10.- Continued.

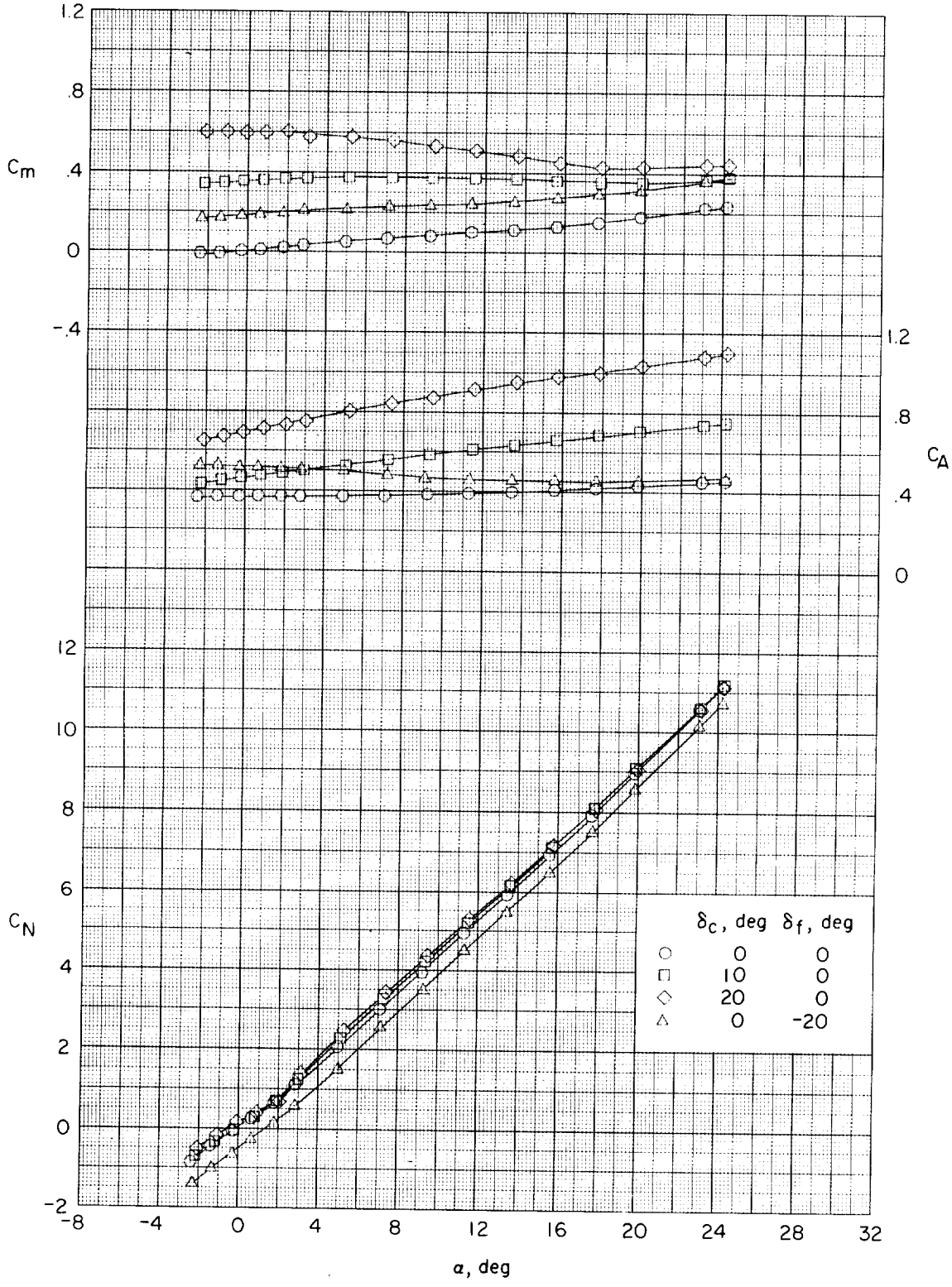

(b) M = 1.90.

Figure 10.- Continued.

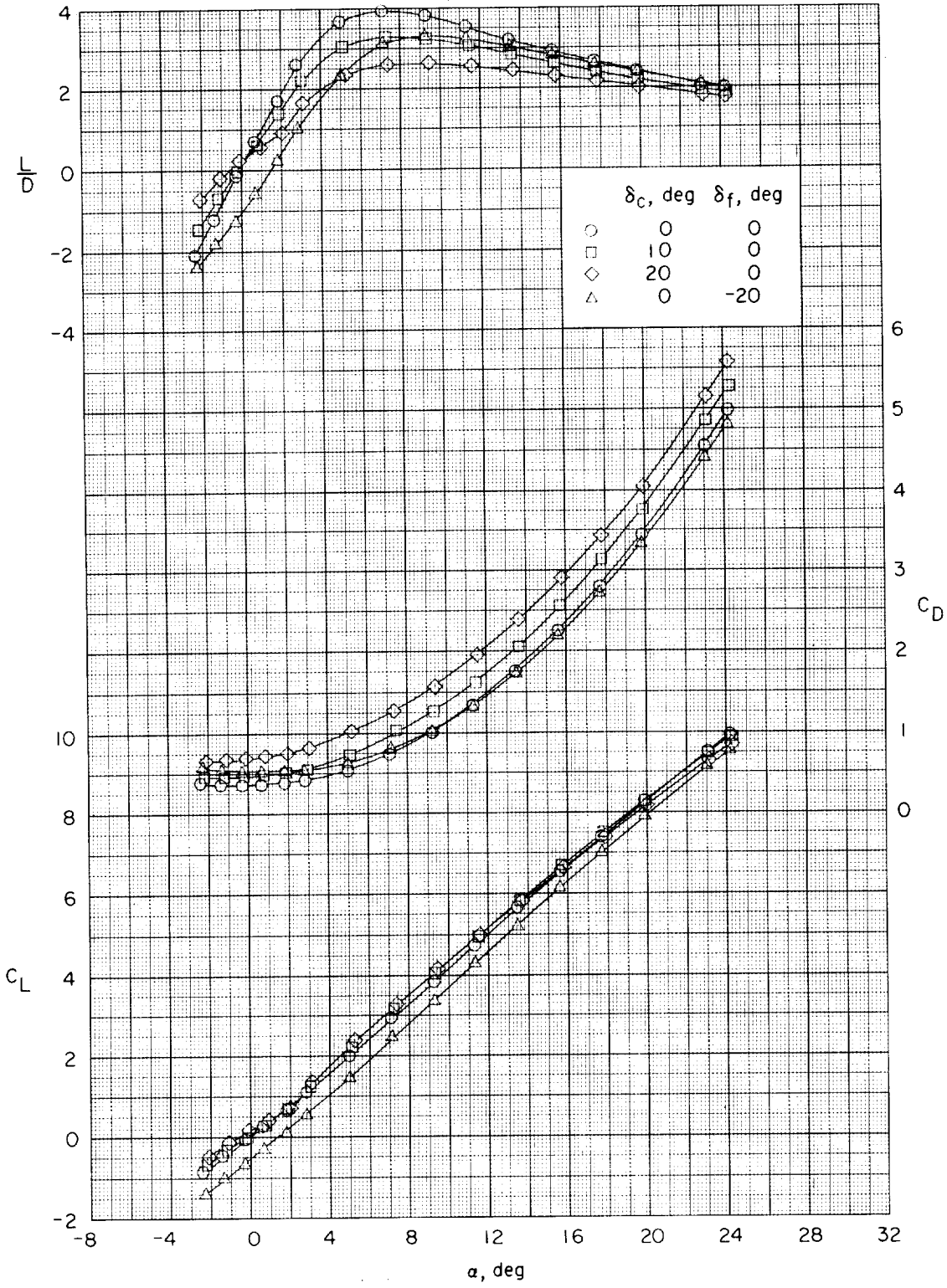

(b) Concluded.

Figure 10.- Continued.

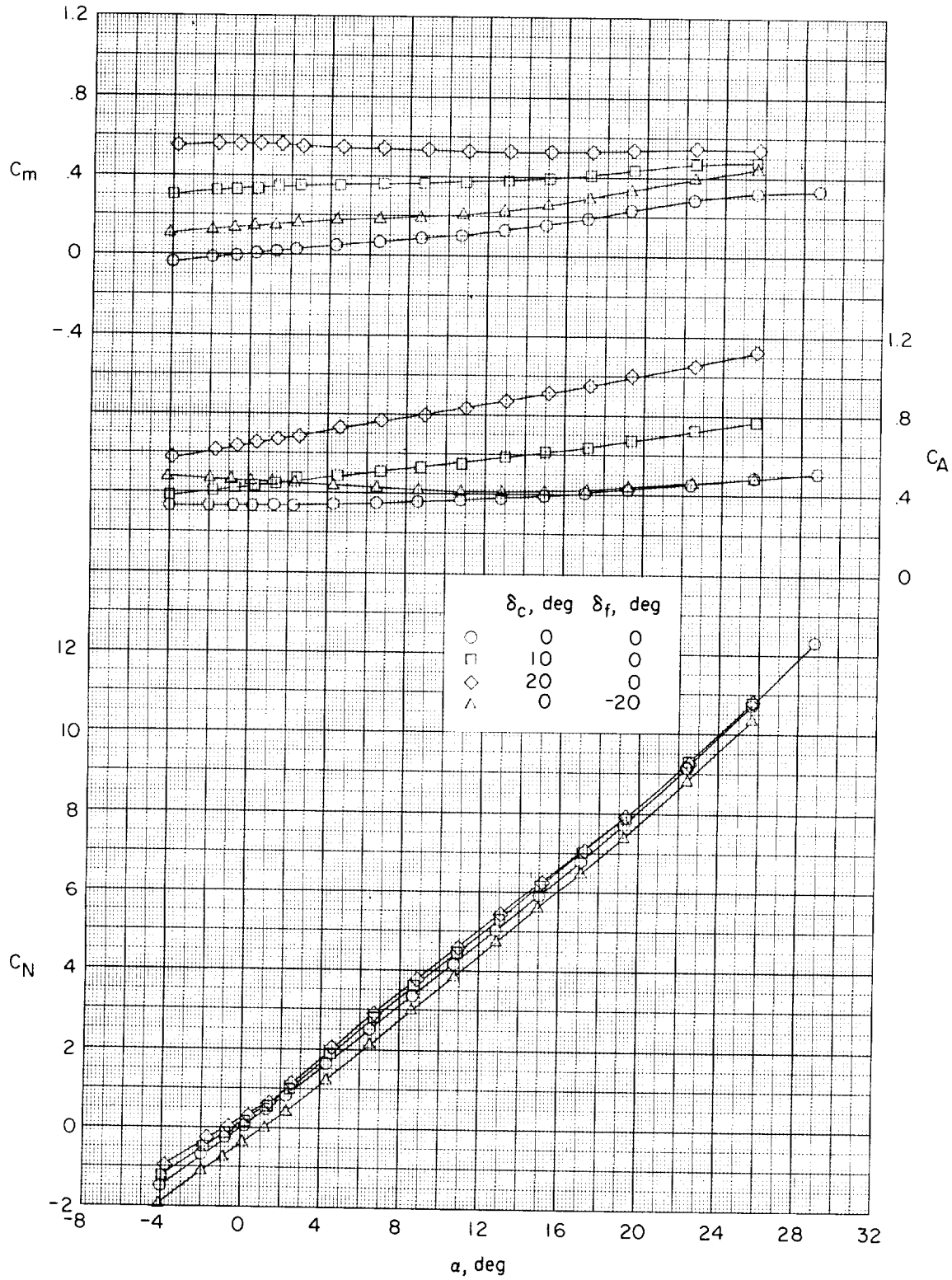

(c) M = 2.30.

Figure 10.- Continued.

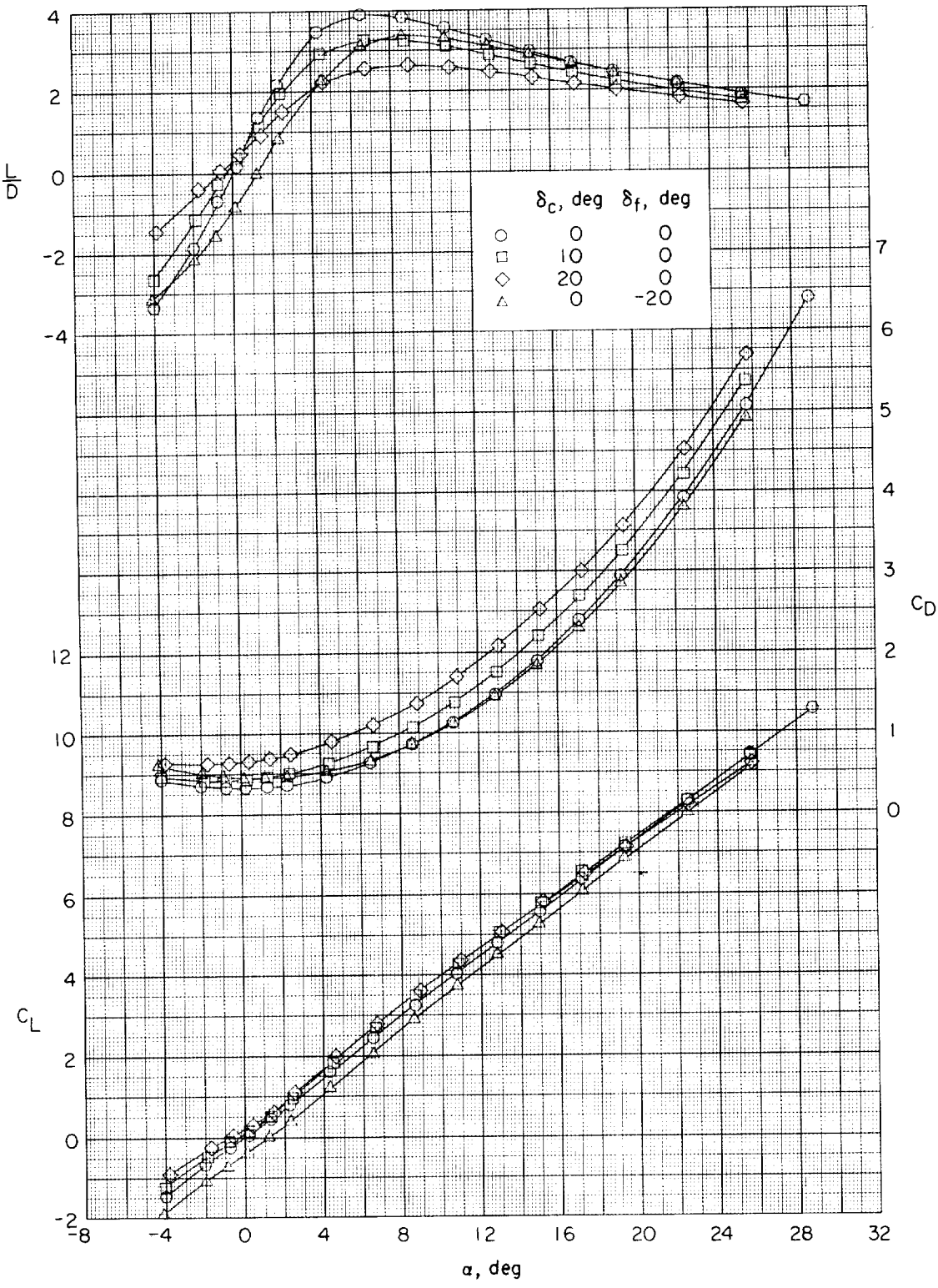

(c) Concluded.

Figure 10.- Continued.

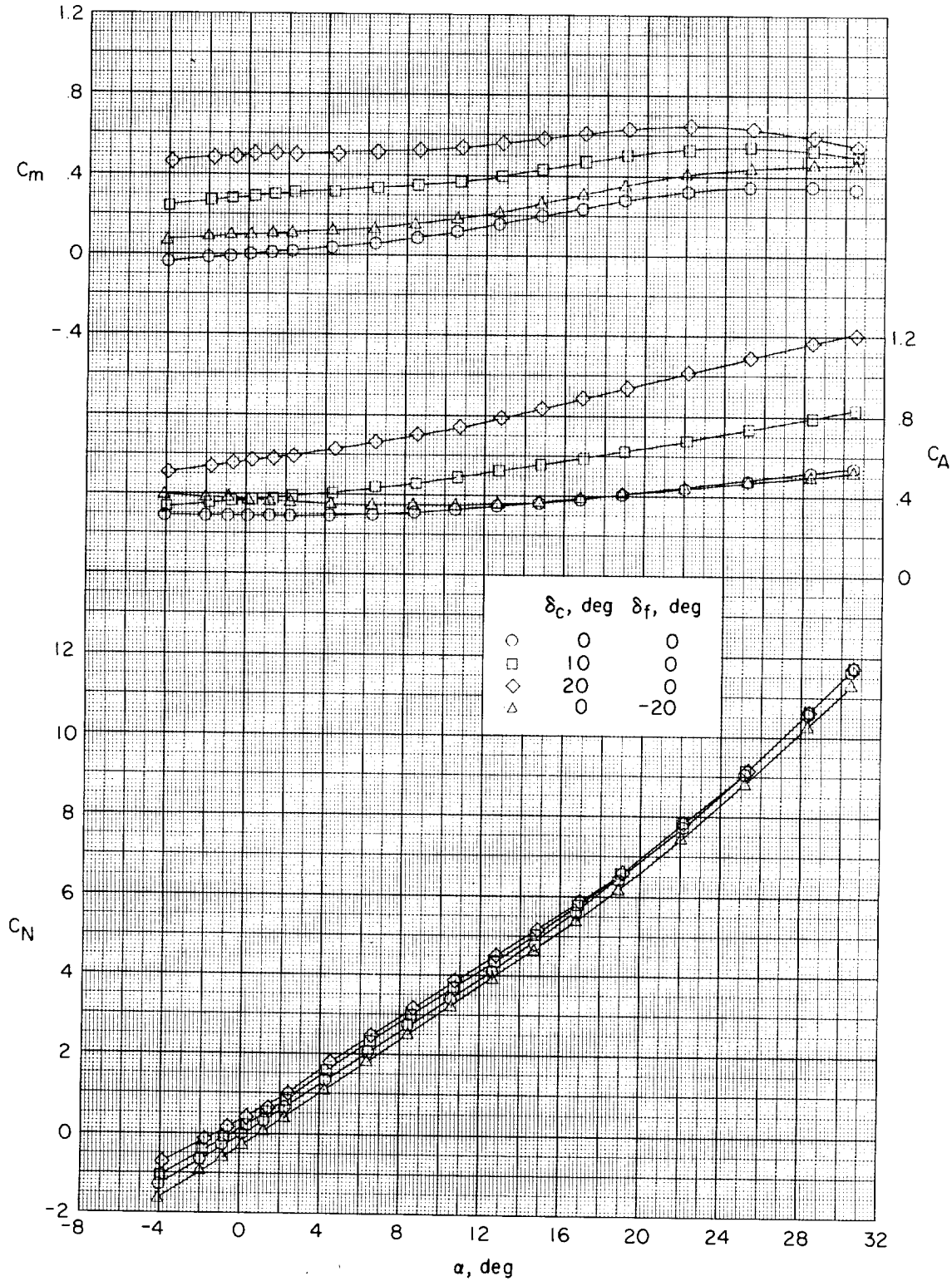

(d) M = 2.96.

Figure 10.- Continued.

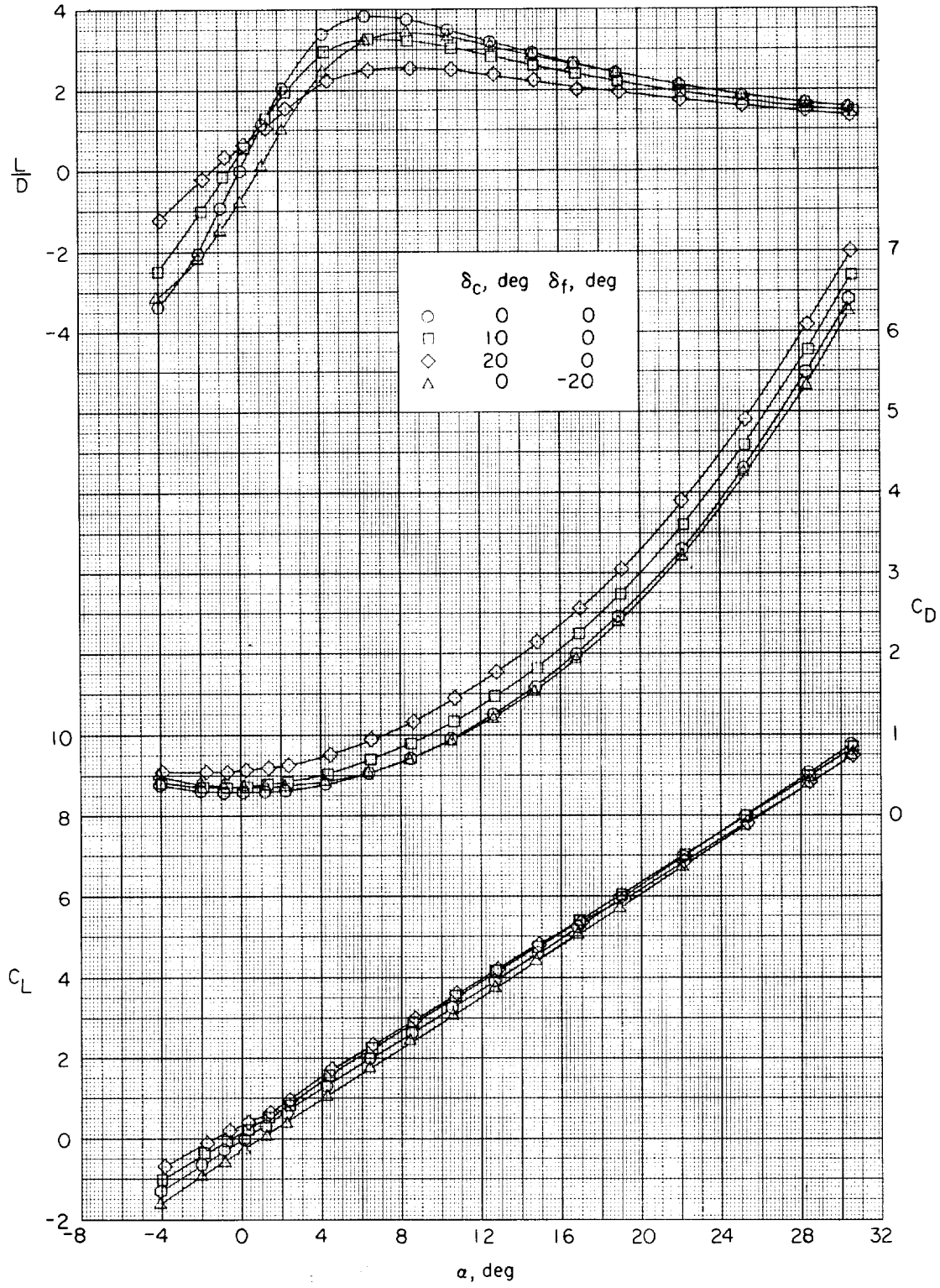

(d) Concluded.

Figure 10.- Continued.

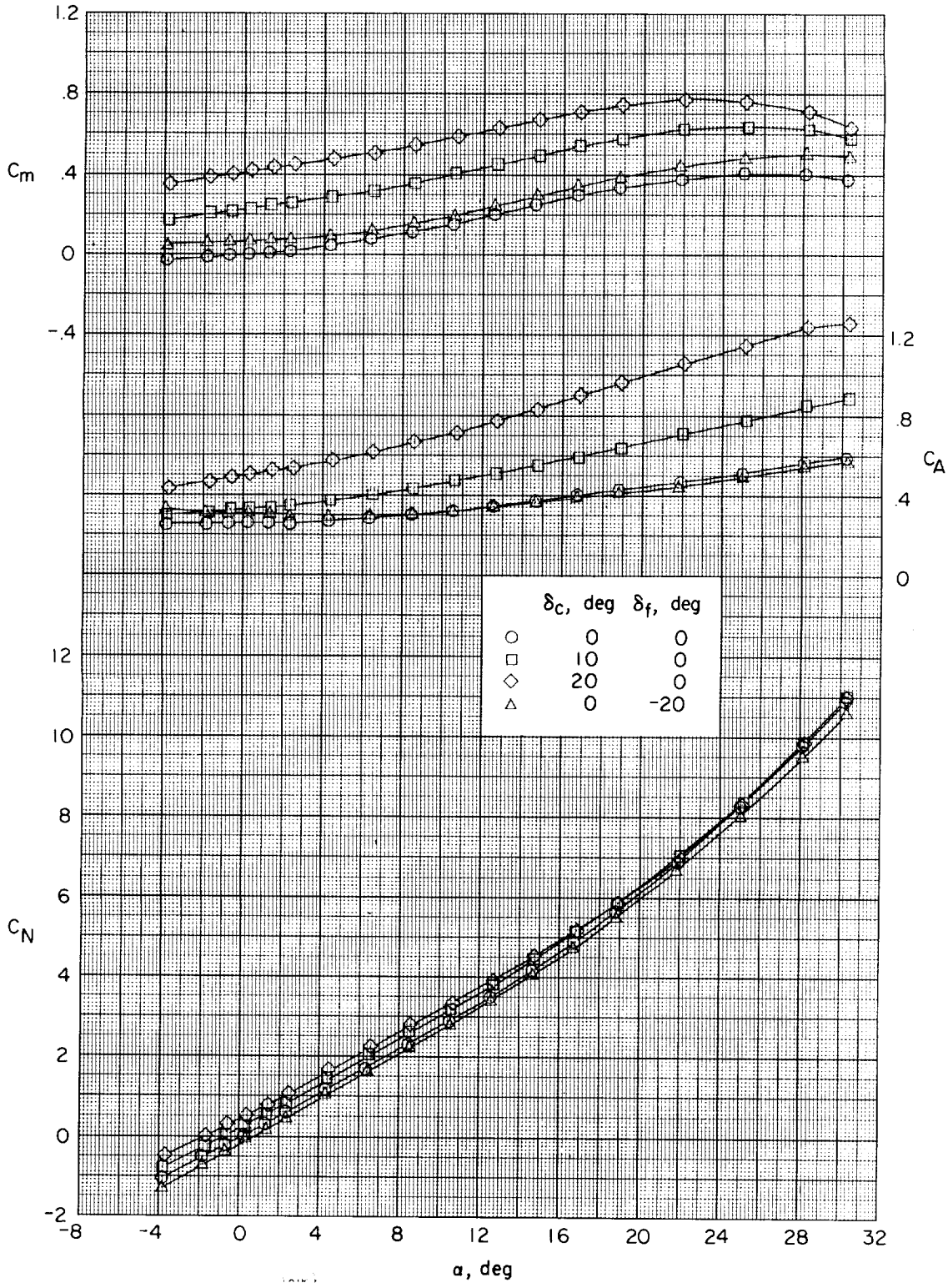

(e) M = 3.95.

Figure 10.- Continued.

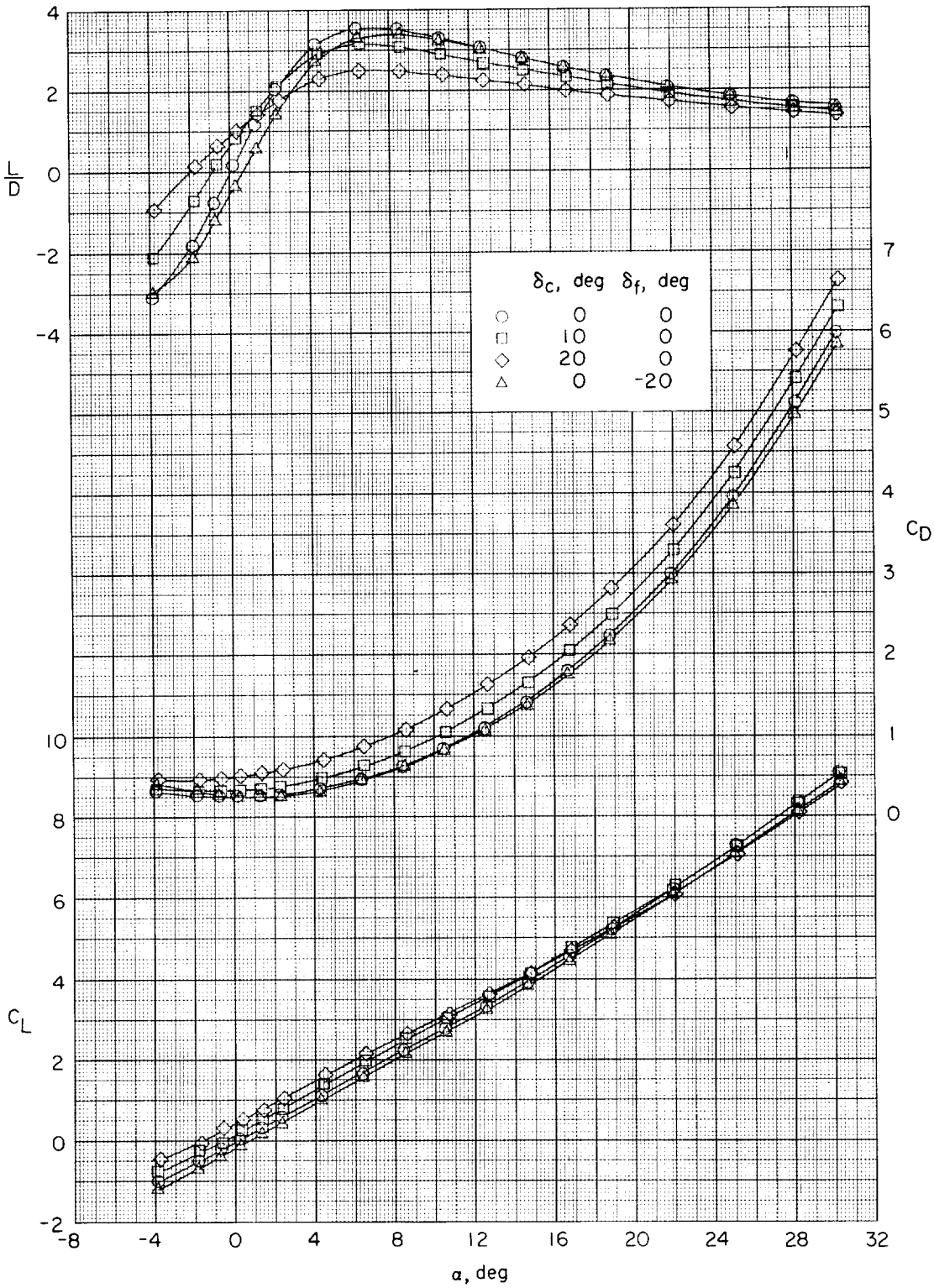

(e) Concluded.

Figure 10.- Continued.

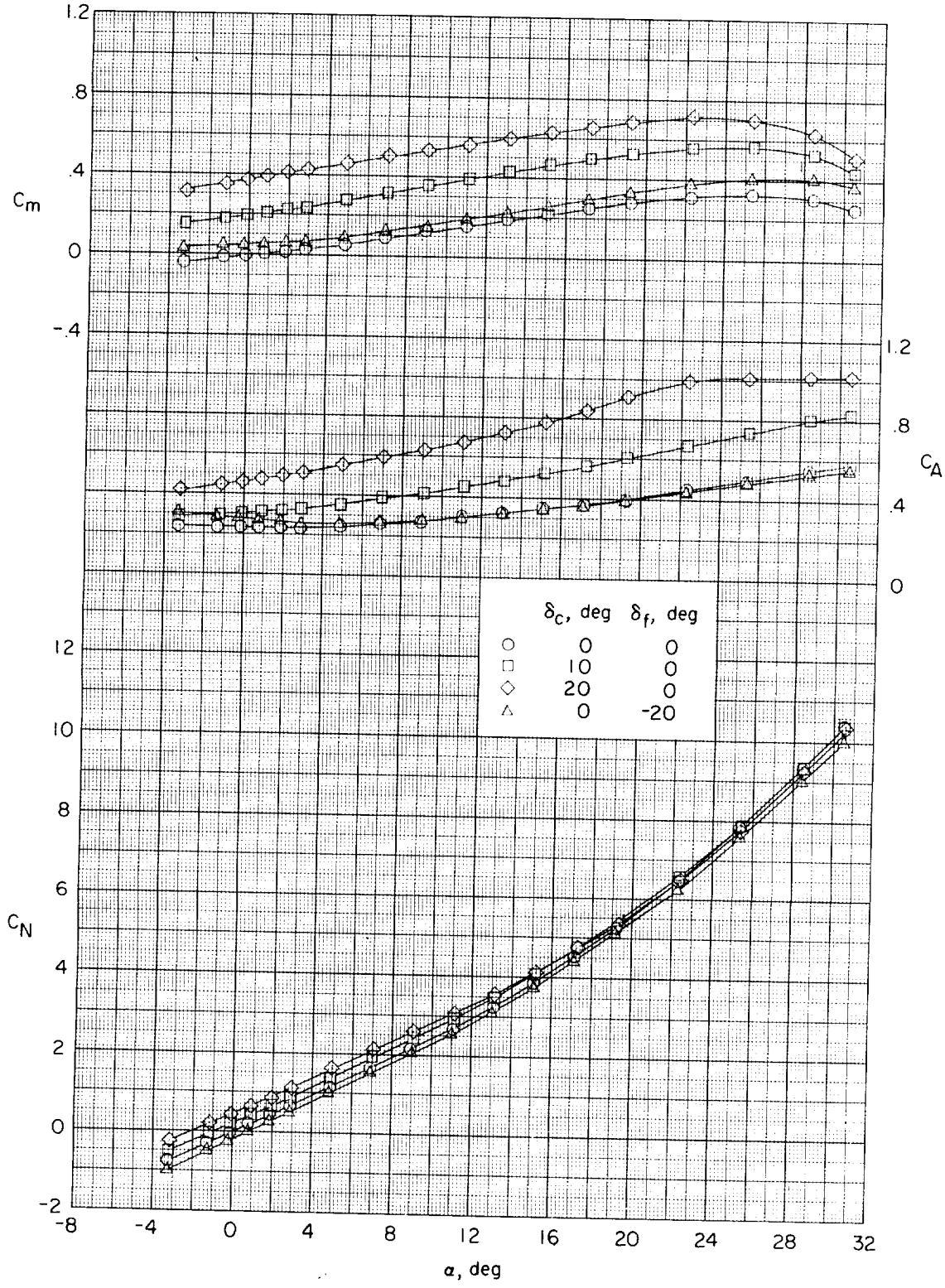

(f) M = 4.63.

Figure 10.- Continued.

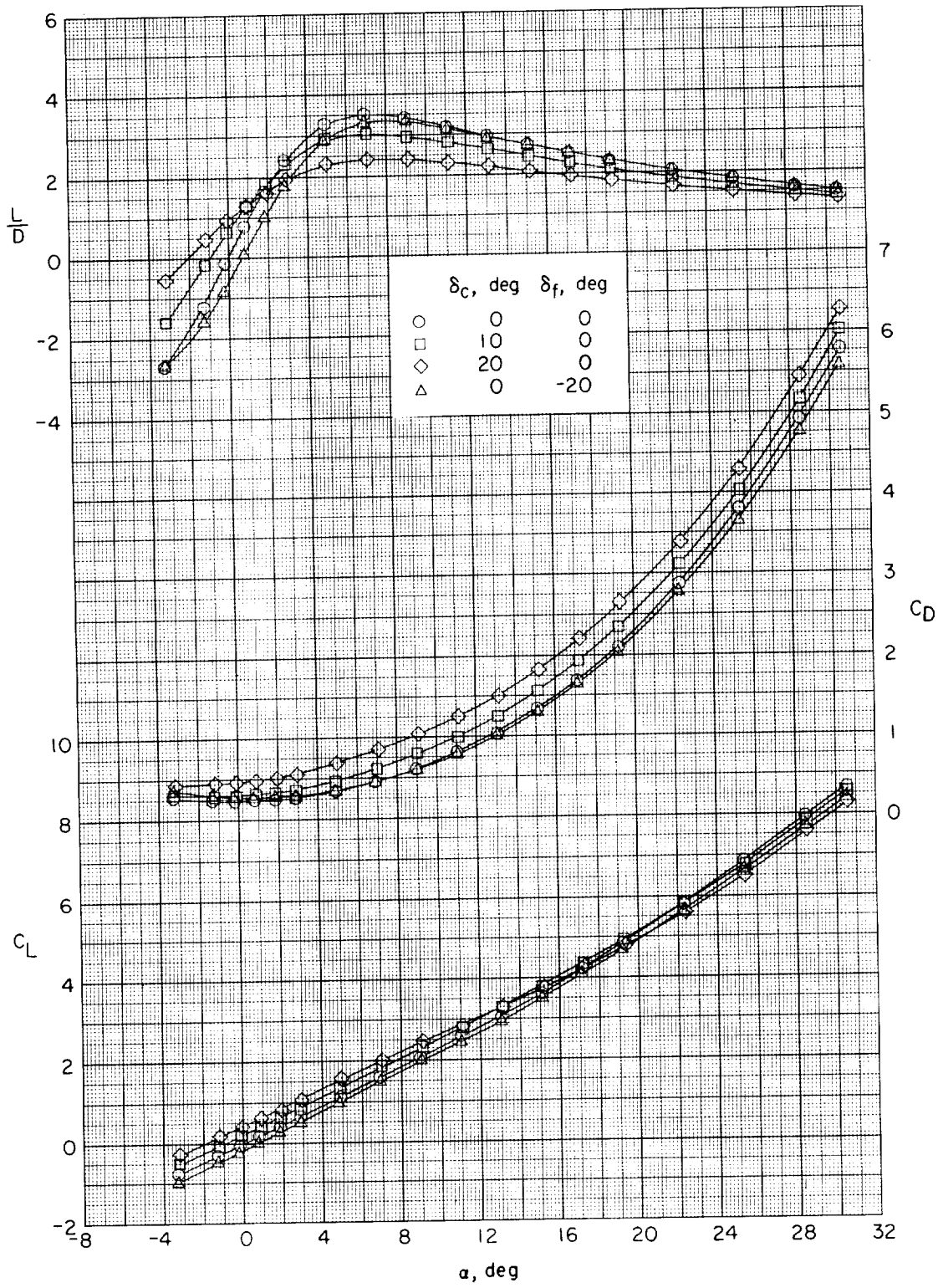

(f) Concluded.

Figure 10.- Concluded.

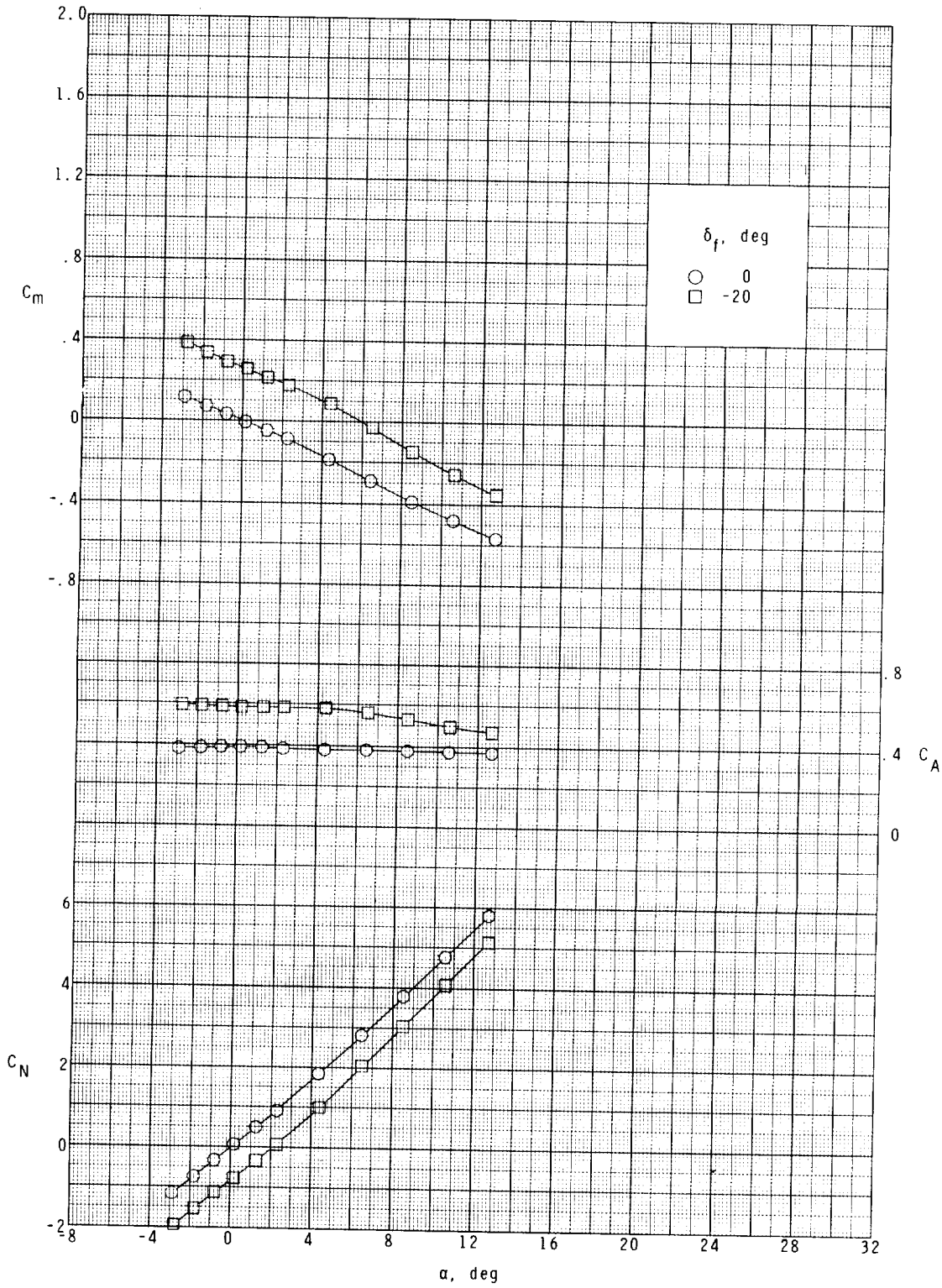

(a) M = 1.50.

Figure 11.- Effects of wing-flap deflection on the longitudinal aerodynamic characteristics of the model. Canard off; WB.

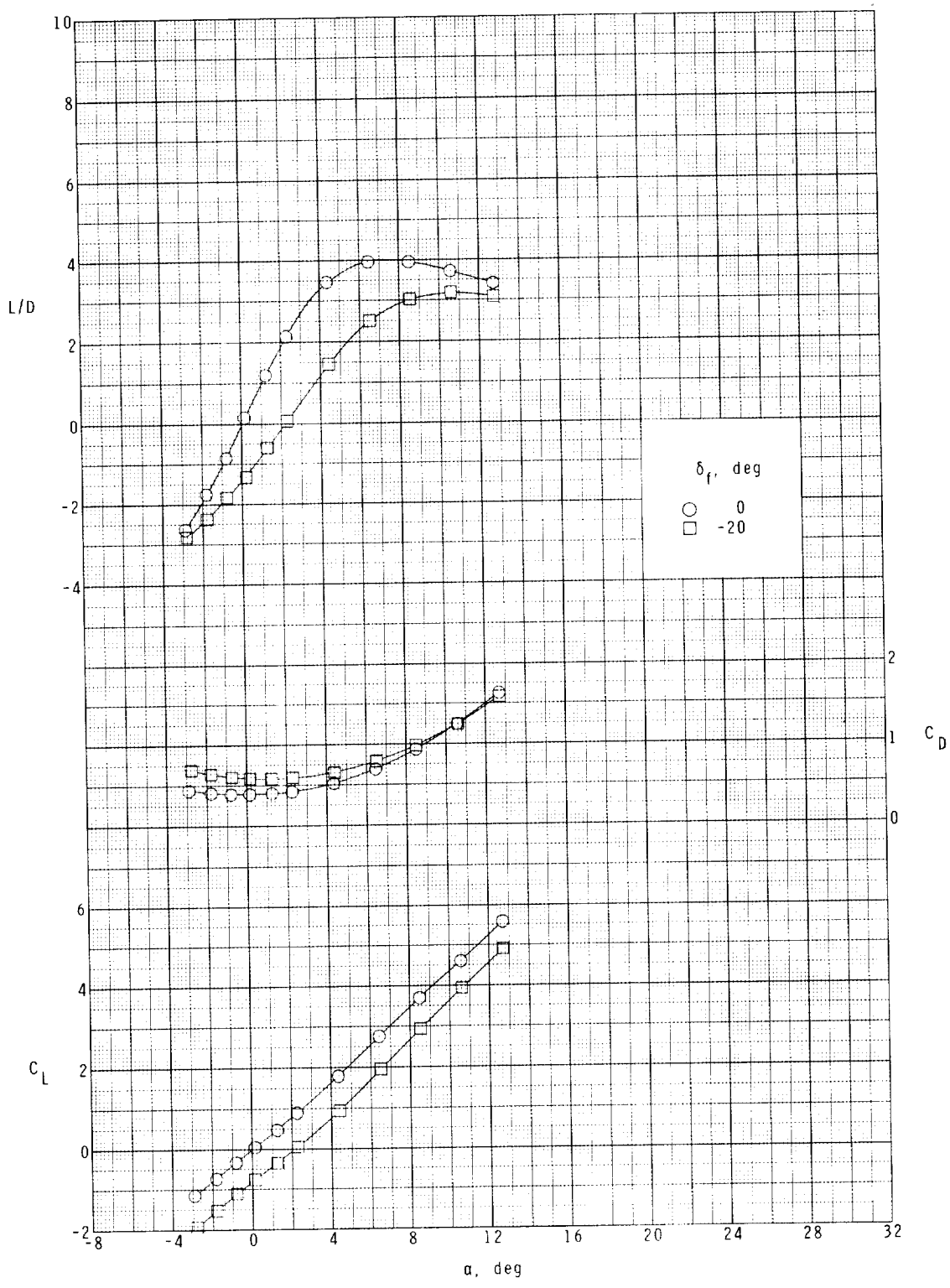

(a) Concluded.

Figure 11.- Continued.

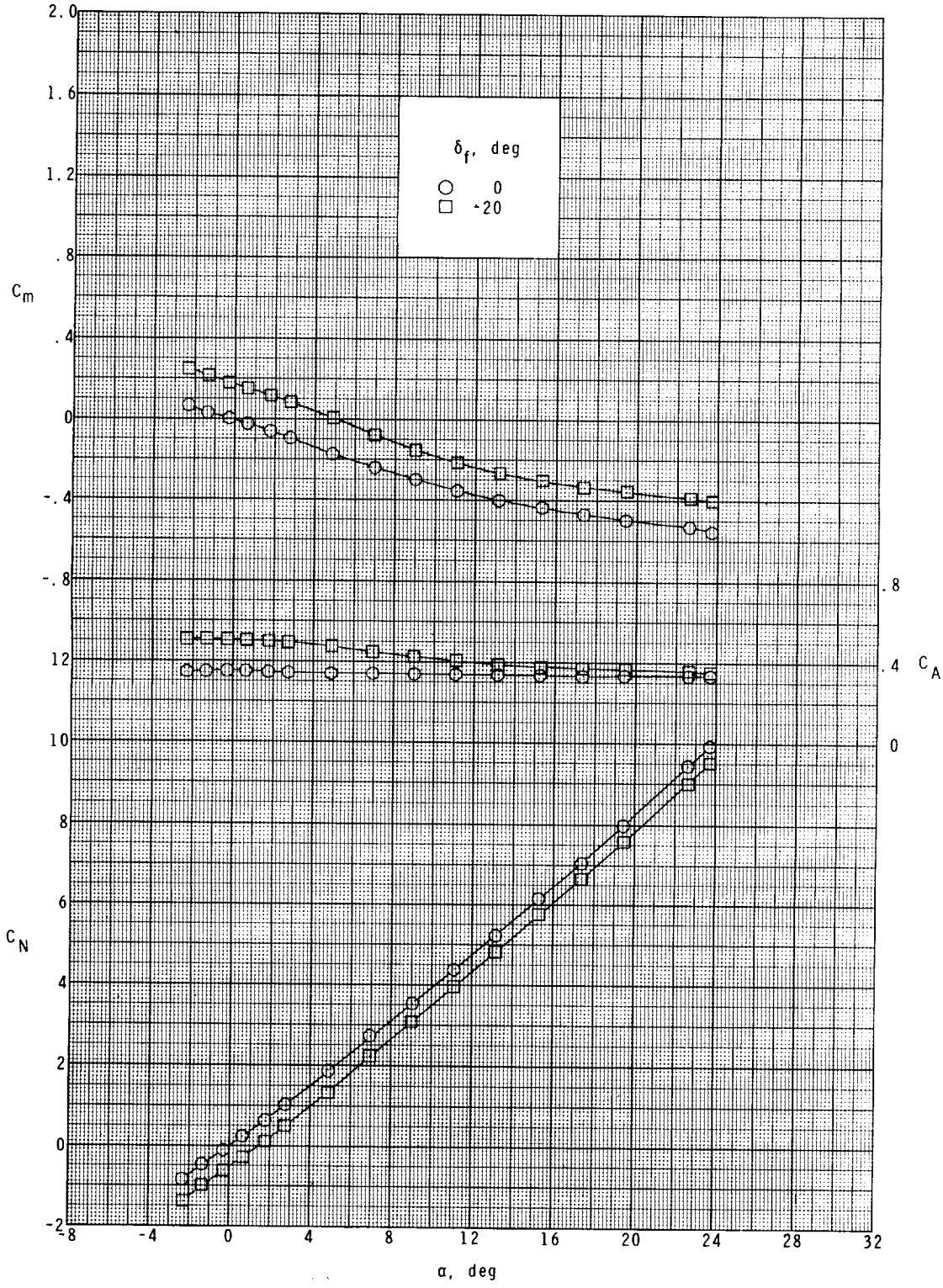

(b) M = 1.90.

Figure 11.- Continued.

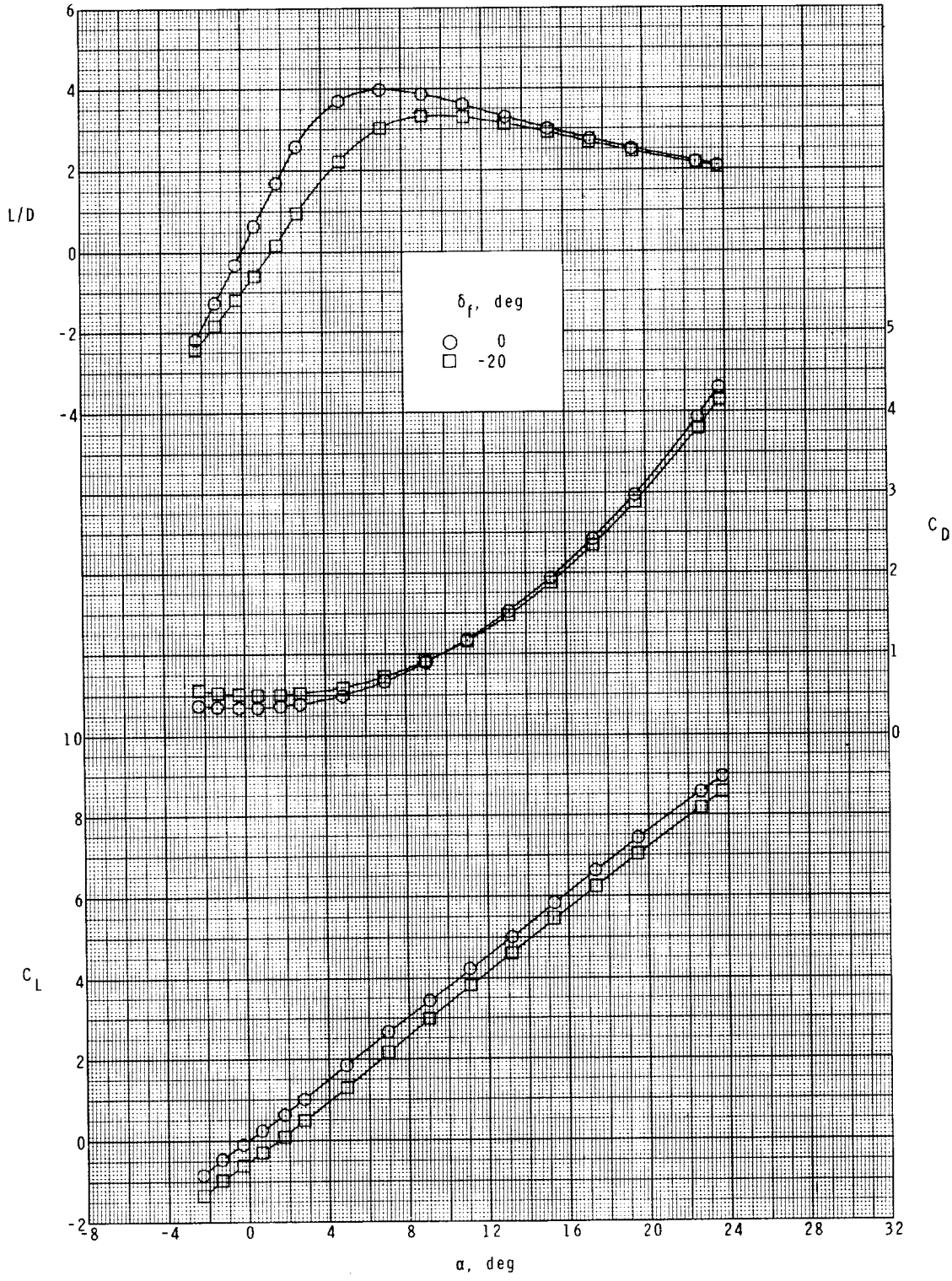

(b) Concluded.

Figure 11.- Continued.

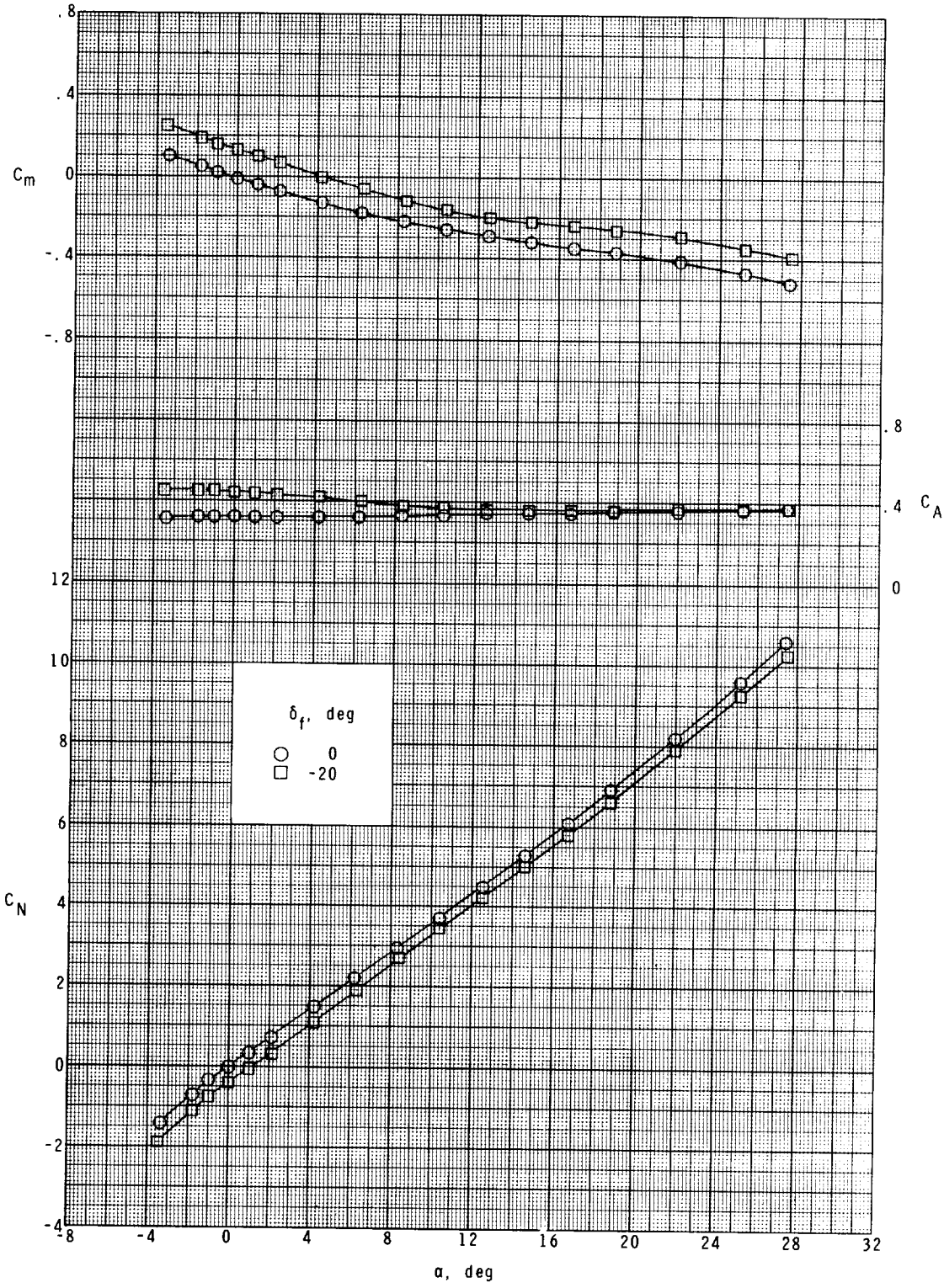

(c) M = 2.30.

Figure 11.- Continued.

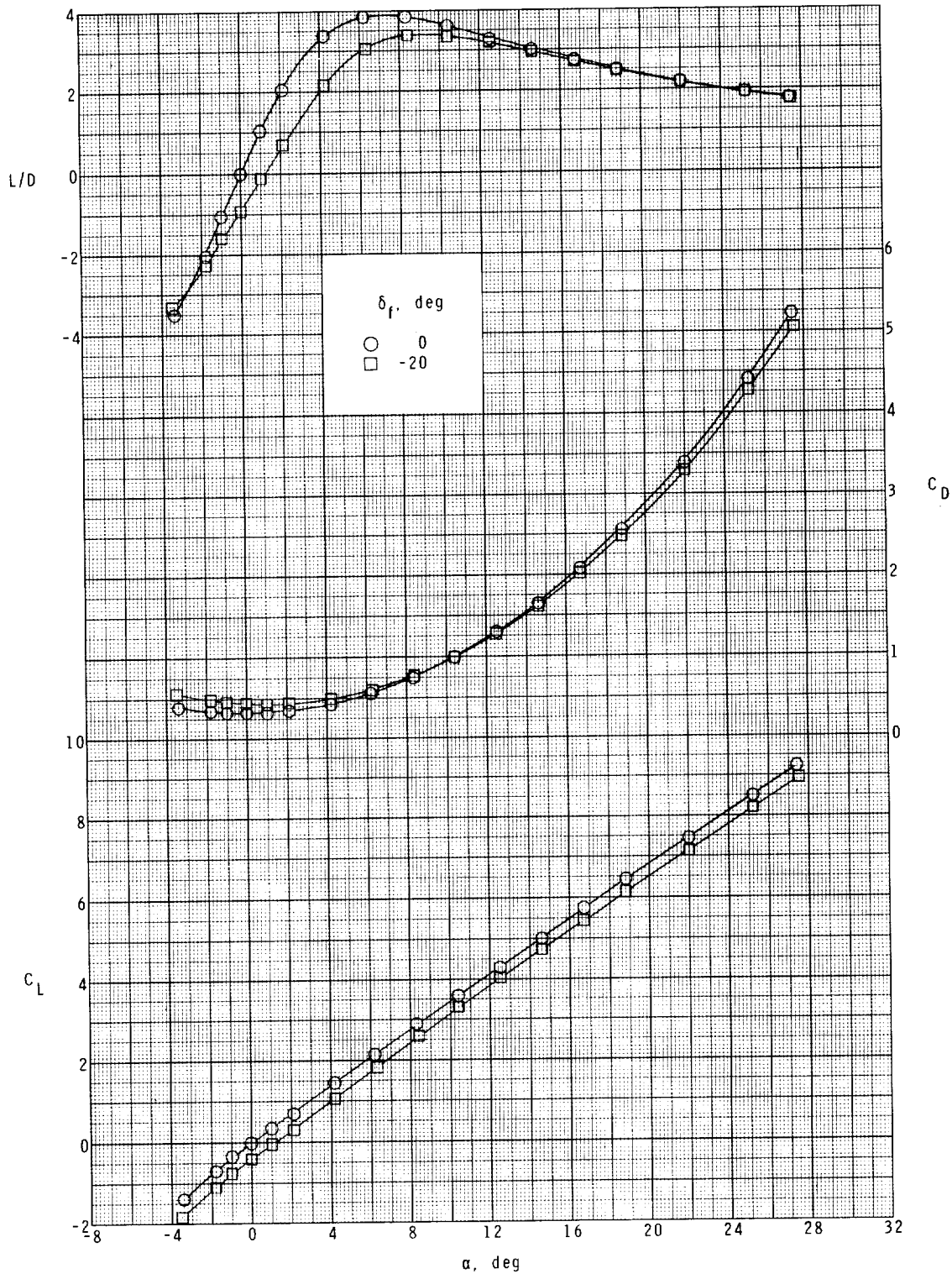

(c) Concluded.

Figure 11.- Continued.

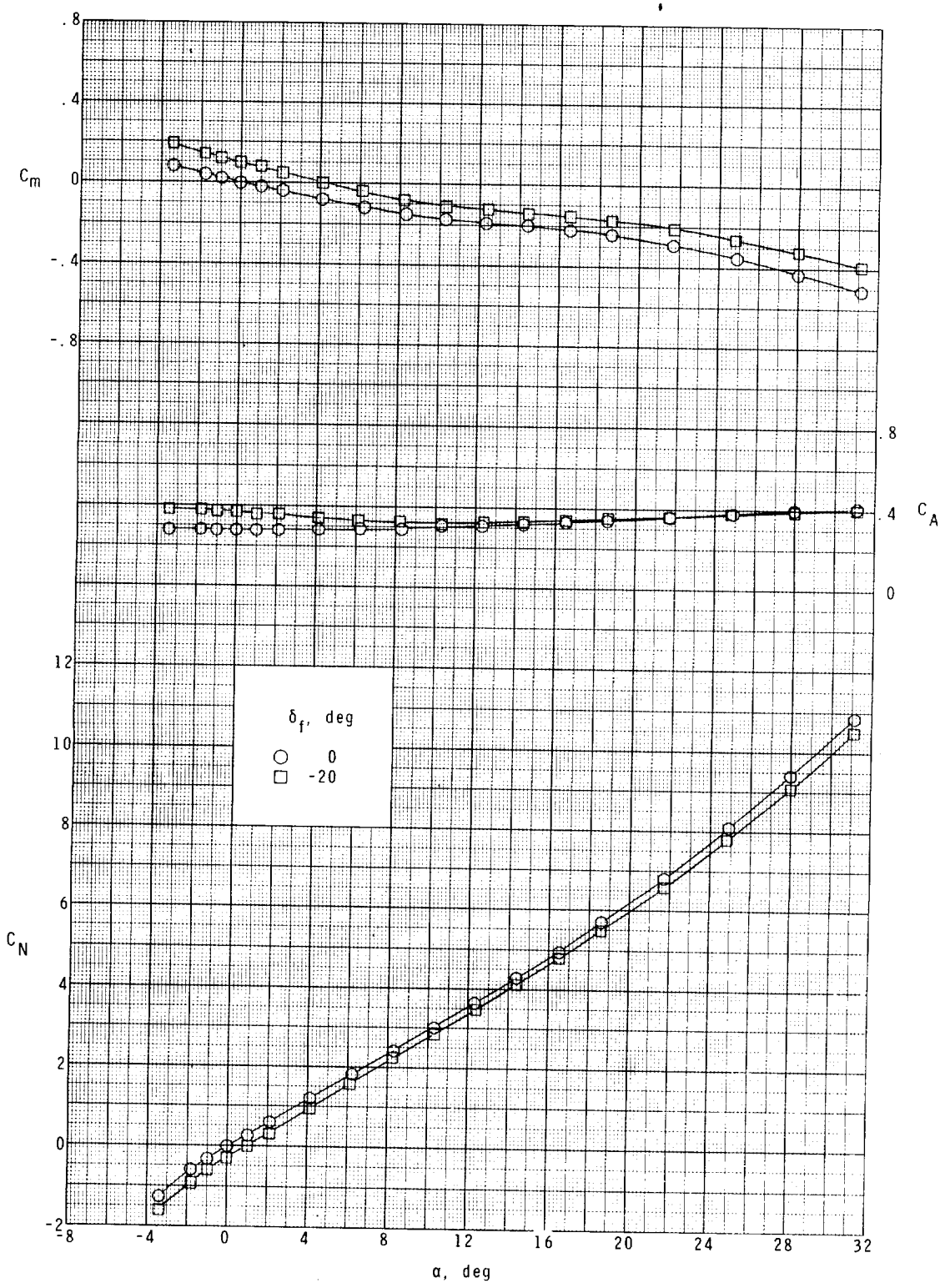

(d) M = 2.96.

Figure 11.- Continued.

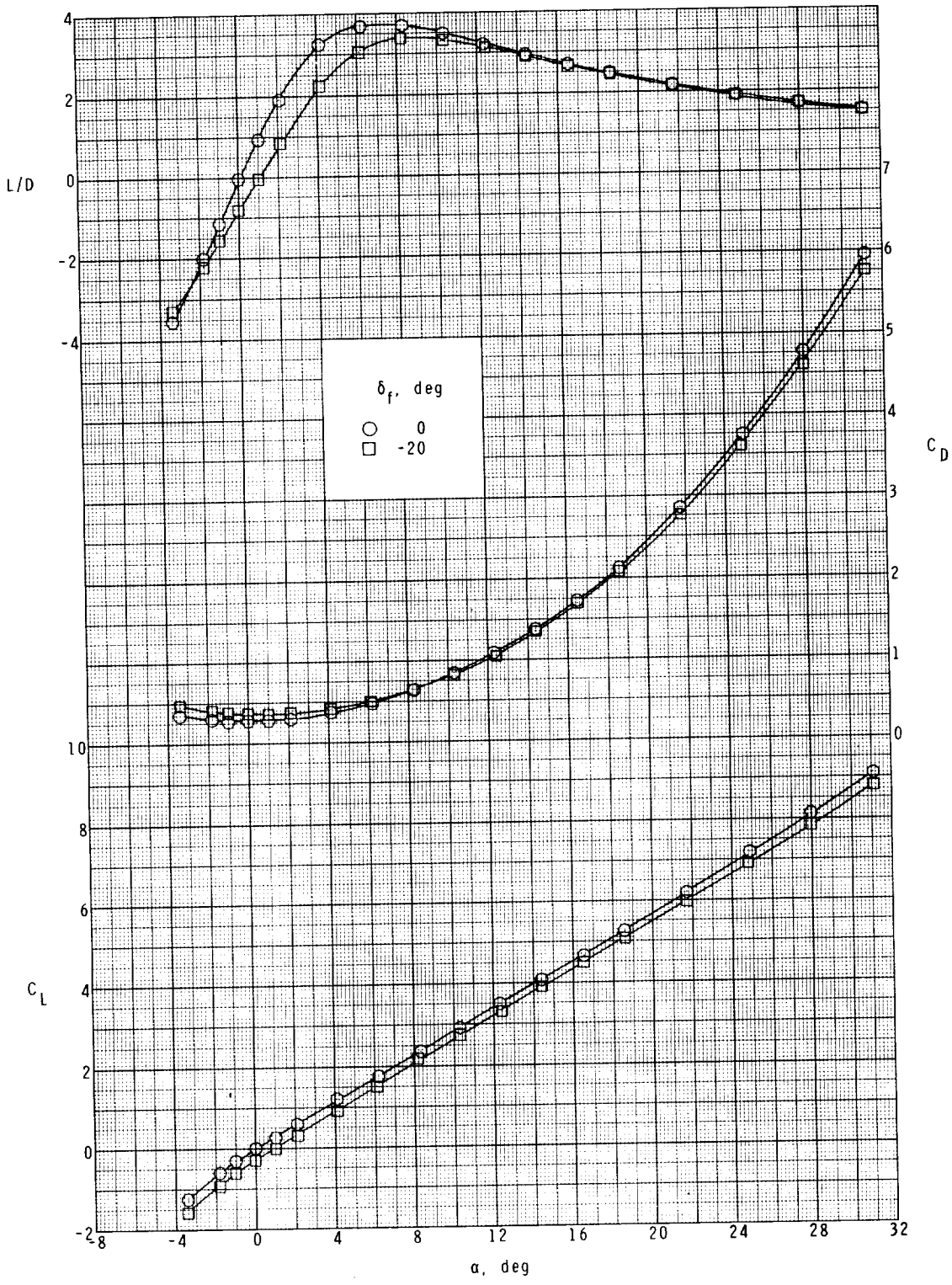

(d) Concluded.

Figure 11.- Continued.

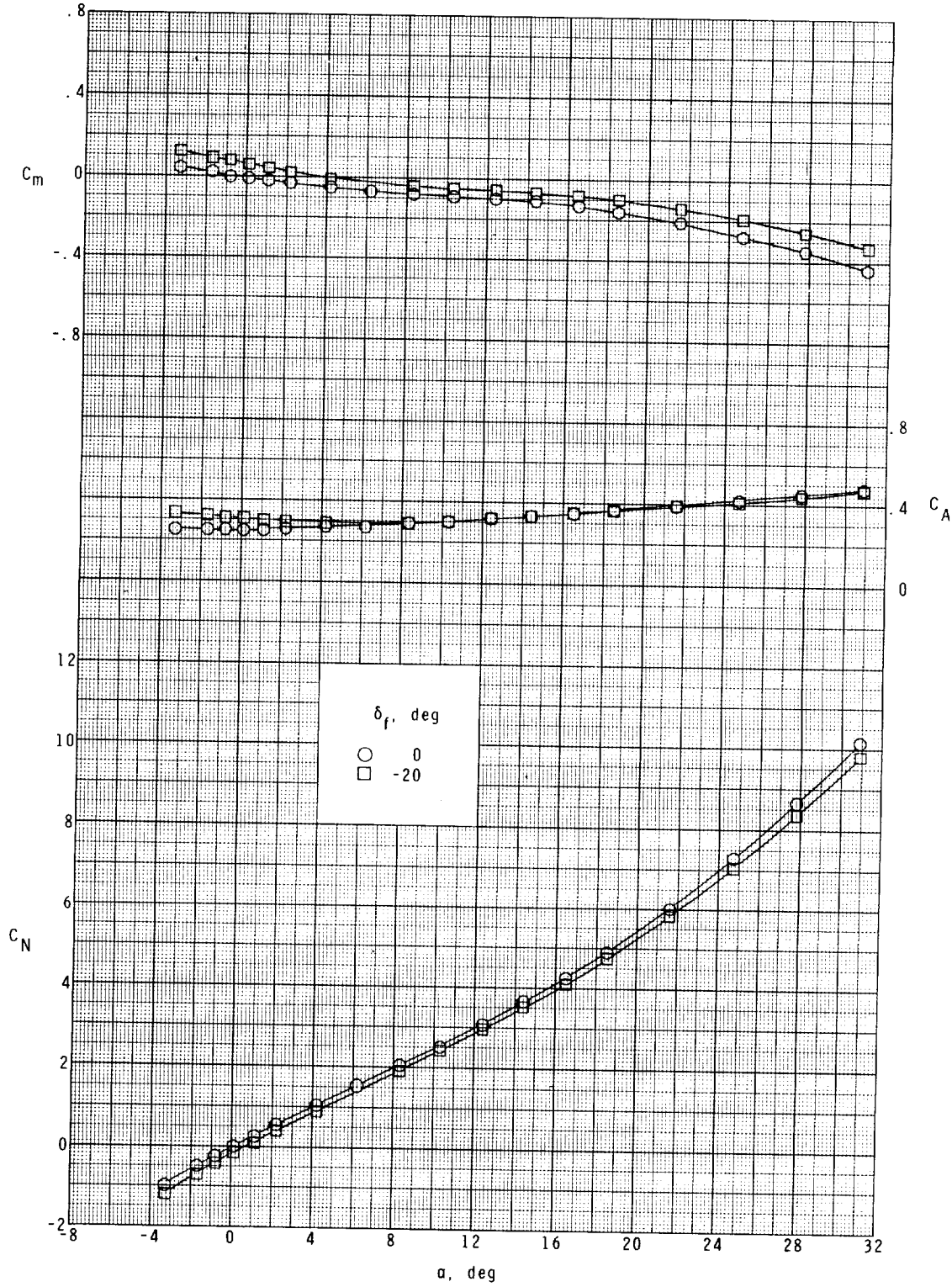

(e) M = 3.95.

Figure 11.- Continued.

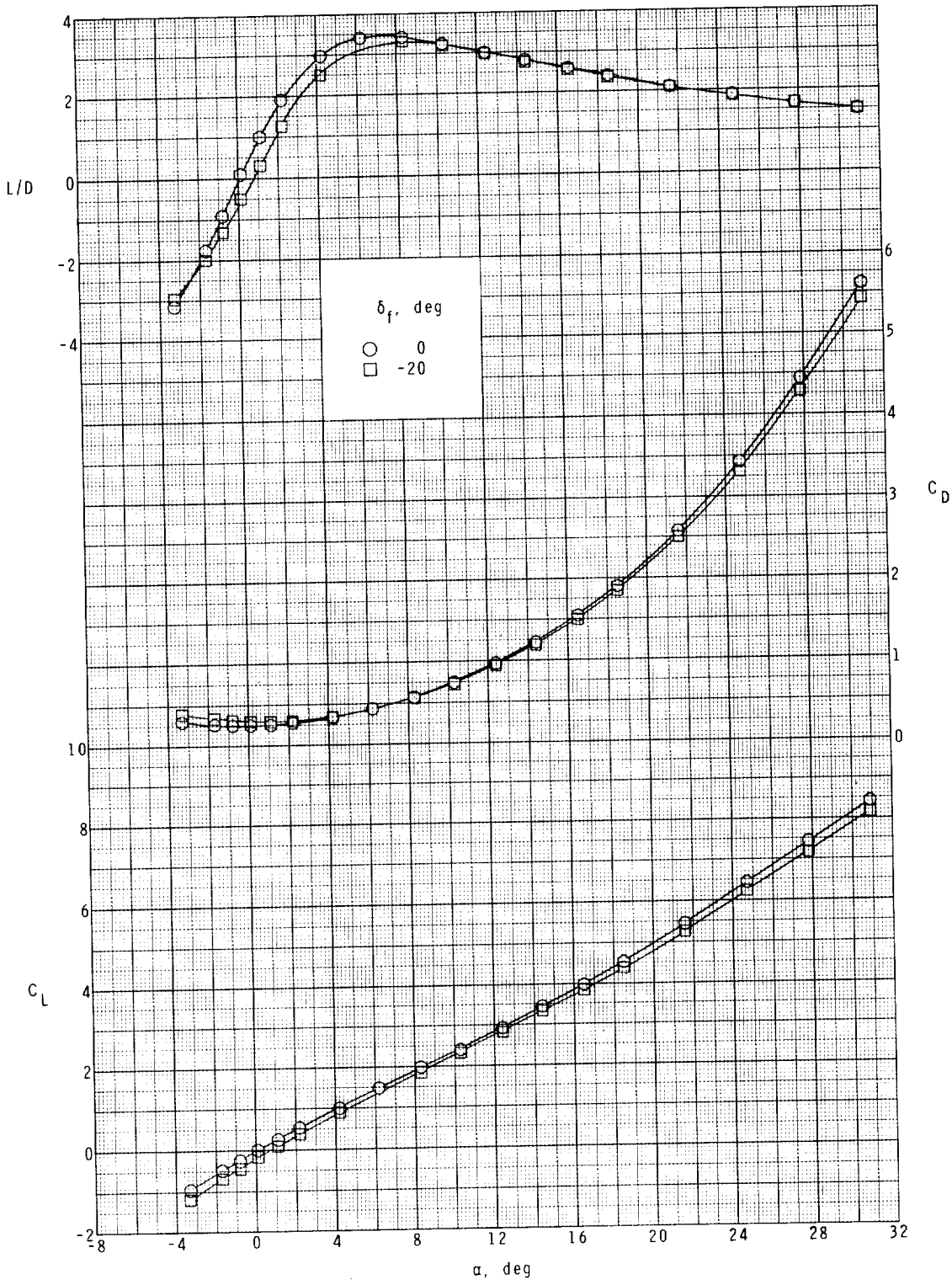

(e) Concluded.

Figure 11.- Continued.

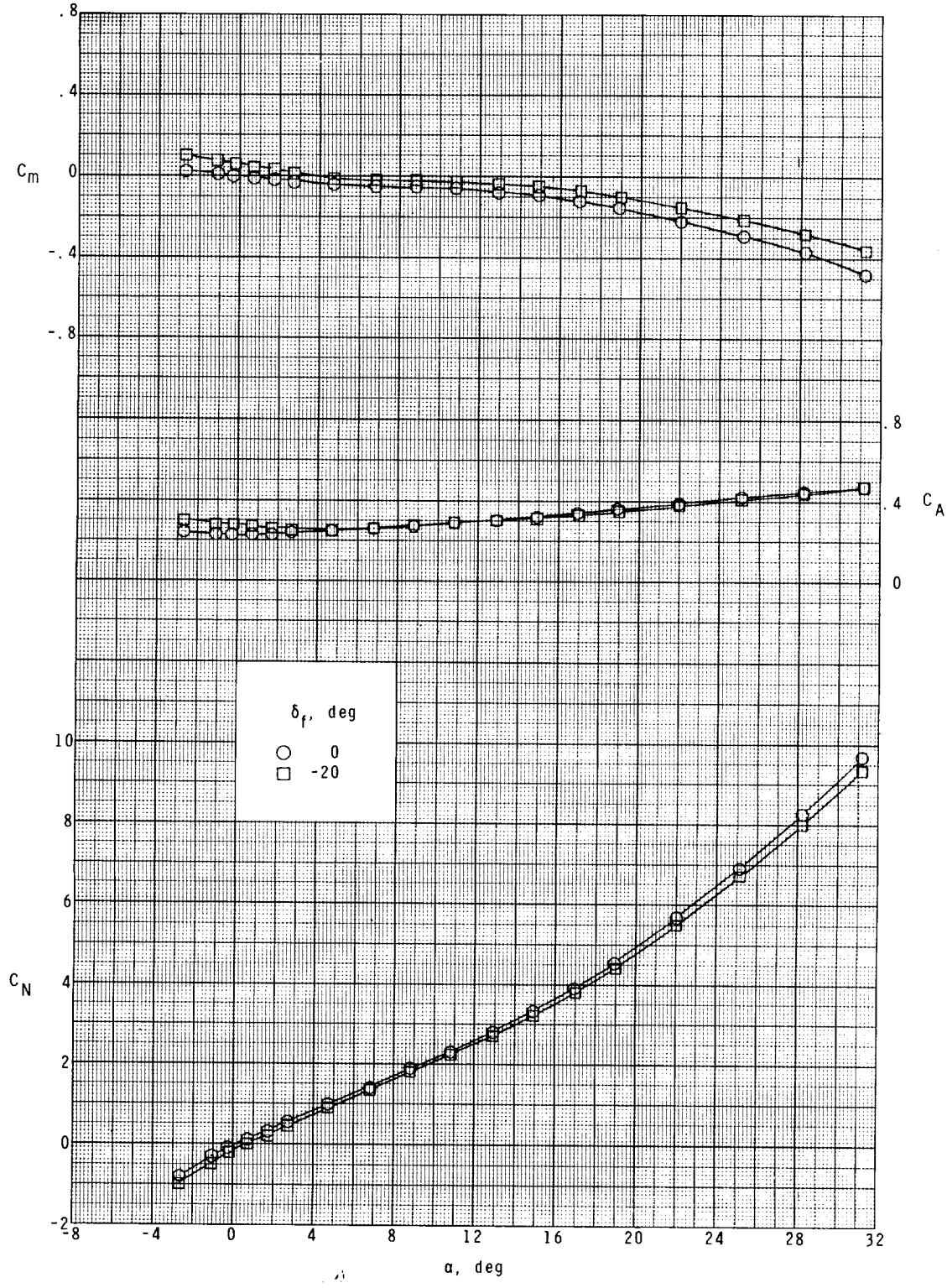

(f) M = 4.63.

Figure 11.- Continued.

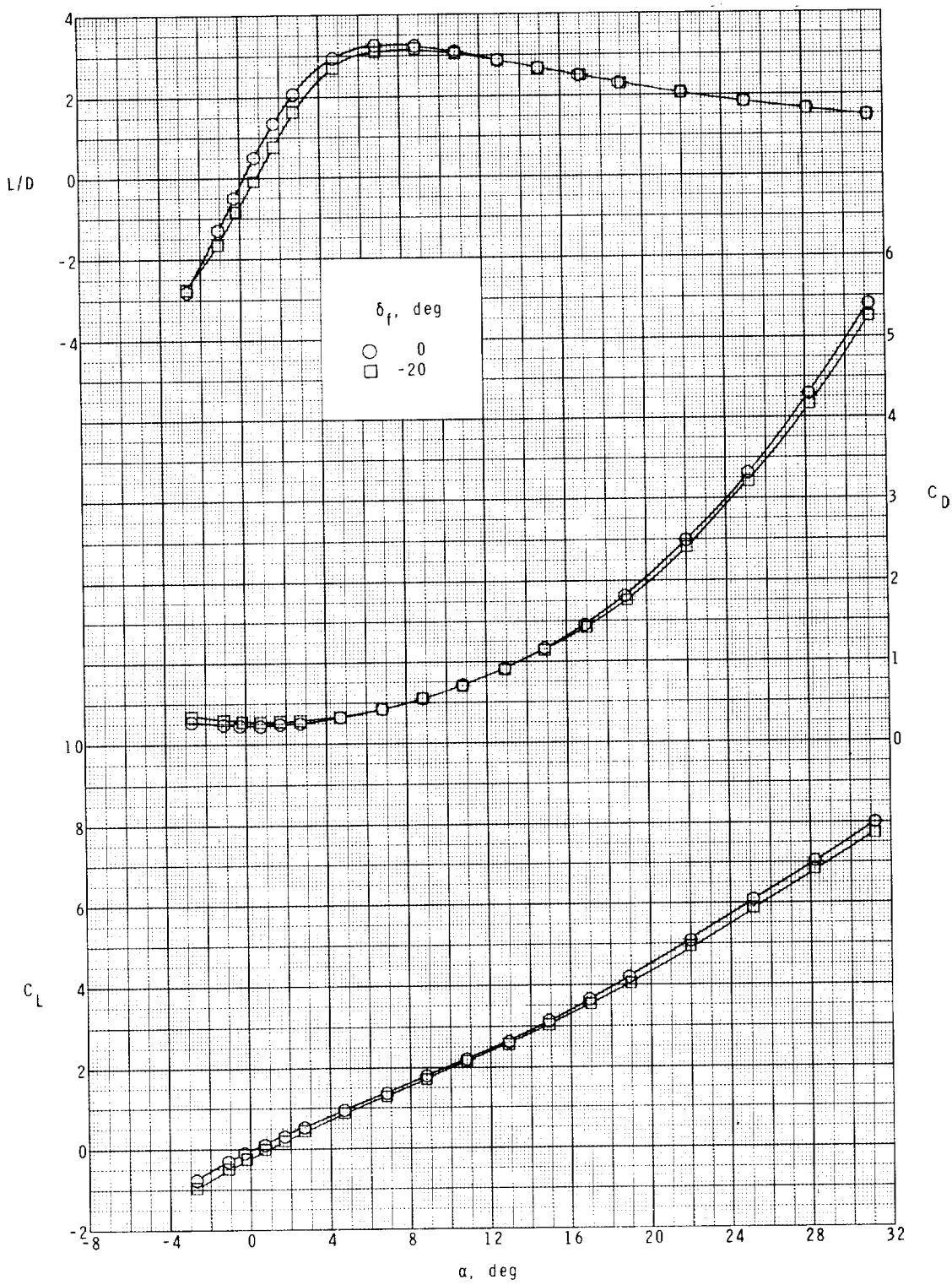

(f) Concluded.

Figure 11.- Concluded.

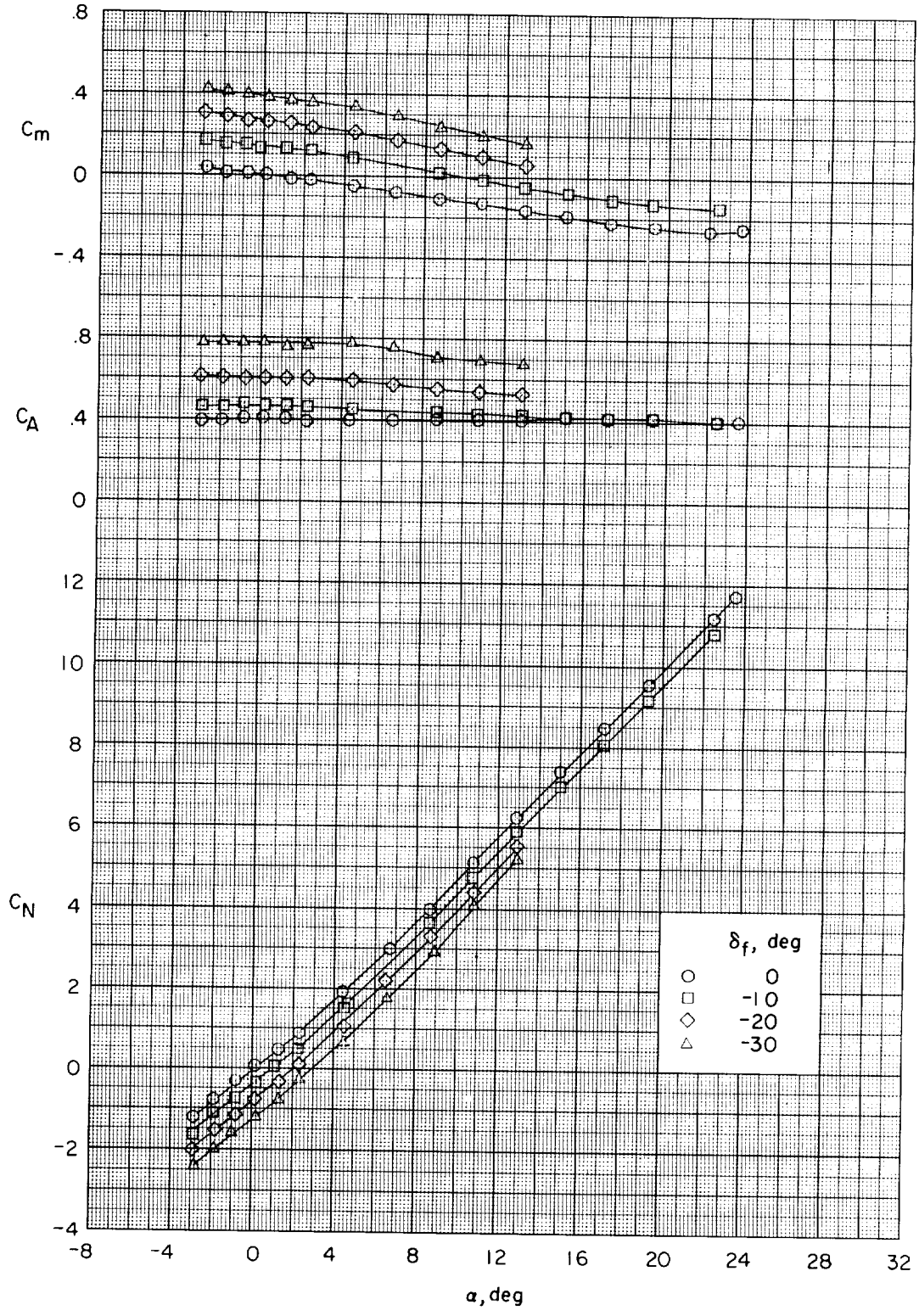

(a) M = 1.50.

Figure 12.- Effects of wing-flap deflection on the longitudinal aerodynamic characteristics of the model with canard C_2 and $\delta_c = 0^0$. Configuration WBC_2.

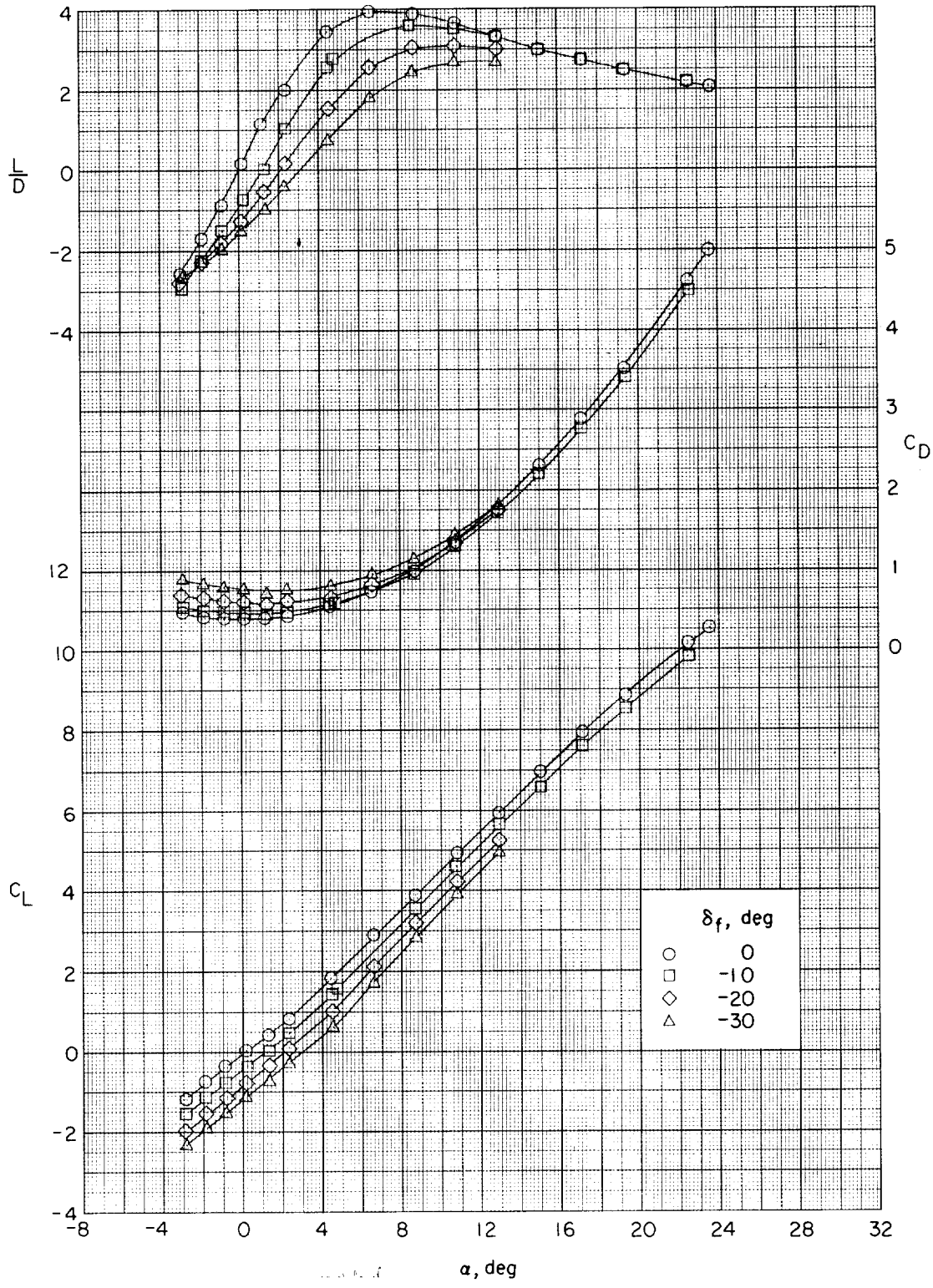

(a) Concluded.

Figure 12.- Continued.

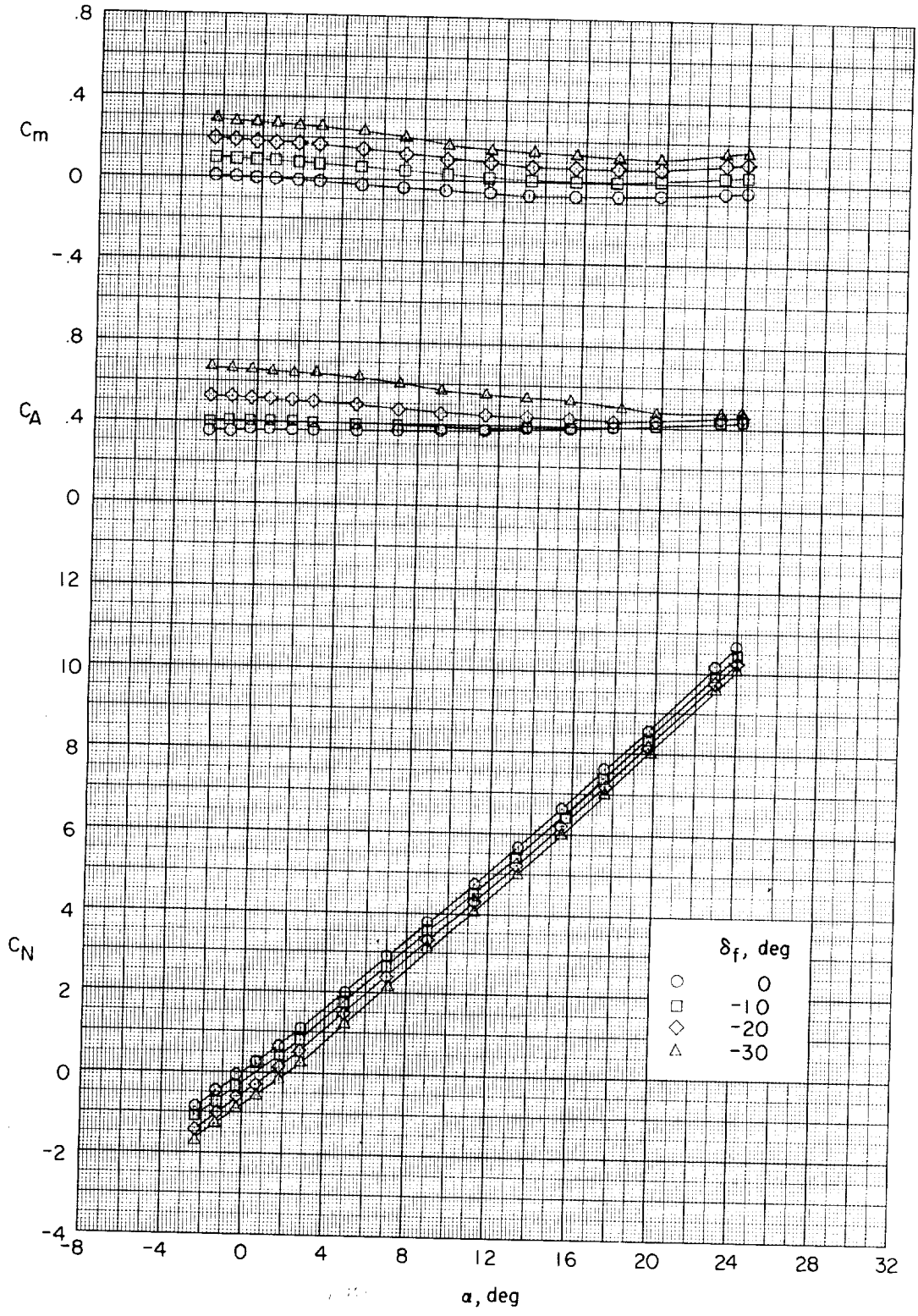

(b) M = 1.90.

Figure 12.- Continued.

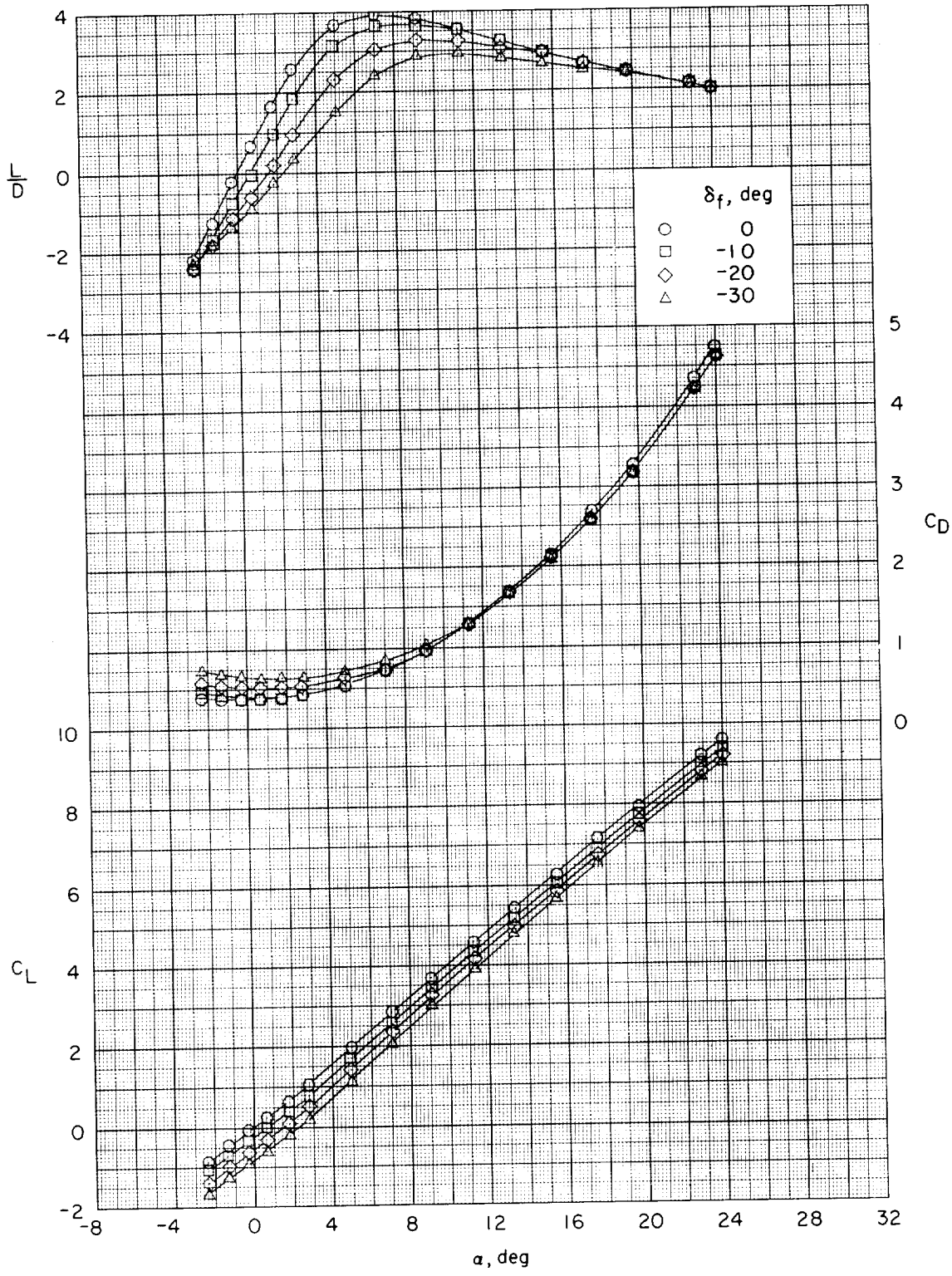

(b) Concluded.

Figure 12.- Continued.

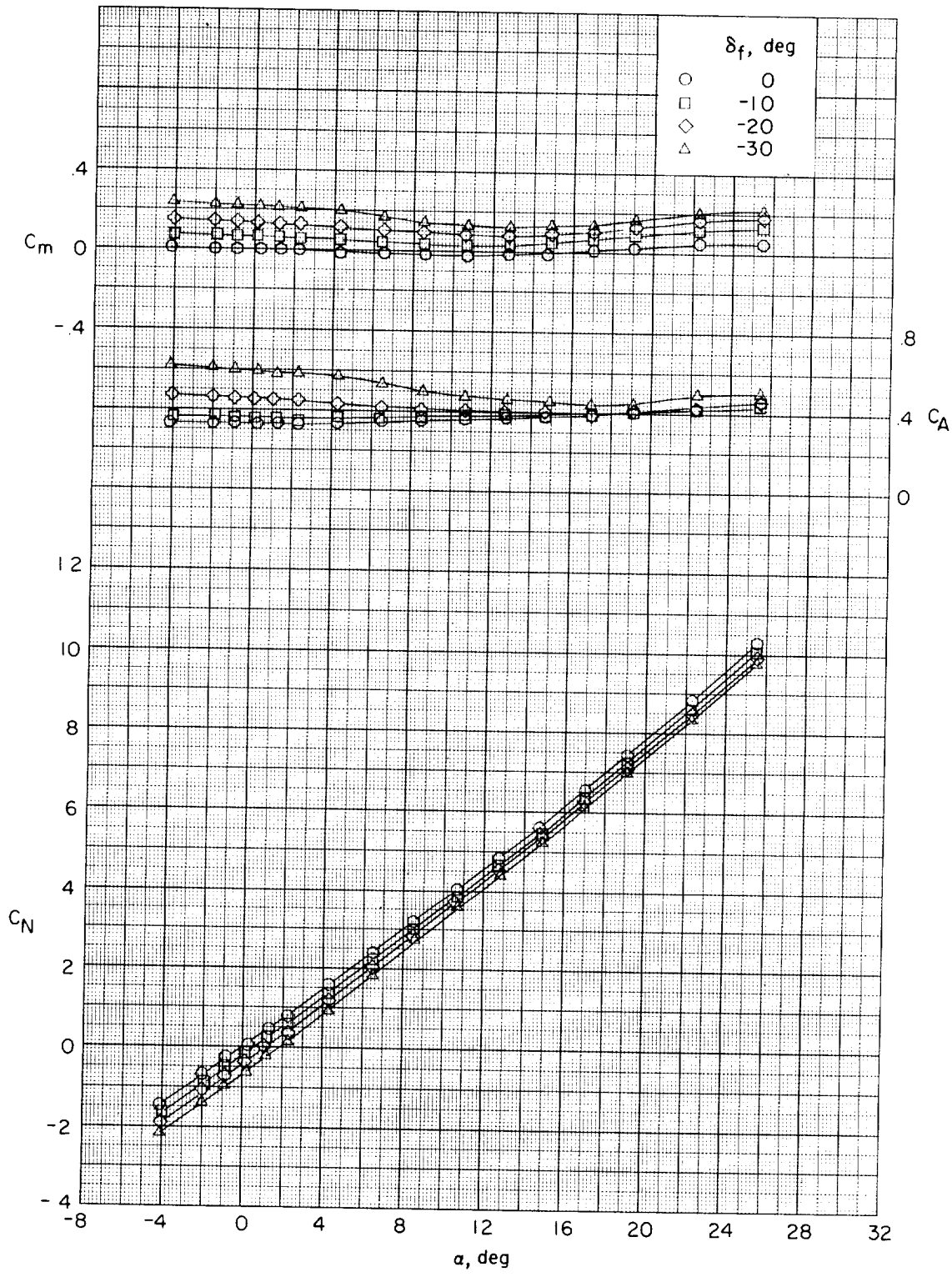

(c) M = 2.30.

Figure 12.- Continued.

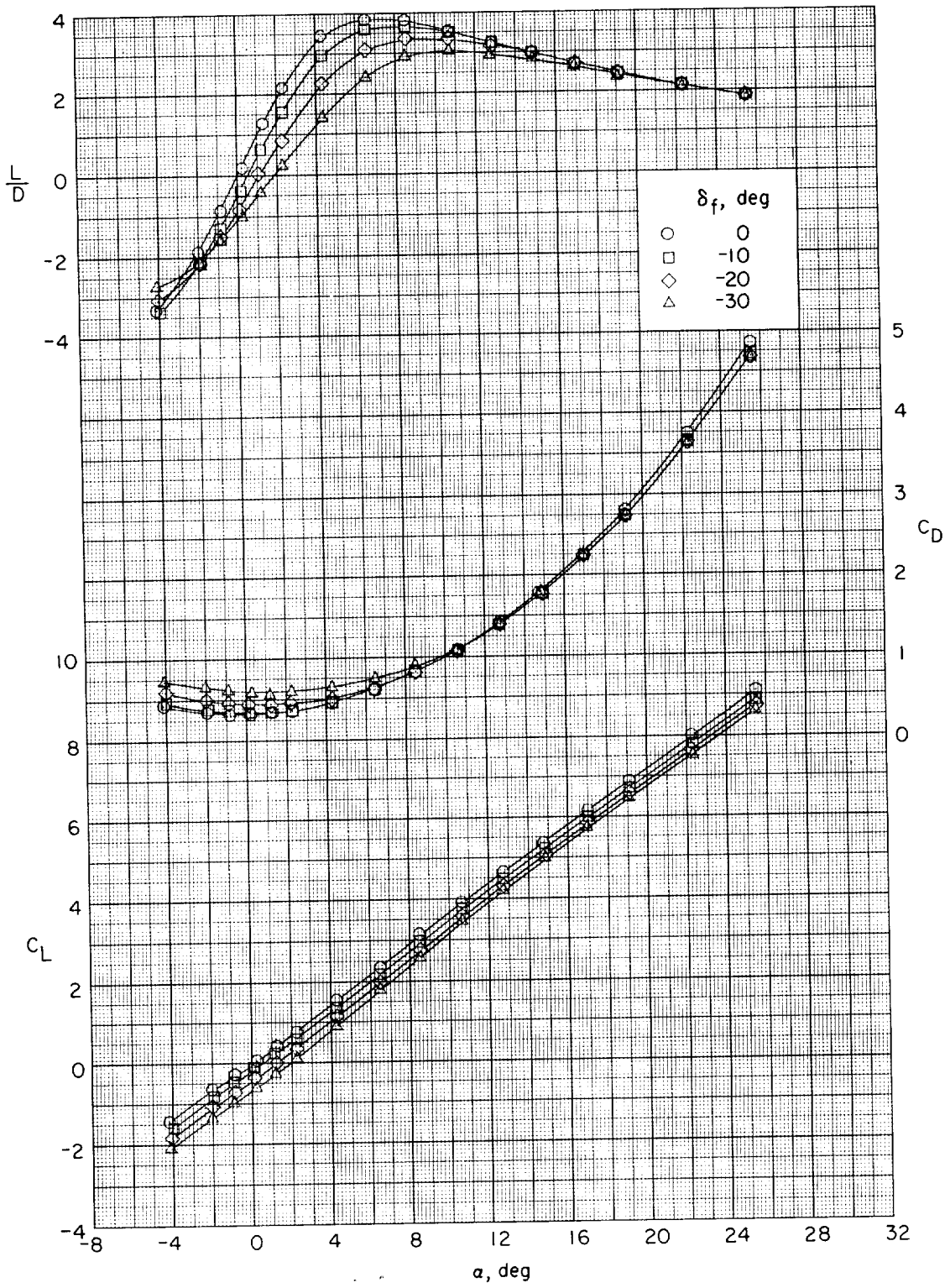

(c) Concluded.

Figure 12.- Continued.

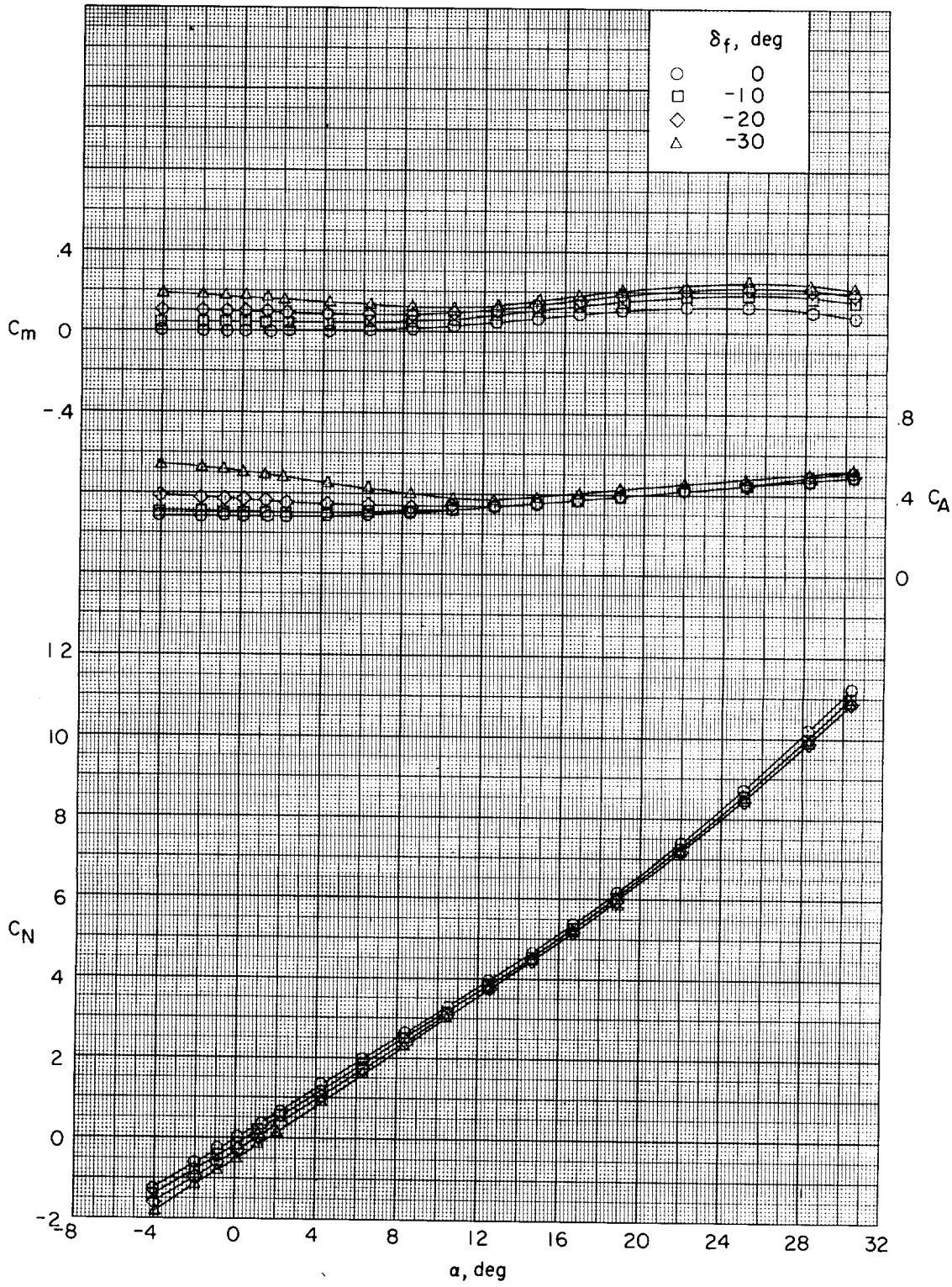

(d) M = 2.96.

Figure 12.- Continued.

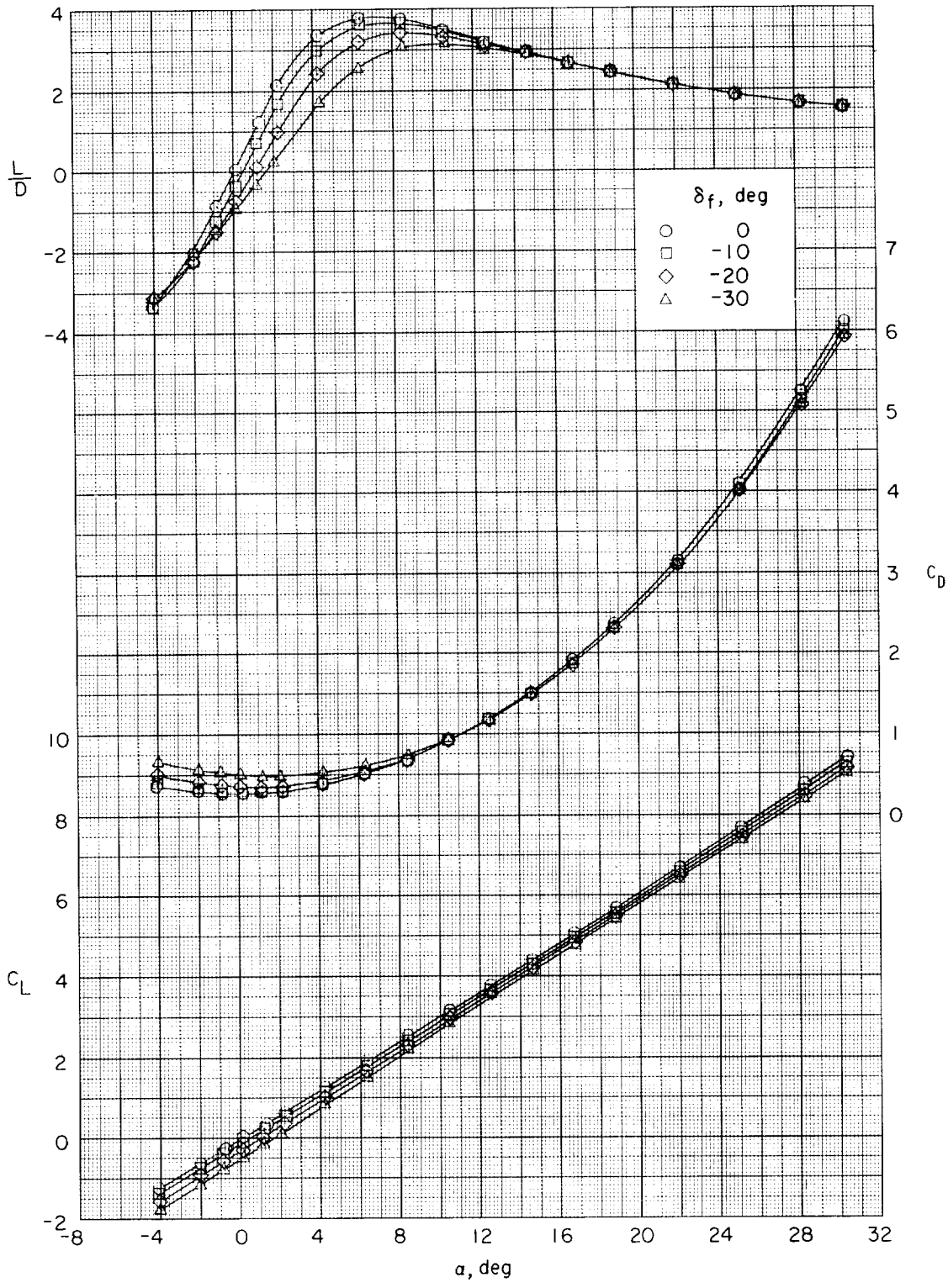

(d) Concluded.

Figure 12.- Continued.

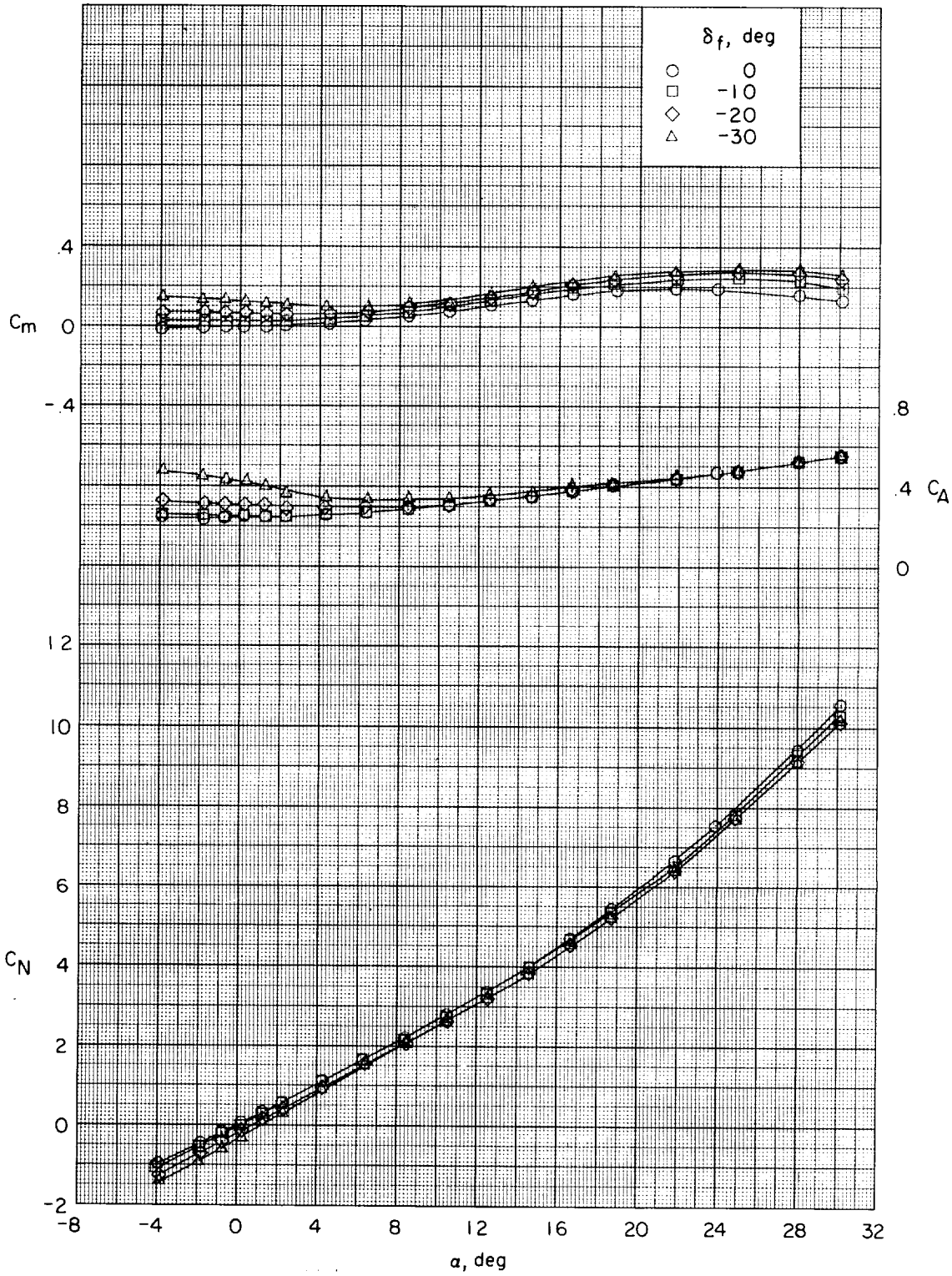

(e) M = 3.95.

Figure 12.- Continued.

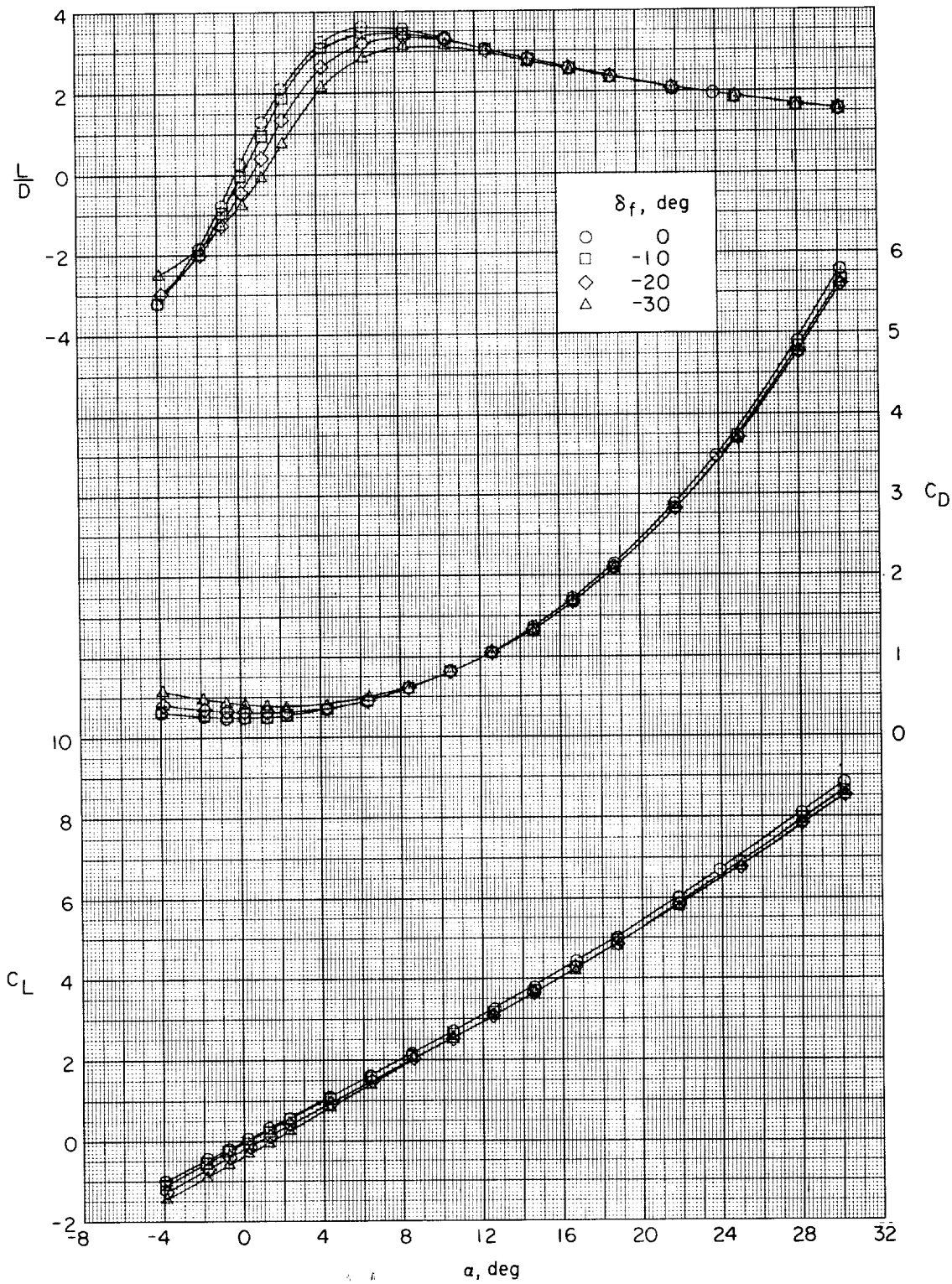

(e) Concluded.

Figure 12.- Continued.

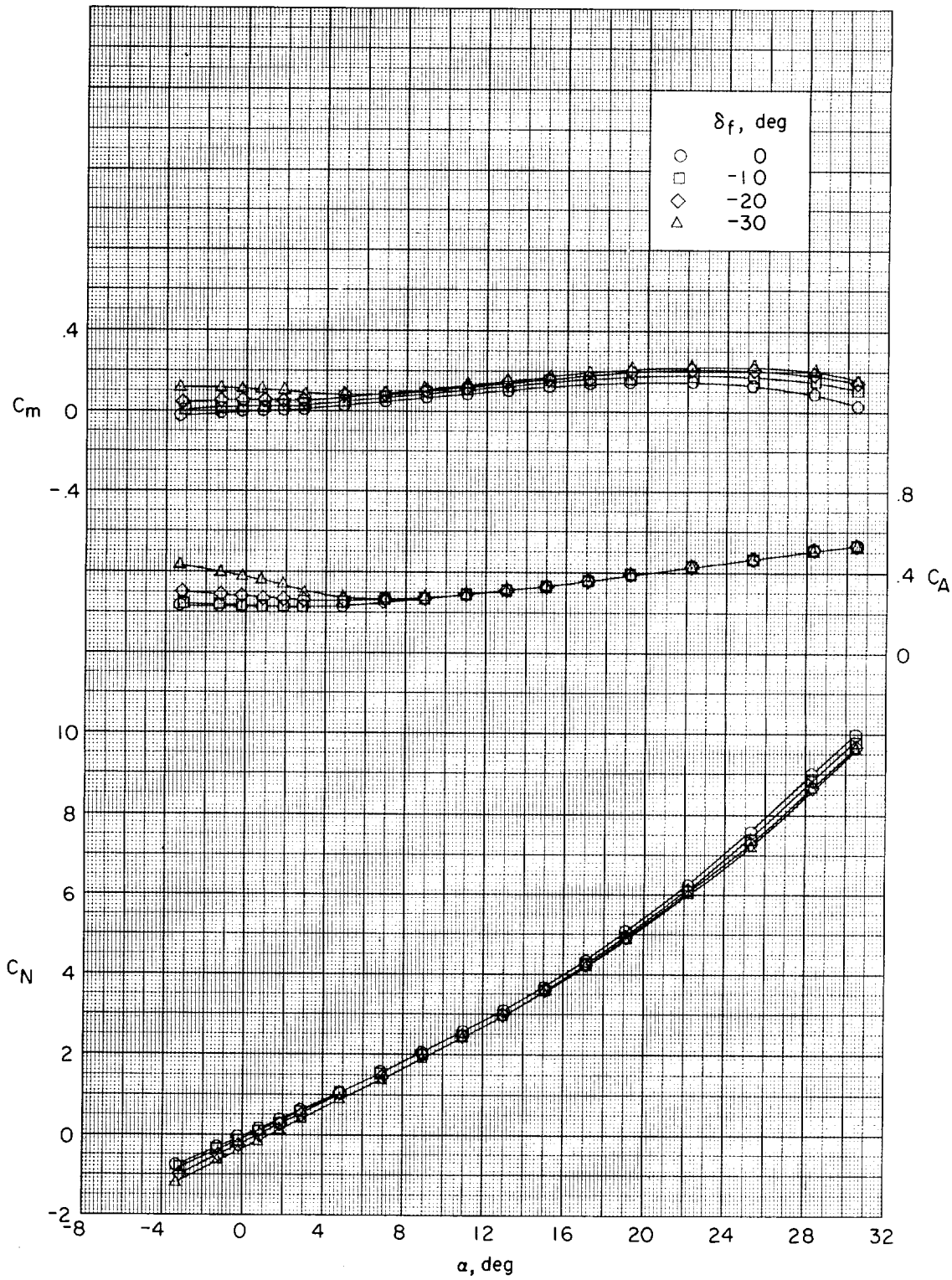

(f) M = 4.63.

Figure 12.- Continued.

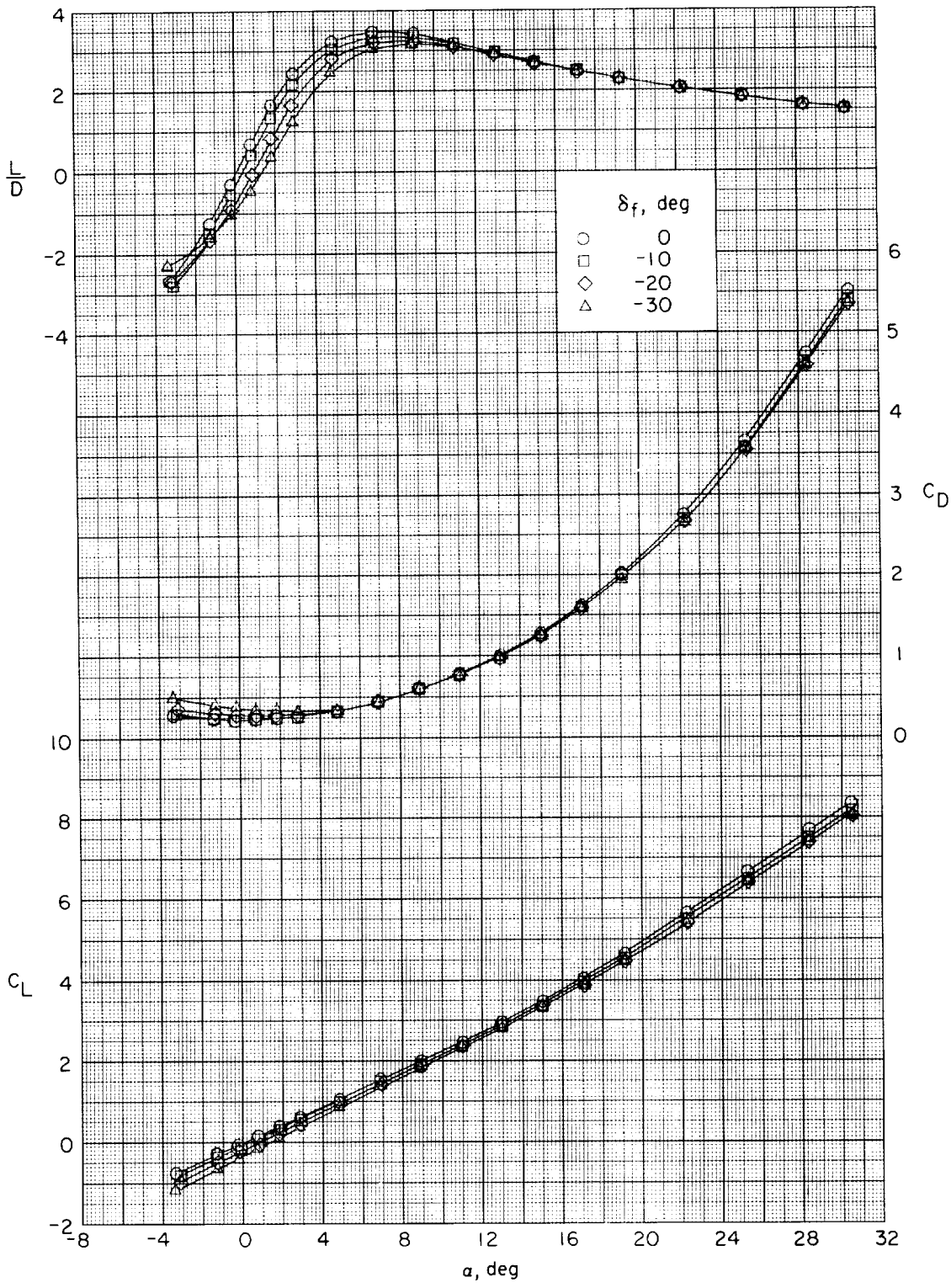

(f) Concluded.

Figure 12.- Concluded.

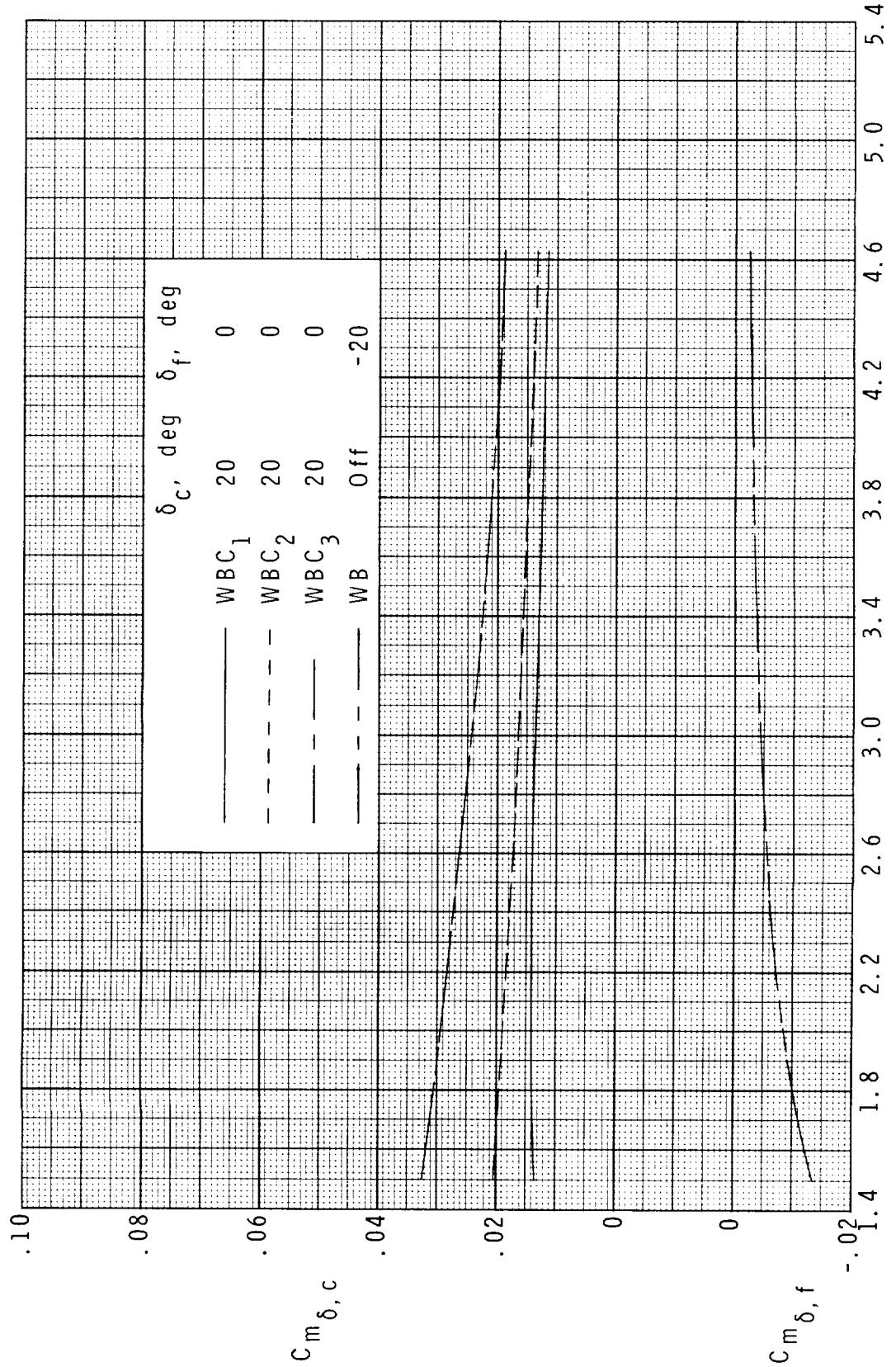

Figure 13.- Summary of pitch-control effectiveness.